Il desiderio è rivoluzionario perché

cerca quello che non si vede.

Platone

UNIVERSITÀ DEGLI STUDI DI MILANO

PhD Course in Molecular and Cellular Biology

XXX Cycle

Unravelling the role of novel factors involved in double-strand break repair.

Simona Aliprandi

PhD Thesis

Scientific Tutor: **Dott.ssa Federica Marini**
Prof. Achille Pellicioli

Academic year 2016-2017

Thesis performed at Department of Bioscience

University of Milan, 20133 Italy

Summary

Abstract

Each day every cell of a living organism is constantly exposed to numerous DNA damages deriving both from the environment but also from its own metabolism. The high number of lesions and the consequent genome instability make of DNA damages one of the weightiest challenge to face for a cell. Indeed the ability to detect, recognise and repair a lesion is of pivotal importance, since on these events depend the stability of the genome and, ultimately, cell viability. The main shield eukaryotic cells have evolved to face this challenge is the DNA damage response, a protein network that allow repair of the lesions. Human cells can rely on two main mechanisms to repair double strand breaks, one of the most harmful lesions: homologous recombination and non-homologous end joining. The correct balance between these two pathways depends on cell cycle, chromatin conformation and on the interplay among different factors. In addition, important for the correct pathway choice is the DNA end resection process. It consists in a nucleolytic degradation of the DSB ends to generate a 3' protruding tail to invade the homologous sequence, used as a template to accomplish the HR. Fine regulation of resection is particularly important to correctly repair the damage and prevent genome instability, fuel of cancer.

In this Thesis I present the work performed during my three years of PhD, in which I've been involved in two projects. Using human cells as a model system I've analysed the role of two different proteins, both involved in DNA repair pathway choice: DAXX and SLX4.

In the first and half year of my PhD, I analysed the effect of double strand break-dependent phosphorylation of DAXX on its activity as a chaperone of the histone variant H3.3. In brief, we found that upon double strand break, DAXX is

phosphorylated by the apical kinase ATM on two serine (S424 S712) and the ability of DAXX to depose H3.3 at the lesion relies on these modifications. The accumulation and maintenance of H3.3 at the damage impact on the histone post-translational modification pattern, impairing 53BP1 protein foci formation and favouring the damage to be repaired through homologous recombination. Our results highlight the important role of histones chaperones and modifications in double strand break repair and suggest a possible mechanism explaining the prediatric glioblastoma occurrence in case of H3.3 mutations.

During the last part of my PhD I focused my attention of the role of SLX4 protein in double strand break repair pathway choice. Preliminary data of our laboratory suggested an SLX4 pro-resection activity, favouring homologous recombination occurrence. Staring from these results, I analysed resection in Fanconi Anemia patient-derived cells, SLX4 null. In collaboration with Pablo Huertas' laboratory (CABIMER, Sevilla, Spain) I verified an impairment of the resection process in these cells, confirming SLX4 pro-resection role. Further analysis will be required to elucidate the molecular mechanism of SLX4 activity but these first results are very promising to shed light on a new player of the intricate network of double strand breaks repair pathway choice.

Part I

State of the art

DNA damages and genome stability maintenance.

The deoxyribonucleic acid (DNA) is the macromolecule containing all the information required for cell life. Nuclear DNA constitutes the genetic heritage of cell and, once replicated, is divided and transmitted to the subsequent generations. Maintenance and faithful inheritance of the genome are essential processes to avoid the propagation of altered information that could threat cell life and, in a multicellular organism, the health of the entire organism itself. As a matter of fact nuclear DNA integrity is constantly challenged by both chemical compounds and physical agents able to damage DNA structure and alter its sequence. Indeed, it has been estimated that each cell of our body undergoes up to 70000 DNA lesions per day, deriving from endogenous sources as by-product of the cellular oxidative metabolism, spontaneous base hydrolysis (Nussenzweig 2017), replication errors and also incorporation of ribonucleotides (Potenski & Klein 2014; Mertz et al. 2017). Moreover, from the environment also exogenous agents, like UV, viruses and drugs can threat DNA integrity (Figure 1). Among the different kind of lesions DNA can experience, double strand breaks (DSBs) are one of the most deleterious, despite being some of the less frequent (25 per cell each day) (Nussenzweig 2017). Indeed, if not correctly and immediately repaired, DSBs can lead to mutations, loss of heterozygosity, chromosome rearrangements and deletions (Cannan & Pederson 2016), globally considered index of genome instability, the main feature of cancer cells (Bakhoum & Compton 2012; Pikor et al. 2013). To face the daily challenge of DNA damage, eukaryotic cells have evolved a complex network of mechanisms, named DNA damage response (DDR), to repair DNA lesions and protect genome stability (Ciccia & Elledge 2010). Moreover if lesions are too many or severe, cells

can undergo apoptosis or premature senescence to prevent the transmission of a mutated genome to subsequent generations (Jeggo et al. 2016).

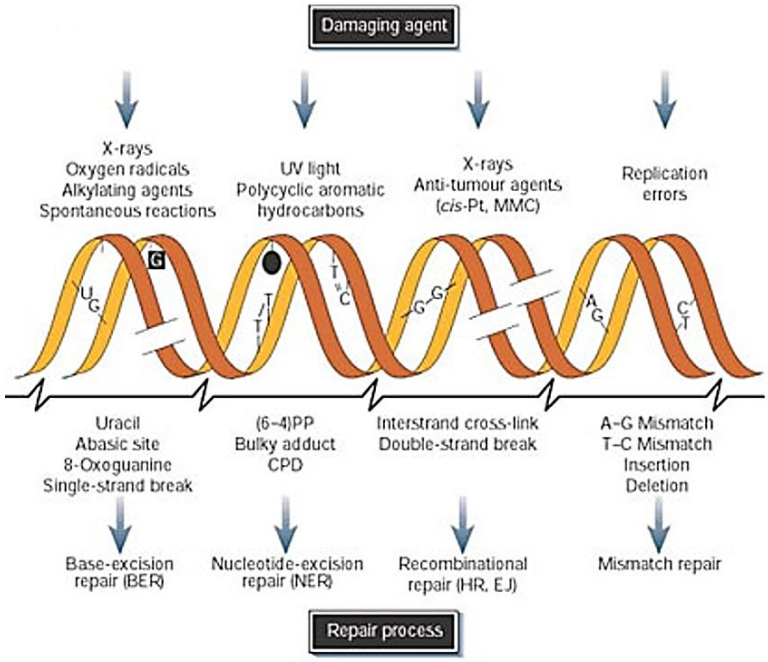

***Figure 1**: DNA damages and lesion-specific repair pathways* (modified from Hoeijmakers 2001).

The molecular response to DSBs is one of the most studied due to the dangerousness of this kind of damage. Since this response is the main focus of this PhD thesis, in the next chapters I'll extensively describe the specific events of the DDR in occurrence of DSBs.

DNA damage response.

In human cells, DDR consists in a kinase cascade triggered by the apical kinases ATM and ATR, serine/threonine kinases belonging to the phosphatidylinositol

kinase (PIKK) family, and carried out by the transducer kinases Chk1 and Chk2 that spread the signal to the thousands effectors of the DDR.

The proteins involved in this process are usually divided in: sensors and PIKKs, mediators, transducers and effectors (Sulli et al. 2012) (Figure 2).

The Sensors

The DDR cascade sensors are the proteins responsible for DNA damage detection, shared with the DNA lesion repair mechanism (see "The double-strand break repair pathways" chapter). This tight interconnection of the two processes ensure the correct and coordinated activation of the DDR network and the faithful repair of the damages. In case of DNA damage, both factors acting as sensors and the PIKK apical kinases detect the presence of a lesion and start the signal of DDR. Among the sensors currently known in human cells are included protein of the PARP family, the MRN complex, composed by Mre11-Nbs1-Rad50 (Sulli et al. 2012) and the 9-1-1 (Rad9-Rad1-Hus1) complex. The first can identify and bind single-strand DNA stretches, deriving from processing of DSBs or UV radiations, the second is loaded on DSBs ends and the 9-1-1 complex localise at the junction between double strand (dsDNA) and single strand DNA (ssDNA). The ssDNA binding protein complex, RPA, plays a relevant role in DDR triggering. The association of RPA to ssDNA leads to 9-1-1 complex recruitment. Successively, TopBP1 binds DNA damaged regions and interact with ATRIP, essential to ATR apical kinase localization and activation (Ueda et al. 2012).

The MRN complex is one of the most characterised among the DSBs sensors. Indeed, in few seconds after DSB occurrence, MRN sense it and act as a bridge keeping the ends of the lesion in close proximity. This complex favour ATM apical kinase recruitment and activation at the damage site (Paull 2015). A further branch of DDR, responsible for DSBs recognition and repair involves Ku70/80 heterodimer. It localize at the lesion, and recruits DNA-PKcs, another PIKKs

family member, that assure a rapid re-ligation of the DSBs ends (Chang et al. 2017).

The apical kinases

The serine-threonine kinases that regulates and trigger the DDR in mammals are ATM (ataxia telengectasia mutated), ATR (ataxia telengectasia rad3 related) and DNA-PKcs (DNA-dependent protein kinase catalytic subunit). The genes encoding ATM and ATR are mutated in the human genomic instability syndrome ataxia-telangiectasia and in a related syndrome, respectively. All the three kinases of the DDR belongs to the phosphatidil-inositol-3-kinase-like proteins (PIKKs) and are preferentially activated by specific kind of lesions: ATM is triggered by DSBs while ATR by ssDNA (Smith et al. 2010). ATR activation requires the binding with the ATR-interacting protein (ATRIP) and replication protein A complex (RPA). This interaction leads ATR auto-phosphorylation, that starts the targets phosphorylation wave, triggering the so called ATR-Chk1 axis (Smith et al. 2010; Acevedo et al. 2016).

The process leading to ATM activation is similar to the one described for ATR. In unperturbed condition ATM is present in the nucleus as an inactive homodimer. When a DSB occur, the ATM dimers dissociate and auto-phosphorylate on serine 1981 (S1981). Then a fraction of ATM is recruited at the lesion, thanks to the MRN complex, while the remaining subpopulation remains in the nucleoplasm (Paull 2015). Notably, the interaction between specific domains of ATM and Nbs1, component of the MRN complex, is central to ATM recruitment and retention at DSB sites.

The DNA-PKcs kinase has peculiar features and orchestrates the repair of DSB through the NHEJ pathway (see below).

The mediators

The first signalling event mediated by ATM and ATR kinases, during DDR, is the phosphorylation of the histone H2AX, on serine 139 (γH2AX) (Rogakou et al. 1998). The variant H2AX of the canonical histone H2A is already present into the chromatin in unperturbed condition and, after a DSB, it is phosphorylated by the PIKKs for megabases away from the damage site (Rogakou et al. 1999). Differently from sensors, accumulating at the lesion independently from apical kinases, the mediators of DDR localize at the damage and promote the recruitment of active PIKKs in the lesion proximity. Prominent accumulation of γH2AX and other mediators is easily detectable, through immunofluorescence and microscopy, as foci into the nucleus of damaged cells (Pilch et al. 2003).

Other main mediators of DDR are: Mdc1, 53BP1, Brca1 for ATM and TopBP1, claspin and Brca1 for ATR.

MDC1 (mediator of DNA damage checkpoint 1) specifically interacts with γH2AX and Nbs1, member of the MRN complex, at the damage where it's phosphorylated by ATM. This MDC1 modification constitutes the scaffold for the recruitment of ATM and other DDR factors binding, allowing the signal amplification. In addition MDC1 promote localization at the lesion of chromatin remodelling factors as for example RNF8 and RNF168, two ubiquitin ligases responsible for Brca1 and 53BP1 localization at the damage (Ciccia & Elledge 2011).

53BP1 protein

The tumour suppressor p53 binding protein 1 (53BP1), initially identified as a p53 interactor, is a key regulator of the DSBs repair and is characterised by a complex multidomain structure. The N-terminal portion display a sequence of 28 S/TQ sites, phosphorylated by ATM or ATR upon DNA damage, responsible for 53BP1 interaction with Rif1 and PTIP (Wu et al. 2009; Zimmermann & de Lange 2014). These two factors, together with 53BP1, inhibit Brca1 recruitment, promoting

NHEJ repair mechanism (see “The double-strand break repair pathways” chapter). The central part of 53BP1 comprises a nuclear localization signal and a tandem Tudor domain required for its localization. Indeed thanks to this domain 53BP1 can recognise the H4K20Me2 and is recruited at the damage (Hartlerode et al. 2012). Another domain essential for 53BP1 localization is an ubiquitin binding UDR motif that binds the H2AXK15Ub, induced at the vicinity of the damage thanks to the RNF168 E3 ubiquitin-ligase (Panier & Boulton 2014). Finally, at the C-terminal, 53BP1 contains a pair of BRCT (Brca1 C-terminus) domains required to heterochromatin DSBs repair. Indeed 53BP1 promotes the phosphorylation of the KRAB-associated protein 1 (KAP1) by ATM, involved in heterochromatin maintenance, enhancing its localization at the lesion and a general chromatin de-condensation, essential for an efficient repair (Noon & Goodarzi 2011).

Noteworthy, 53BP1 participates to the finely tuned process of the DNA repair pathway choice. Indeed upon DSB, 53BP1 localises at the damage where, interacting with Rif1, promotes the NHEJ pathway, blocking resection (essential step of the HR, see below) (Zimmermann et al. 2013). The activity of 53BP1 and its partner Rif1 is counterbalanced by the pro-HR activity of another mediator, Brca1, in S/G2 phase cells (Daley & Sung 2014).

Brca1 protein

The breast and ovarian cancer susceptibility gene 1 (Brca1), located on chromosome 17, encodes for the Brca1 protein and fits the so called “two hit” model for a tumour suppressor gene (King et al. 2007). According to this model a cell require two hits (mutations), in each allele of a tumour suppressor gene to undergo transformation. In hereditary cancer the first hit is a germ-line mutation while the second occurs in somatic cells of a specific tissue (Knudson 1971). Mutation in Brca1 gene account for 50% and 75% respectively of hereditary breast and ovarian cancer cases (Alli & Ford 2015). Moreover, a significant fraction of

sporadic breast and ovarian cancer displays a lower or absent Brca1 protein expression (Welcsh & King 2001).

The Brca1 protein is a 220KDa molecule containing two C-terminal BRCT domains, characteristic of cell cycle and DNA damage related protein, demonstrated to be phosphopeptide-binding motifs (Wu et al. 2015). At the N-terminal portion of Brca1 is present a RING domain responsible for Brca1 interaction with the BARD protein, mediating Brca1 E3 ubiquitin-ligase enzymatic activity (Meza et al. 1999). Brca1-BARD1 complex ubiquitination targets are, up to now, unknown. Interestingly, independently from BARD1, Brca1 has been found to form a bridge between many different transcription factors (p53, the estrogen receptor, c-Myc) and transcription machinery components or chromatin remodeller (Rosen 2013). Another Brca1-containing complex is composed by Brca1 itself and BACH1 but its function is not clear yet. It has been proposed that association of Brca1 with BACH1 is necessary to the correct progression through S-phase and replication fork stalling bypass (Cantor et al. 2001). Particularly interesting for this Thesis is the complex composed by Brca1, CtIP and the MRN hetero-trimer, which associates thanks to Brca1 interaction with phosphorylated S327 of CtIP. This complex is involved in DSBs repair pathway choice stimulating the resection of the DSB ends and committing the lesion to be repaired through homologous recombination (see below) (Polato et al. 2014; Aparicio & Gautier 2016; Isono et al. 2017). Indeed in S/G2 cell, when the HR repair can occur (see below), Brca1 protein interact with CtIP and the MRN complex (composed by Mre11, Nbs1 and Rad50 protein) favouring 53BP1 relocalization at the DSB ends periphery. These events counterbalance the 53BP1-dependent barrier allowing the first wave of resection to take place (Daley & Sung 2014). Interestingly defects in DSB-ends resection and HR observed in Brca1-deficent cells are restored by depletion of 53BP1 (Bunting et al. 2010) further sustaining the antagonistic relation between 53BP1 and Brca1. Interestingly a Brca1 role as an negative regulator of

resection has been described. In complex with Abraxas and RAP80, Brca1 is recruited at the lesion site where, thanks to interaction with the de-ubiquitinating enzyme BRCC36, limits an excessive processing of the DSB ends (Coleman & Greenberg 2011; Wang et al. 2013). In conclusion, thanks to its many interaction partners, Brca1 is a versatile protein connecting sensors and effectors of the DDR, acting as a mediator for both ATM and ATR. Moreover, interacting with phosphorylated proteins and displaying an E3 ubiquitin-ligase activity, Brca1 plays different roles in DSBs repair and cell cycle checkpoint activation (Deng 2006) as to be considered a caretaker of genome stability.

TopBP1 protein

The human DNA topoisomerase IIβ-binding protein 1 (TopBP1) is a 180KDa nuclear protein, characterised by eight BRCT domains, commonly present in DNA damage response and cell cycle regulation proteins (Wardlaw et al. 2014). TopBP1, initially identified as an interactor of DNA topoisomerase IIβ, was then discovered to modulate cell proliferation, apoptosis and DNA synthesis, regulating E2F1 transcription factor (Liu et al. 2003). Furthermore, TOPBP1 was described to monitor DNA replication and to participate to intra-S checkpoint activation (see below) (Kim et al. 2005; Jones & Petermann 2012). Indeed it was discovered to form foci co-localizing with Brca1 ones, upon hydroxyurea and ionizing radiation exposure and to interact with Rad9 (component of the 9-1-1 clamp). The binding with Rad9 favour TopBP1 recruitment at the lesion, where, in turns, it promote ATR activation (Greer et al. 2003). The exact mechanism how TopBP1 activates ATR is poorly understood but one possibility is that ATR kinase activity is triggered by conformational changes of the ATR-ATRIP complex due to TopBP1 binding (Mordes et al. 2008). The current model proposes that, after the formation of ssDNA due to the processing of a DSB (see below), the 9-1-1 complex favour both TopBP1 and ATR recruitment at the lesion and TopBP1-ATRIP interaction. This lead to a TopBP1-ATR contact and a consequent conformational change in the

kinase domain of ATR, allowing phosphorylation of its targets (Burrows & Elledge 2008; Wardlaw et al. 2014). This, combined with a putative TopBP1 role as a platform for ATR targets recruitment, makes of TopBP1 one of the major regulator of ATR activity. In addition claspin, another mediator specific for ATR, localize at the damage and favour the transducer kinase Chk1 activation (Liu et al. 2006).

The transducer kinases

Once activated by ssDNA, ATR triggers the checkpoint signal transduction cascade, phosphorylating another serine-threonine kinase, Chk1, in two residues localised in the C-terminal regulatory region of Chk1 (S317 and S345) (Walker et al. 2009). These phosphorylations increase the basal Chk1 kinase activity allowing replicative forks stabilization, cell cycle progression slowdown through checkpoint activation, repair of the damage and, ultimately, cell viability (Goto et al. 2015). Chk2 is the other transducer kinase of DDR, mainly activated by ATM through phosphorylation on T68, located in the N-terminal region. This modification leads to conformational changes in Chk2 structure, homodimerization and Chk2 auto-phosphorylation to complete the activation (Smith et al. 2010). Targets of Chk2 are Cdc25A, Cdc25C, p53, E2F-1, Brca1 and TRF2. Through the phosphorylation of these proteins Chk2 regulates cell cycle progression, DNA repair, premature senescence and apoptosis. Interestingly, several proteins phosphorylated by Chk2 are also ATM targets, including KAP1, Brca1 and 2 and p53, suggesting an ATM signalling reinforce and modulation role of Chk2 (Zannini et al. 2014).

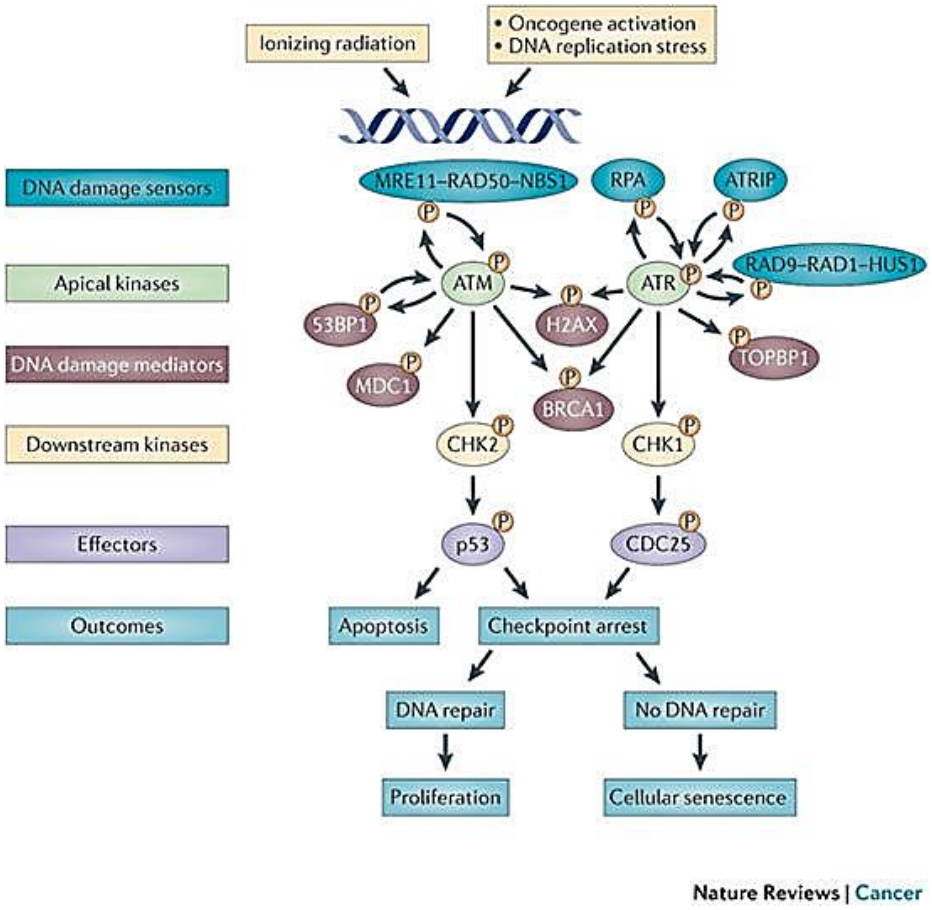

Figure 2: *The DNA damage response cascade (Sulli et al. 2012).*

The cell cycle and checkpoints

A fine tuned crosstalk of DNA damage response and cell cycle regulation is an essential condition for the correct progression of events necessary to face and repair the DNA damages. Therefore in this section of the Thesis I'm briefly discussing cell cycle regulation and checkpoints activation.

The cell cycle

The cell cycle is the life path leading a cell to replicate the genome and equally divide it among daughter cells. It consists in a sequence of finely regulated events

divisible in four phases: G1, S, G2 and M. In addition there is also a fifth phase called G0, defined as a non-dividing state from which cells can exit whether exposed to growth stimuli (Cheung & Rando 2013). Each of these steps is characterised by specific activities and factors leading to cell growth, DNA replication (synthesis), DNA segregation into daughter cells and their physical separation. On the correct sequence of cell cycle events rely the ability of cells to faithfully replicate and equally divide the chromosomes among the daughter cells (Satyanarayana & Kaldis 2009). Thus, fine regulation of cell cycle progression is of pivotal importance.

The master regulators of the cell cycle are the cyclin-dependent kinases (CDKs), proteins belonging to the serine-threonine kinases family, highly conserved among all eukaryotes. CDKs are small proteins (34-40kDa) which activity depends on the binding with activator factors: the cyclins (Satyanarayana & Kaldis 2009). In mammals four CDKs are responsible for cell cycle regulation: CDK4 and 6 controlling G1 phase, CDK2 involved both in G1/S transition and S phase and CDK1 controlling M phase. Cyclins expression levels, as suggested by the name, fluctuate during the cell cycle. The activation of a specific CDK in a precise phase depends on the fine tuning of cyclins synthesis and degradation.

The cyclins expressed in human cells are:

- In G1 phase: cyclin D, required for CDK4/6 activation
- During G1/S transition: cyclin E, binding partner of CDK2, is produced in G1, peaks in G1/S transition and is progressively degraded in S.
- In S phase: cyclin A, responsible for CDK1 and 2 activation, starts to be produced together with cyclin E in G1 but reach the maximum level of expression in G2 phase.

- In M phase: cyclin B, interacts with CDK1, produced in S phase and, once accomplished its function during M phase, is rapidly degraded (Malumbres & Barbacid 2009).

However CDK interaction with the specific cyclin is a necessary but not sufficient event to trigger the kinase activity of the CDKs that undergo to multiple regulation levels: post-translational modification, inhibitors association and ubiquitin-dependent degradation (Reinhardt & Yaffe 2013; Lim & Kaldis 2013; Sullivan & Morgan 2007).

The great majority of human cells, in physiological condition, are in G0 but when exposed to grow factors can restart the cell cycle progression from G1 phase. Due to the activity of mitotic factors cyclin D transcription increases and activates the CDK4/6 which in turn phosphorylates pRb. This event disenganges the transcription factor E2F permitting the expression of its target genes, required for G1/S transition, as cyclin A and E (Dick & Rubin 2013). The consequent accumulation of cyclin E activates CDK2 and enhances cyclin A expression inducing the formation of the pre-replication complex on the replication origins. During S phase, DNA has to be faithfully replicated: this process starts in specific DNA loci, called replication origins. To ensure the correct origin firing, the crosstalk of the DNA replication proteins with CDKs and cell cycle regulation mechanisms is extremely important (Wu et al. 2014). During the S phase cyclin B accumulates in the cytoplasm, in G2 phase translocates to the nucleus and, binding CDK1, leads the cell toward G2/M transition. During M phase, the E3-ubiquitin ligase APC promotes securins degradation, essential to for sister chromatid segregation. Then cyclin A and B degradation allow the exit from M phase. Finally, cytokinesis, the physical separation of the two daughter cells, can occur (Sullivan & Morgan 2007; Manchado et al. 2010).

Cell cycle checkpoints

In physiological conditions, cell cycle is characterised by the presence of specific regulation steps that prevent the entrance in the next phase if all passages required for the previous one haven't been completed. These steps are called cell cycle checkpoints and in human cells there are three: the G1/S checkpoint and the G2/M, regulating the transition respectively from G1 to S and from G2 to M, and the intra S checkpoint, monitoring the correct DNA replication. A forth checkpoint regulate the transition from metaphase to anaphase, during mitosis. DNA damages can activate a transient arrest at the checkpoint of the phase in which the lesion has occurred, thus blocking cell cycle progression (Houtgraaf et al. 2006).

Checkpoint G1/S

When a DSB occur in G1, a cell can activate two different mechanisms both blocking G1/S transition: the first involves Cdc25A, a phosphatase responsible for CDK activation, and the second, slower than the previous, requiring $p21^{Waf1}$ transcription. The first can be triggered by both ATM-Chk2 and ATR-Chk1 pathways and results in phosphorylation of Cdc25A and in its consequent degradation. Since Cdc25A is required for CDK2-cyclin E activation, this blocks the G1/S transition. However the pathway considered of primary importance for G1/S checkpoint is the one involving $p21^{Waf1}$, an inhibitor of CDK4/6-cyclin D and CDK2-cyclin E complexes. This process is slower that the previous requiring transcription and accumulation of proteins to arrest cell cycle. In this case the DNA damage checkpoint promotes $p21^{Waf1}$ expression through stabilization of p53, an oncosuppressor mutated in 50% of human cancer and regulating transcription of many factors necessary for DDR, apoptosis and senescence. As a consequence, $p21^{Waf1}$ promotes cell cycle arrest (Bouwman & Jonkers 2012).

Checkpoint G2/M

The control mechanism inhibiting the mitotic entry of damaged cells is the G2/M checkpoint. It's triggered by the ATM-Chk2 signalling that can act, as described for the G1/S checkpoint, through both a fast and a slow processes. (Löbrich & Jeggo 2007). The first mechanism consists in the inhibition of CDK1-cyclin B complex and Cdc25C translocation into the cytoplasm, both mediated by Chk2. While the second process requires p53 accumulation and $p21^{Waf1}$ transcription, inhibiting cell cycle progression (Smith et al. 2010).

Checkpoint intra-S

Whether a DNA damage occurs during S phase, replication forks, encountering a lesion, take part to the damage recognition process and the ssDNA, coated by RPA, induces the recruitment of all the factors required for checkpoint activation. The intra-S checkpoint relies mainly on ATR activity, that localise at the damage interacting with the previously described mediator TopBP1 (Acevedo et al. 2016; Iyer & Rhind 2017) avoiding new origins firing, and triggering the transducer kinase Chk1. As a consequence, Chk1 phosphorylates a plethora of targets involved in replication forks stabilization and DNA damage repair (Houtgraaf et al. 2006)

DNA repair

The repair of DNA damages involves a huge amount of enzymes that, coordinating their activity, chemically modify the structure of the DNA double helix. The activity of each protein has to be carefully regulated since an improper activation or localization can threat genome integrity and stability.

Cells can rely on many machineries specific for the different kind of lesions, conventionally divided in four classes:

- Excision repair pathway, takes advantage of the undamaged strand of DNA to accomplish repair. Classified as:
    - MMR (mismatch repair), specific for un-correct base pair (Li 2008)
    - BER (base excision repair), repairs chemical bases alterations (Krokan & Bjoras 2013)
    - NER (nucleotide excision repair), specific for bulky adduct lesion, like pyrimidine dimers produced by UV exposition, that distort the DNA helix structure (Schärer 2013)
- ICL (inter-strand crosslinking) repair pathway, also known as the Fanconi Anemia pathway, is required in case of inter-strand crosslinking during S phase (Williams et al. 2013)
- DSB (double strand breaks) repair pathway relying on two mechanisms:
    - HDR (homologous direct repair) also known as HR (homologous recombination), requires the presence of the homology sequence on the sister chromatid that is used as a template to repair the lesion. For this reason is the preferred pathway in case of DSBs in late S and G2 phases of the cell cycle. Moreover, being considered error free, it is the preferentially used mechanism to repair euchromatin lesions (Brandsma & Gent 2012b).
    - NHEJ (non-homologous end joining) that re-join the DSB ends with no need of the homologous sequence. Whether the lesion display modified bases or overhanging edges, the repair by NHEJ requires a nucleolitic processing of the ends that makes this process considered error prone. This kind of repair is the largely predominant pathway in human cells, used in all the phases of the cell cycle and both in heterochrmatin and euchromatin (Shibata 2017)
- SSB (single strand break) repair, require mechanisms still poorly understood (Caldecott 2008).

The double strand break repair.

The DSBs are one of the most dangerous lesions for the cells. Indeed if not correctly and immediately repaired, DSBs can lead to mutations and chromosome aberrations, compromising genome stability. Thus eukaryotic cells evolved several mechanisms to efficiently and faithfully repair DSBs, among which the main are HR and NHEJ (Ciccia & Elledge 2010).

Non-homologous end joining (NHEJ).

This pathway is triggered by the recruitment of the Ku complex at the DSB ends. It consists in a hetero-dimer of the Ku70 and Ku80 proteins forming a ring structure essential to keep the tethering of the DSB ends. The Ku complex favours DNA-PK, one of the apical kinases of the DDR, activation and localization at the lesion, stabilizing and preventing the DSB end resection. Then, the recruitment on the damage of the Artemis protein catalyses the DSB end processing and the intervention of the complex formed by XRCC4 and LIG4, responsible for end re-ligation (Chang et al. 2017). The Artemis-dependent end processing can cause insertion or deletion of some nucleotides, provoking mutations, for this reason NHEJ mechanism is considered error prone but it is still the most frequent pathway in human cells: 70% of the total DSBs are repaired through NHEJ (Shibata 2017).

The homologous recombination (HR).

The HR is a multi-step process requiring the sister chromatid presence to accomplish the repair. This confines HR mechanism in late S and G2 phases of the mitotic cell cycle but, since it exploits the homologous sequence as a template for the repair, this pathway is considered “error-free” (Brandsma & Gent 2012b).

When a cell undergoes DSBs the MRN complex localizes at the lesion favouring, thanks to Nbs1 activity, ATM recruitment and auto-phosphorylation on S1981. From these moment ATM is active and phosphorylates histone H2AX on S139 for megabases from the DBS (Rogakou et al. 1999; Paull 2015). This modification is

essential for the subsequent recruitment of HR factors. Meanwhile Mre11, component of the MRN complex, interacting with Brca1, starts the first wave of resection, called “short-range resection” (Stracker & Petrini 2011). The resection step consists in a nucleolitic degradation of the 5’ strand of the DSB to generate a 3’ ssDNA filament. This process is considered the crucial step committing a DSB towards HR. Indeed once it has occurred the NHEJ pathway cannot be used anymore to repair the lesion (Mimitou & Symington 2011). For these reason a fine tuning of the mechanisms regulating the DNA repair pathway choice is of pivotal importance for cells and will be the next paragraph topic. Conventionally resection is divided in two different but sequential “waves”, the first is Mre11-dependent, while the second, called “long-range resection”, performed by the nuclease EXO1, the BLM helicase and DNA2 nuclease complex that extends the 3’ protruding ssDNA tail length (Mimitou & Symington 2011) (Figure 3).

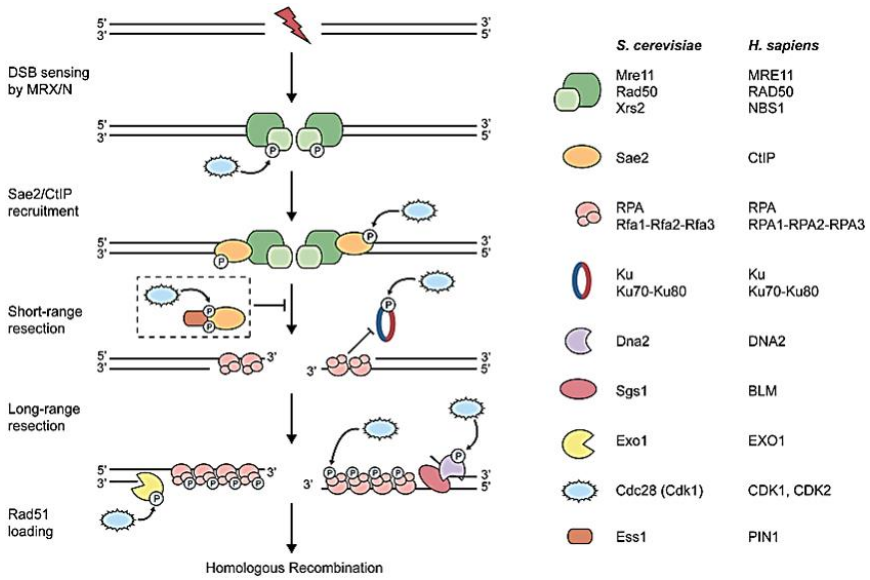

Figure 3: *The resection process (Ferretti et al. 2013).*

The formation of ssDNA filament lead to recruitment of the RPA complex, phosphorylated by DNAPK on S4 and S8 (Ashley et al. 2014), and then replaced by the recombinase Rad51 loaded by the Brca2 protein (Ma et al. 2017). Rad51 forms nucleofilament on the 3' protruding tail, deriving from the resection, and is responsible for search and invasion of the homologous sequence on the sister chromatid. This process generates the so called D-loop structure (Krejci et al. 2012) (Figure 4). In this context DNA-polymerases elongate the 3' end of the invading strand, forming a particular structure, the double Holliday Junction (dHJ), that can be resolved by different proteins: the dissolvase BLM/TOPOIII complex and the resolvases GEN1, MUS81 and SLX1/SLX4. In both cases the normal double helix structure of the DNA is restored but, while in case of dissolution the repair generates a non crossover product, in case of resolution the repair product could display both crossover or non-crossover (Matos & West 2014). Noteworthy, all these mechanisms take place in a specific chromatin context. Indeed the regions flanking the resected DNA display both pre-existing histone marks and DDR-induced histones post-translational modifications (PTMs). (Miller & Jackson 2012).

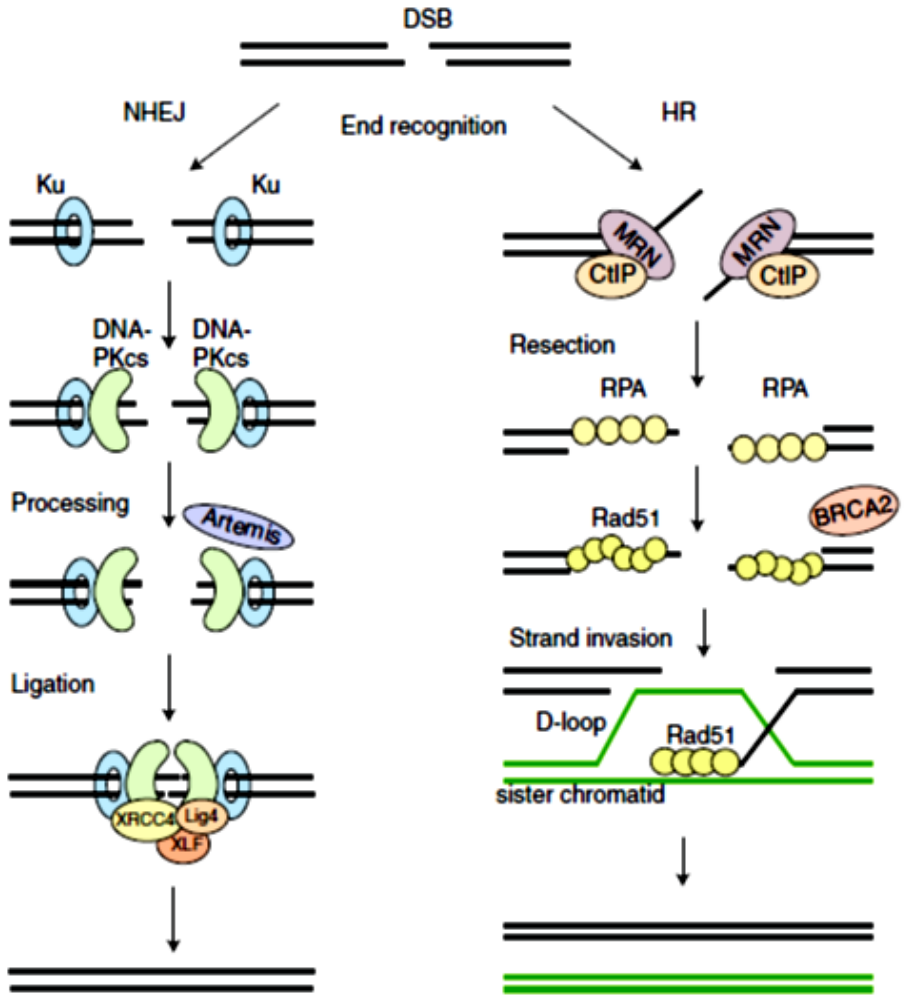

Figure 4: *The two major DSBs repair pathways in human cells, NHEJ and HR* (Brandsma & Gent 2012).

DNA repair pathway choice: a cell cycle and chromatin based decision.

As previously mentioned, both HR and NHEJ are preferentially used in specific moments of the cell cycle. The HR, requiring the presence of an homology sequence on the identical sister chromatid, can correctly take place only after DNA replication (S/G2 cell cycle phases). Indeed, unscheduled HR occurring in G1, when only the homologous chromosome is available, leads to loss of

heterozygosity. Moreover, strand invasion between two DNA molecules bearing non identical homologous sequences (due to possible point or silent mutations) can generate mismatches, translocation and copy number changes, leading to genetic modification of the recipient molecule (Chapman et al. 2012; Le Guen et al. 2015). On the other hand, NHEJ is considered an error-prone pathway since it is accurate only with fully complementary DSB ends. Indeed, in case the ends of the damage are chemically altered, it's required a mild processing, a "cleaning" step, before the relegation (Le Guen et al. 2015). The activity of the Artemis nuclease, involved in this process, can lead to the loss of some bases making of NHEJ an error prone pathway (Yang et al. 2016). Moreover, as previously described, resection is an irreversible process that commits a DSB to be repaired trough HR (Symington & Gautier 2011). Thus fine regulation of the choice among NHEJ and HR pathways acquires a fundamental importance for the maintenance of genome stability. The current hypothesis is that the choice is governed by the interplay between 53BP1 and Brca1 acting in concert with cell cycle regulators and a specific chromatin context (Daley & Sung 2014; Escribano-Díaz et al. 2013; Clouaire & Legube 2015).

When a DSB occurs the 53BP1 protein, one of the DDR mediator and anti-resection factors, localizes at the lesion and, thanks to the ATM-dependent phosphorylation on S25 and S29, interacts with Rif1 blocking Brca1 localization at the damage (Harding et al. 2011). Since Brca1 is responsible for 53BP1 repositioning at the periphery of the DSB region, a Brca1 impaired recruitment promotes 53BP1 localization at the lesion and, interacting with Rif1, resection inhibition due to the 53BP1-dependent barrier effect. These events, blocking the extensive processing of the damage ends, lead to repair the DSB with NHEJ pathway that can take place in all the phases of the cell cycle. (Kakarougkas & Jeggo 2014). However, when a DSB occur in late S or G2 phase this mechanism is counteracted by the CDK1-cyclinB-dependent phosphorylation of CtIP on S327

and T847 (responsible respectively for CtIP interaction with Brca1 and CtIP enzymatic activity) (Yu & Chen 2004; Huertas & Jackson 2009). These events favour both CtIP association with Brca1 and inhibition of Rif1 interaction with 53BP1, promoting resection (Escribano-Díaz et al. 2013). Thanks to a finely regulated balance of these mechanisms, HR is favoured in late S and G2 phases of the cell cycle (Figure 5A). In human cells, NHEJ is the most frequent pathway despite of being error prone while HR is used to repair 60% of late S/G2 phases DSBs (Shibata et al. 2011). For thus DNA repair pathway choice cannot only rely on cell cycle regulation to maintain these balance: a pivotal role is played by chromatin compaction status and histone PTMs.

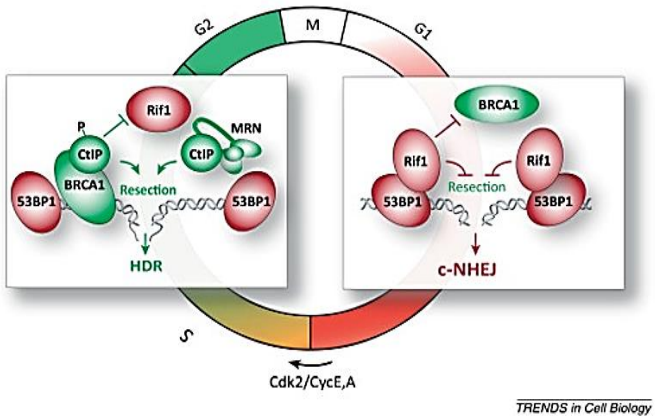

Figure 5A: *DSBs repair pathway choice, a cell cycle based decision.*

In eukaryotes, DNA associates with various proteins forming the chromatin, a highly regulated and dynamic structure whose homeostasis depends on different mechanisms: histones PTMs, DNA methylation, nucleosome density and histone variants incorporation. Classically chromatin is classified as: euchromatin composed by accessible DNA and associated proteins and heterochromatin

characterised by a more compact DNA status. Specific combinations of histones PTMs characterize different genomic regions (as enhancers, promoters, transposons) and their regulatory state (actively transcribed, poised and silenced genes) finely tuning all the DNA metabolism processes (Thompson et al. 2013). Recently, it has been supposed that the pre-existent chromatin structure plays an important role in the DNA repair pathway choice. Depending on where in the genome the lesion occurs, thanks to the histone PTMs code, the DSB is repaired through NHEJ or HR (Clouaire & Legube 2015). This would allow the cell to choose the most suitable mechanism taking in account not only cell cycle phases but also chromatin context, making of the PTMs pattern a pathway choice regulator. For example, in euchromatin, H4K16 acetylation and H3K36Me3, due to SETD2 methyltransferase marking actively transcribed genes, is a binding platform for protein involved in repair pathway balancing. Indeed the pro-resection factor CtIP, upon DSB, is recruited at the lesion via H3K36Me3 recognition while H4K16 acetylation, performed by Tip60 upon damage, inhibits 53BP1 positioning at the lesion, allowing Brca1 recruitment and HR (Hsiao & Mizzen 2013; Pfister et al. 2014) (Figure 5B).

On the other hand in heterochromatin, characterised by H3K9Me3 presence and a high nucleosome density, a DSB triggers three major early events:

1) an ATM-dependent chromatin relaxation relying on phosphorylation of KAP1 (KRAB-domain associated protein 1) that rapidly diffuse throughout the chromatin. This favour detachment of HP1 (heterochromatin protein 1) from H3K9Me3. Being HP1-H3K9Me3 interaction responsible for the maintenance of a compact chromatin status, the axis ATM-KAP1-HP1 leads to a DNA damage dependent chromatin relaxation, facilitating the repair (Ziv et al. 2006) (Figure 5B).

2) the subsequent unmasking of H4K20Me2 and H2AK15Ub, both recruiting 53BP1, leading to a further chromatin relaxation (Figure 5B)

3) replacement of H2A with the histone variant H2A.Z, blocking the CtIP-MRN mediated resection (Price & Andrea 2014).

Taken together these events potentially can favour both HR, since this repair system requires a more “open” chromatin status, but also NHEJ, which is promoted by 53BP1 binding to the newly exposed H4 and H2A modifications (Jacquet et al. 2016). In general, DSBs occurring in euchromatin are repaired trough HR. On the other hand, when a DSB occur in the heterochromatin the DDR could promote a chromatin opening, during S/G2 phases, favouring HR or, in G1 phase, induce NHEJ for which an extensive chromatin opening is not required. A growing number of proteins and chromatin remodelling factors are recognised to be involved in DNA damage response and the “chromatin-based DSB repair pathway choice” model, integrating the cell cycle dependent regulation, constitute a further layer of control of this mechanism (Dabin et al. 2017). This underlines both the importance of a perfect modulation of the repair pathway choice and chromatin signalling versatility in genome stability maintenance.

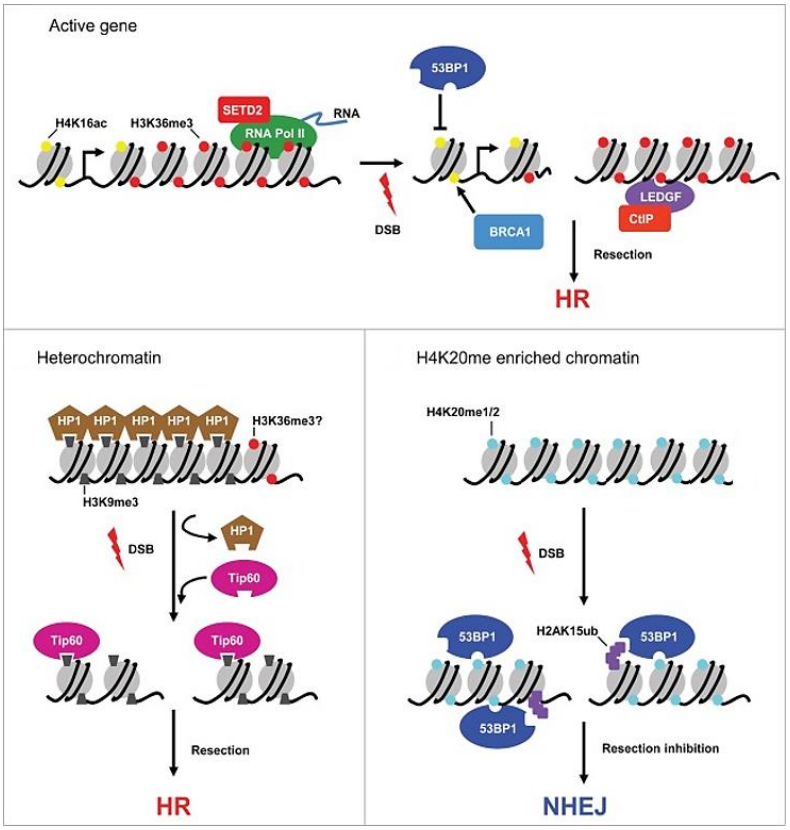

***Figure 5B**: DSBs repair pathway choice, a chromatin based decision* (Clouaire & Legube 2015).

The histone variant H3.3

Histones are small (17KDa), basic proteins fundamental for chromatin structure organization. Eukaryotic DNA is wrapped for 147 base pairs around the nucleosome, an octamer composed by two copies of histones H2A, H2B, H3 and H4, while H1 histone connects two contiguous nucleosomes. Histones are responsible for chromatin compaction status and regulate chromatin dynamics through PTMs or substitution of canonical histone with histone variants (Sarma & Reinberg 2005). Indeed, both these mechanisms modulate the density and accessibility of the chromatin to transcription and/or repair factors. Histone variants are highly similar isoforms of canonical histones that, in the last years, are gaining a pivotal role in transcription regulation, chromatin compaction modulation and, main topic of this Thesis, DNA damage response and repair (Sarma & Reinberg 2005; Biterge & Schneider 2014). While canonical histone expression peaks during S-phase and incorporation into the chromatin occurs in a DNA replication dependent-manner, histone variants are expressed and deposed during the whole cell cycle, independently from DNA replication. The canonical histone genes are organised in cluster, don't display introns and the mRNA, without the poli-A tail, is characterised by a stem-loop structure regulating the translation. On the contrary, histone variants are coded by genes composed by both exons and introns and once transcribed the mRNA are poli-adenylated (Biterge & Schneider 2014). Due to a different aminoacidic sequence, the replacement of a canonical histone with a variant modify reciprocal interactions into the nucleosome and with other proteins regulate chromatin compaction status, stability of the nucleosome itself and all DNA metabolic processes. An emblematic example of histone variants involved in DDR is constituted by H2AX, phosphorylated in an ATM-dependent manner upon DSBs, considered one of the triggering signals of the DDR (Rogakou et al. 1998), and by the enrichment of the H2AZ at the DSB region that promotes both chromatin decondensation and NHEJ repair pathway (Xu et al. 2012). Of great

interest for my PhD project is the fact that recent studies are underlying a possible involvement of the histone variant H3.3 in DNA damage response and repair (Adam et al. 2013; Luijsterburg et al. 2016). For these reason in the next sections I'm extensively presenting both H3.3 and its specific chaperon DAXX.

The histone H3.3 is a variant of the canonical histone H3.1, conserved from yeast to human. At the protein sequence level, H3.3 differs from H3.1 just for 5 amino acids, but this is sufficient to show a different PTMs pattern than H3.1 (Szenker et al. 2011) (Figure 6). In the recent years the histone variant H3.3 has been reported to play a multifaceted role in chromatin compaction and transcription regulation. Indeed it has been reported that tri-methylation of H3.3 on lysine 9 decorates telomeric regions and contribute to the silencing of transposable endogenous retroviral elements in embryonic stem cells (Udugama et al. 2015; Elsässer et al. 2015) suggesting a role in the maintenance of repressed heterochromatin. In contrast with this hypothesis, recently has been found that H3.3K36Me3 is enriched at bodies of actively transcribed genes where it favours transcription elongation and it is specifically recognised by the oncosuppressor ZMYND11 (Wen et al. 2014). Moreover other studies have detected H3.3 enrichment at promoters, transcription start sites and regulatory elements in both embryonic stem and differentiated mammalian cells (Daury et al. 2006; Goldberg et al. 2010; Chen et al. 2013; Deaton et al. 2016)). Taken together these findings suggest a double role of H3.3 in transcription and chromatin compaction regulation (Goldberg et al. 2010).

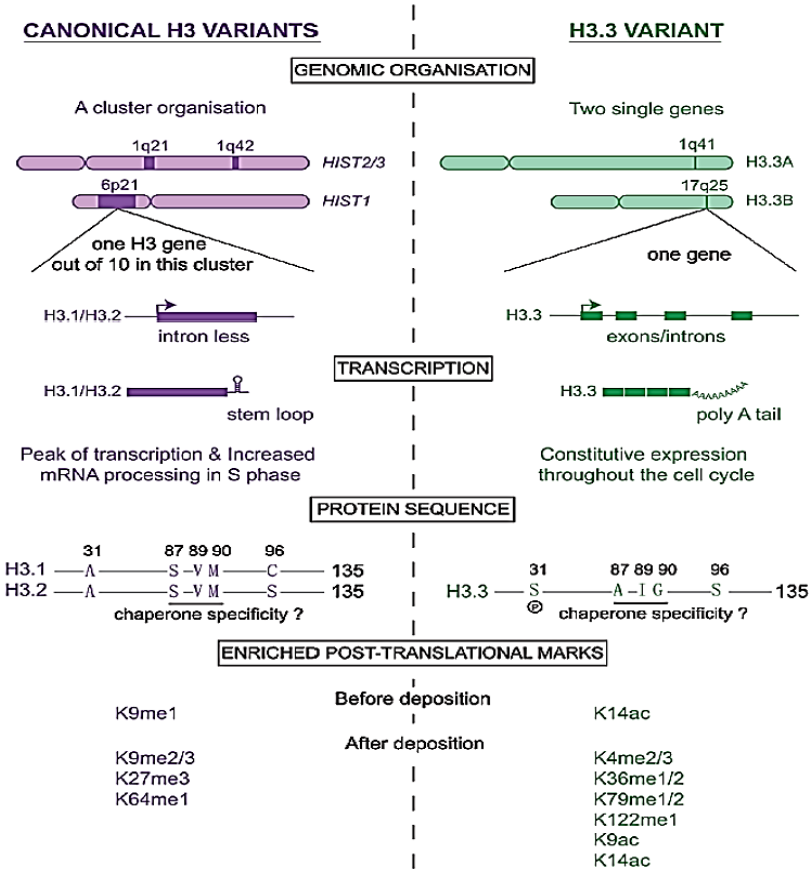

Figure 6: *The canonical histone H3.1 vs the histone variant H3.3* (Szenker et al. 2011).

The deposition of an histone inside a nucleosome requires the presence of a chaperon protein: the two most studied chaperon proteins for H3.3 deposition are HIRA and DAXX.

HIRA (histone regulator A) was initially involved in the replication independent deposition of H3.3 at promoters and bodies of actively transcribed genes (Goldberg et al. 2010). Then, it has been reported that Cabin and UBN1 human protein co-purify with H3.3 and HIRA forming a complex also present in yeast, known as His (Szenker et al. 2011). Interestingly, HIRA depose H3.3 in UV damaged region of

actively transcribed genes to prime transcription restart after the repair, suggesting an involvement of this histone variant in DNA damage repair process (Adam et al. 2013). DAXX is the other most studied H3.3 chaperon. DAXX can interact with H3.3 in complex with ATRX that seems to guide the deposition at specific heterochromatin regions (Goldberg et al. 2010; Dunleavy et al. 2011). Indeed while DAXX-ATRX interaction is dispensable for deposing H3.3 in actively transcribed genes bodies and promoters, it is required to enrich H3.3 presence at telomeric and peri-centromeric regions (Lewis et al. 2010) (Figure 7). In this context, it is not clear yet whether H3.3 deposition promotes an open chromatin status, favouring transcription, or chromatin compaction and transcription repression.

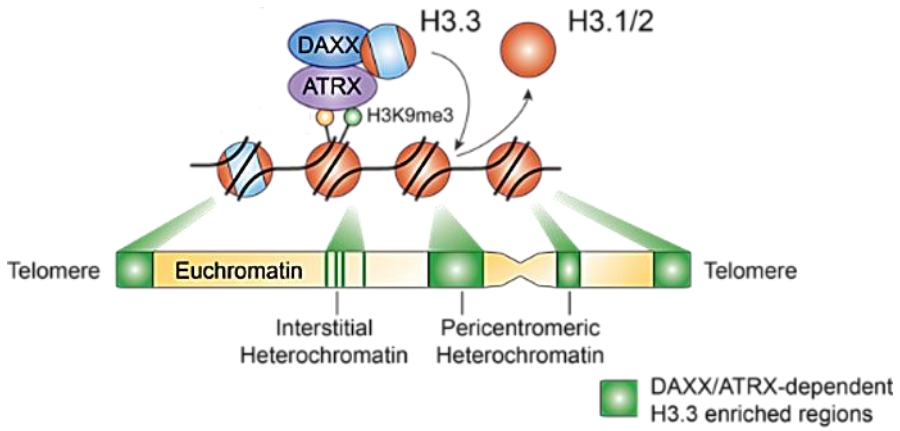

Figure 7: *H3.3 deposition by the DAXX-ATRX complex (modified Banaszynski group website).*

Particularly interesting for the topic of this Thesis is the fact that in 2013 it has been demonstrated that H3.3 is deposed at the DSB promoting HR repair pathway (Yang et al. 2013). Moreover, as previously mentioned, one year later, modified H3.3K36Me3 was reported to be involved in transcription elongation and to be specifically bound by the oncosuppressor ZMYND11 (Wen et al. 2014). Since H3K36Me3 is one of the histone PTMs involved in DSBs repair pathway choice in euchromatin, where it favours HR occurrence, this result could suggest a crucial

role of H3.3 and its modification in the repair pathway choice. In contrast with these hypothesis, recently, it has been demonstrated that H3.3 deposition at the DSB, by the histone chaperone CHD2, favour an open chromatin status and NHEJ repair pathway (Luijsterburg et al. 2016). Considering this scenario, the elucidation of H3.3 role in the DSB repair requires further analysis but could possibly shed light on H3.3 participation to the genome stability mechanisms.

DAXX protein

Death-associated protein 6 (DAXX) is an 80KDa nuclear protein, highly post-translationally modified but poorly structurally characterised. The known domains are:

- A PAH domain (paired amphipatic helix) (Hollenbach et al. 1999) also called DHB (DAXX helix bundle), (Escobar-Cabrera et al. 2010) responsible for interaction with MDM2 and HAUSP proteins
- An acidic rich region required for DAXX-H3.3 interaction (Elsässer et al. 2012)
- A C-terminal domain containing a S/T/Q rich portion and a SUMO interacting motif (SIM). Both these domains are important for DAXX interaction with PML and the consequent localization in PML-Nuclear Bodies (Lin et al. 2006) (Figure 8).

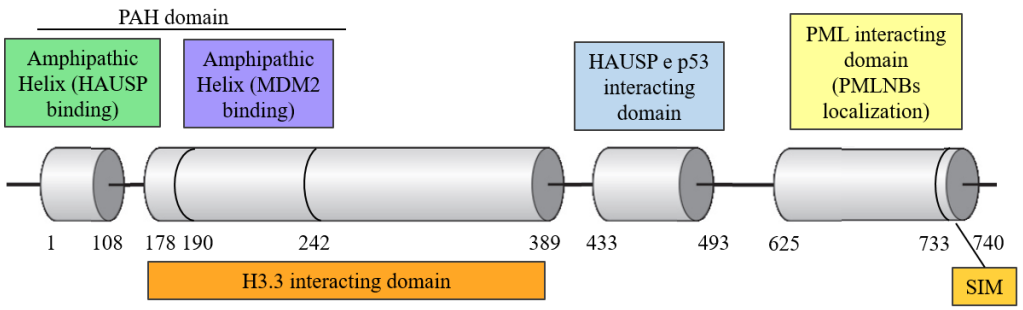

Figure 8: *DAXX protein domains.*

Initially DAXX was identified as a cytoplasmic protein interacting with the Fas death receptor and involved in the JNK (JUN N-terminal kinase) pathway (Yang et al. 1997). Successively, it has been demonstrated that DAXX is localised in the nucleus where it interacts with some nuclear sub-structures as the PML-Nuclear Bodies (PML-NBs) and with a high number of protein involved in many nuclear processes (Tang et al. 2004). The PML-NBs are clustered structures, composed mainly by the PML protein (promyelocytic leukemia protein), in which localise a growing number of factors. Noteworthy, it has become clear that many DDR proteins temporary are recruited in PML-NBs as: Chk2, p53, Nbs1, Mre11, Brca1, Rad52 and more (Guo et al. 2000; Carbone et al. 2002; Bernardi & Pandolfi 2007). The role of these structures in the DDR is further underlined by the fact that, upon DNA damage, the number of PML-NBs and their contacts with chromatin increase, particularly in the damaged region. An hypothesis about PML-NBs role is that they constitute a storage structure to accumulate proteins to impair or favour their activity/interaction (Mao et al. 2011). The DAXX interaction with PML relies on DAXX SUMO interacting motif (SIM) that mediates the contact with SUMOylated PML, present in the Nuclear Bodies (Lin et al. 2006).

Moreover, DAXX has been involved in transcription regulation of multiple genes required for muscle development (Salsman et al. 2017) , immune response (Yao et al. 2014), viral infection (Khaiboullina et al. 2013) and tissue homeostasis (Sakaue et al. 2017). The DAXX role in transcription modulation is further sustained by interaction with multiple chromatin modifiers as HDAC2 (Hollenbach et al. 2002) and Dnmt1 (Puto & Reed 2008).

In the last five years new functions are emerging for DAXX. Indeed, DAXX has been identified to be phosphorylated by the apical kinases ATR and ATM upon damage induction (Stokes et al. 2007; Matsuoka et al. 2007), suggesting a possible

involvement of DAXX in DDR. This hypothesis is further sustained by the finding that DAXX is a regulator of p53 stability upon DNA damage, acting in complex with MDM2 and HAUSP (Zhao et al. 2004; Song et al. 2008; Tang et al. 2013). In unperturbed condition, DAXX is bound to both MDM2 and HAUSP. This create a bridge allowing HAUSP, a de-ubiquitinase, to remove the basal auto-ubiquitination of MDM2, thus stabilizing MDM2 and promoting p53 degradation. In case of DNA damage, ATM phosphorylates DAXX on S564 disrupting the bridge through MDM2-HAUSP dissociation. As a consequence, HAUSP does not remove the auto-ubiquitination of MDM2 that is rapidly degraded and p53 can accumulate and accomplish its transcriptional and pro-apoptotic function (Tang et al. 2013). Interestingly, this DAXX role has been recently disputed (Brazina et al. 2015).

Recent studies pointed out a new role of DAXX: it is involved in chromatin remodelling processes, not only thanks to interaction with chromatin remodelling factors, but since DAXX has been found to be a specific chaperon of the histone H3.3 (Lewis et al. 2010). DAXX is able to depose H3.3 in peri-centromeric and telomeric regions, interacting with the helicase ATRX (α-thalassemia mental retardation X-linked protein), a 280KDa protein member of the chromatin remodeller family SWI/SNF2 (Udugama et al. 2015). As previously mentioned, the complex DAXX-H3.3ATRX deposes H3.3 in heterochromatin regions, probably thanks to DAXX interaction with histone PTMs or G rich DNA regions (Goldberg et al. 2010). While in an ATRX-independent manner, DAXX deposes H3.3 at regulatory elements of some genes, modulating transcription (Lewis et al. 2010). Up to now, it has not been clarified if DAXX deposition of H3.3 is a mechanism of transcription regulation or it possess other structural roles that can be influenced by other cellular processes, such as DDR.

Inter-strand crosslinking and the Fanconi Anemia pathway

Among the 70000 DNA damages a cell can undergo every day, approximately ten are ICLs, covalent binding of the leading and lagging DNA strands (Grillari et al. 2007). This kind of lesion is particularly deleterious since it blocks any DNA metabolism process, provoking the stall of both replication and transcription forks. In non S-phase cells the NER (nucleotide excision repair, see DNA repair section) pathway is responsible for the ICLs repair, in which the XPF/ERCC4 nuclease has an essential role . On the other hand, in case of ICLs occurring in S phase, eukaryotic cells rely on the Fanconi Anemia (FA) pathway for the repair. It consists in subsequent steps, involving proteins of the Fanconi Anemia complementation groups, that allow the cleavage of crosslinked DNA portion and, through an HR based process, the reconstitution of the two DNA strands (Williams et al. 2013). The 20 FA proteins identified to date, have been conventionally divided in three groups basing on their principal function in the FA pathway: core complex components, D2-I heterodimer and HR factors (Anderson T Wang & Smogorzewska 2015). When an ICL occurs during S phase and a fork collide on it, the helicase FANCM localize at the damage and, upon ATR activation, promote both the replisome machinery disassembly and core complex members recruitment (FANCA, FANCB, FANCC, FANCE, FANCF, FANCG and FANCL). The core complex, thanks to the E3 ubiquitin-ligase enzymatic activity of FANCL, ubiquitinates FANCD2 and promote its interaction with FANCI, forming the D2-I heterodimer (Williams et al. 2013). FANCD2-I complex favors SLX4 localization at the lesion where, interacting with XPF (FANCQ), unhooks the ICL, generating a DSB and a portion of ssDNA (Klein Douwel et al. 2014). The gap of ssDNA is refilled by translesion synthesis polimerases (TLS) as Polζ, while the DSB undergoes repair through the HR process (Anderson T. Wang & Smogorzewska 2015) (Figure 9). Indeed, FANCD2, interacting with the acetyl-transferase Tip60, promote H4K16Ac accumulation (Renaud et al. 2015). This histone modification is

known to counteract 53BP1 recognition of H4K20Me2, limiting 53BP1 recruitment at the lesion and interaction with Rif1, favoring resection and HR (Hartlerode et al. 2012). Interestingly, it has been reported that NHEJ impairment, through downregulation of Ku70 or inhibition of DNA-PK, result in partial rescue of mitomycin (MMC) sensitivity of FANCA mutated cells, underlying the essential role of NHEJ/HR balance in ICLs repair (Adamo et al. 2010). In these scenario, ICLs and DSBs repair are tightly interconnected mechanisms as they share regulation mechanisms and factors of pivotal importance for DNA repair like Brca2 (FANCD1) and Brca1 (FANCS), Rad51 (FANCO) and SLX4 (FANCP). Indeed SLX4, recruited at the lesion through interaction with ubiquitinanted FANCD2 (Yamamoto et al. 2011), is involved in two steps of the FA pathway: the unhooking of the ICL, requiring SLX4 interaction with XPF (FANCQ) and SLX1 nucleases, and the dHJ resolution, final part of the HR step, that allows the restoration of the two DNA strands (Yamamoto et al. 2011; Klein Douwel et al. 2014).

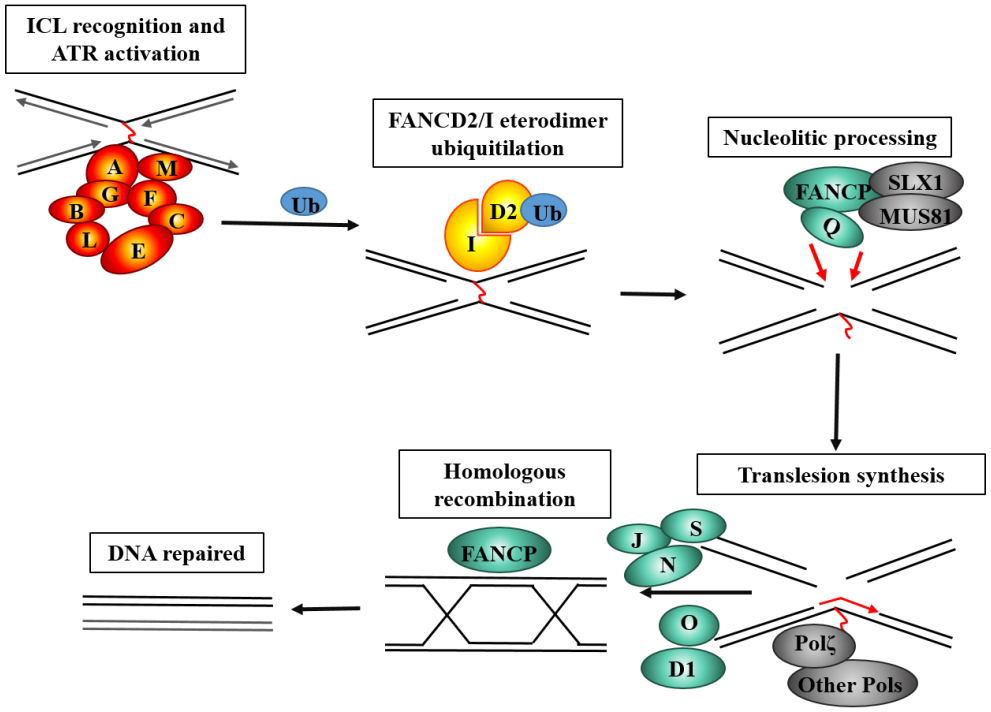

Figure 9: *The Fanconi Anemia pathway* (modified from Wang & Smogorzewska 2015).

The Fanconi Anemia syndrome

Mutations in most of the 20 genes involved to date in the FA pathway lead to the Fanconi Anemia Syndrome (Table 1). This is one of the genome instability disorders and it is characterised by an autosomal recessive and X-linked genetic transmission, bone marrow failure, congenital developmental abnormalities and early onset of acute myeloid leukemia and solid tumours (D'Andrea & Grompe 2003). Mutations in FANCA, FANCC and FANCG genes, all coding for a FA core complex component, consist of nearly 90% of the total mutated FA genes (Wu 2013). Interestingly has been demonstrated that mutation of one of the core complex components is sufficient to develop FA phenotype. Indeed, despite FANCL is the only component characterised by an E3 ubiquitin-ligase enzymatic

activity, mutation in one of the other genes of the core complex result in its destabilization, lack of FANCD2 mono-ubiquitination and ICLs repair defects. On the other hand mutations of the downstream effectors of FA pathway, shared with DSB repair mechanisms, do not impair proficient FANCD2 mono-ubiquitination by the core complex, excluding a possible involvement of these effectors on the apical part of FA pathway (Yao et al. 2013). Noteworthy, SLX4 mutations have recently been found causative of six Fanconi Anemia disease cases (Kim et al. 2011; Stoepker et al. 2011; Schuster et al. 2012). Typical feature of Fanconi Anemia cells is the displacement of radial chromosomes, upon diepoxybutane treatment (an ICL agent), deriving from unrepaired ICLs (Newell et al. 2004). Indeed SLX4, also known as FANCP, is involved in the Fanconi Anemia (FA) pathway, responsible for ICL repair during S phase (Bakker et al. 2012).

	Gene	Name (alias)	Patient frequency	Protein function
Genes mutated in FA patients	**FANCA**	-	64%	Core complex
	FANCB	-	2%	Core complex
	FANCC	-	12%	Core complex
	FANCD1	BRCA2	2%	HR protein
	FANCD2	-	4%	D2-I complex, direct downstream events
	FANCE	-	1%	Core complex
	FANCF	.	2%	Core complex
	FANCG	.	8%	Core complex
	FANCI	.	1%	D2-I complex, direct downstream events
	FANCJ	BRIP1	2%	HR protein
	FANCL	-	0.4%	Core complex, E3 ubiquitin ligase
	FANCM	-	0.1%	Core complex, contributes to ATR activation
	FANCN	PALB2	0.7%	HR protein
	FANCO	RAD51C	0.1%	HR protein
	FANCP	SLX4	0.5%	HR protein, unhooking of ICL and dHJ resolution
	FANCQ	XPF	0.1%	HR protein, unhooking of ICL
	FANCS	BRCA1	0.1%	HR protein
	FANCT	UBE2T	-	Core complex, E2 ubiquitin conjugating enzyme
	FANCU	XRCC2	-	HR protein
	FANCV	REV7	-	Translesion DNA synthesis

Table 1: *The Fanconi Anemia proteins* (modified from Anderson T. Wang & Smogorzewska 2015; Mamrak et al. 2017). *In red core complex component, in yellow the D2-I heterodimer monomers, in green HR step proteins.*

For the purpose of this Thesis I'll extensively discuss the features of SLX4/FANCP protein and of a FANCP mutated cell line, derived from one FA patient, since it is the one on which I mainly focused my last year work.

SLX4 protein

The Synthetic lethal for unknown reason 4 (SLX4) is a nuclear protein of 1834 amino acids, considered to act as a scaffold necessary for endonucleases coordination during DNA repair and telomeres homeostasis maintenance (Wan et al. 2013). SLX4 orthologues have been found from yeast to higher eukaryotes but sharing low amino acids identity, except for the C-terminal portion (Kim 2014).

SLX4 structure is compose of:

- Two UBZ domains at the N-terminus, required for SLX4 interaction with ubiquitinated proteins and its localization at the inter-strand crosslinks (Lachaud et al. 2014)
- An MLR domain responsible for SLX4 association with the XPF nuclease (Fekairi et al. 2009)
- A BTB domain necessary for SLX4 dimerization required for dHJ resolution (Yin et al. 2016a).
- Two SIM domains, thank to which SLX4 interact with SUMOylated proteins and is recruited at the DSBs region (Guervilly et al. 2016)
- A SAP domain, at the C-terminus, is the most conserved domain of SLX4. Indeed, evolutionary conserved from yeast to human, it confers to SLX4 the docking platform role, mediating interaction with Mus81 and SLX1 (two DNA branched structure specific nucleases) (Gaur et al. 2015) (Figure 10).

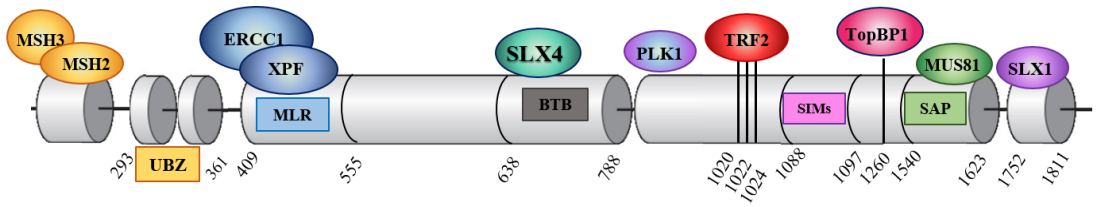

Figure 6: *SLX4 protein domains and interaction partners.*

Moreover, SLX4 has been found to interact with the shelterin TRF2, promoting telomere homeostasis maintenance and resolution of branched intermediates during telomere replication (Wan et al. 2013). Although SLX4 regulation remains elusive, this protein has been recently discovered to interact with ubiquitinated and SUMOylated proteins, through its UBZ and SIM domains, that promote SLX4 localization at ICLs, DSBs and ALT telomeres (Wan et al. 2013; Lachaud et al. 2014; Guervilly et al. 2016). In addition, the SIMs are responsible of the SUMO-ligase activity of SLX4, targeting SLX4 itself and the XPF/ERCC1 endonuclease, a core component of the nucleotide excision repair machinery, involved in ICLs and DSBs repair (Ahmad et al. 2008; Klein Douwel et al. 2014; Guervilly et al. 2015). Thanks to interaction with multiple DNA structure-specific nucleases (XPF, Mus81 and SLX1), several evidences underline the essential role of SLX4 in dHJ resolution, in both yeast and human cells (Fekairi et al. 2009; Garner et al. 2013). Recently, our group has demonstrated that this SLX4 activity is coupled with a more upstream role in DSBs repair, controlling checkpoint activation and DNA end resection during replication stress and at the DSB. Indeed, in *S. cerevisiae*, it has been reported that SLX4 acts as a pro-resection factor, competing with Rad9, homologue of 53BP1, for binding Dpb11 (TopBP1 in human cells) at the DSB. This inhibits the barrier effect of Rad9/53BP1 and dampens the checkpoint signalling, favouring resection and HR (Dibitetto et al. 2016). Interestingly, SLX4 interaction with TopBP1, upon DSB, is conserved in human cells, where TopBP1

can interact with both Brca1 and 53BP1. These two factors, compete for TopBP1 binding at the DSB: when Brca1-TopBP1 association is favoured, HR can occur otherwise TopBP1-53BP1 interaction blocks resection allowing NHEJ (Liu et al. 2017). Thanks to its role in telomere homeostasis maintenance and involvement in the DDR, SLX4 is considered to be a genome stability guardian (Holloway et al. 2011).

In addition, a controversial role of SLX4 in HIV infection is emerging. Indeed, initially, SLX4 was identified to interact with Vpr, accessory protein of HIV1 and 2 viruses, triggering an untimely activity of Mus81, leading to replication stress and DDR activation (Laguette et al. 2014). In 2016 this SLX4 role has been disputed and it has been demonstrated that Vpr trigger DDR through a still unknown SLX4-indipendent mechanism (Fregoso & Emerman 2016) .

As previously mentioned, from 2011 SLX4 mutations have been associated with six Fanconi Anemia disease cases identifying the new subtype P of Fanconi Anemia (Kim et al. 2011; Stoepker et al. 2011; Schuster et al. 2012). Therefore SLX4, also known as FANCP, a novel players involved in the Fanconi Anemia (FA) pathway (Bakker et al. 2012).

Fanconi Anemia cell line RA3331

The RA3331 cell line derives from skin fibroblast of an American 21 years old male individual (IFAR414/1), carrying a germ line heterozygous frameshift in both SLX4 alleles. The paternal allele mutation result in a predicted truncated protein with N-terminal 171 amino acids of SLX4 followed by 22 non-SLX4 amino acids (p.Leu172Phe*fs*X22). The second allele is characterised by a large genomic deletion from intron 9 to exon 12 resulting in a frameshift producing a predicted truncated protein with 671 SLX4 amino acids at the N-terminal followed by 119 non-SLX4 amino acids due to a frameshift (p.Leu672Val*fsX*119) (Kim et al. 2011) (Figure 11). Since immunoprecipitation of SLX4 with a specific antibody failed to

identify both full length and truncated forms of SLX4, these cells are considered SLX4-null cell (Kim et al. 2013a).

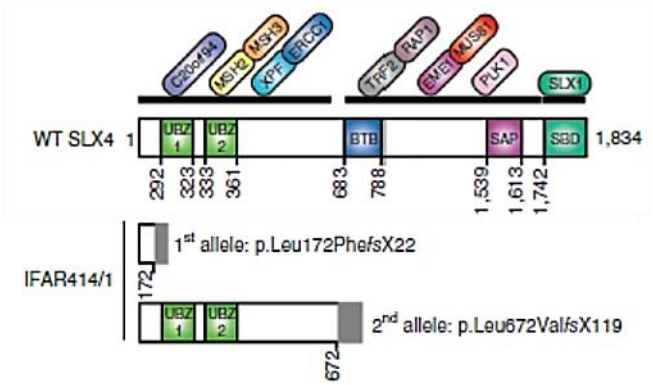

Figure 71: *SLX4 predicted protein in RA3331 cells* (Kim et al. 2011).

RA3331 patient cells are characterised by MMC sensitivity and radial chromosomes upon diepoxibutane exposure, hallmark of FA phenotype, rescued by a complementation assay, re-expressing SLX4 wild type. This confirm the cause-effect relationship between SLX4 gene mutations and FA disease onset (Kim et al. 2011). Interestingly, it has been reported that these patient cells display high levels of INFα and β, probably due to an enhanced LINE1 retro-transposition in absence of SLX4. Indeed SLX4 prevent accumulation of LINE1 reverse transcribe DNA that otherwise would gather in the cytoplasm triggering INFα and β production. These studies suggest a role of SLX4 as a negative regulator of innate immunity (Laguette et al. 2014; Brégnard et al. 2016).

Premature senescence and apoptosis

In case the DNA damages are too many or too severe to be repaired, eukaryotic cells can activate two different processes to block proliferation of damaged or mutated cells, therefore ensuring a faithful genome transmission to subsequent generations: premature senescence and apoptosis.

Premature senescence

This mechanism is defined as permanent exit of cells from the cell cycle. The senescence pathway was originally associated with an excessive telomeres shortening, due to replication (replicative senescence). Telomeres are the terminal structure of chromosomes, composed by specific repetitive DNA sequences and associated to structural protein with protective function, shelterins. In case of an excessive telomeres shortening, due to DNA replication mechanism, these cannot associate with shelterins any more and are detected by the cell as DSBs, indeed common feature of all cellular senescence events is the DDR activation (Kuilman et al. 2010).

Recently it has emerged that the senescence can also be induced by chronic DNA damage (stress induced premature senescence) and hyper-proliferation due to oncogene activation (oncogene induced senescence). The DDR is activated by senescence (replicative, stress and oncogene induced senescence) but, except for this common step, the mechanisms leading to these different phenotypes are nowadays poorly understood (Courtois-Cox et al. 2008).

In general, it is known that the activation of the senescence process relies on two main signalling cascades: the ATM-p53-$p21^{Waf1}$ (Qian & Chen 2013) and the $p16^{INK4A}$-Rb pathways (Takahashi et al. 2007). The activation of the first mechanism takes place in a similar way as mentioned for the G1/S and G2/M checkpoints. Indeed, an essential feature of senescence is a permanent arrest of cell

cycle progression. Noteworthy, p53 transcription activity in the senescence program is regulated by different factors and post-translational modification compared to those occurring during checkpoints activation, as for example SIRT1 dependent de-acetylation (Jingjie Yi & Jianyuan Luo 2010). The second mechanism is p53 independent. Indeed, it requires the activity of p16 ^{INK4A}, one of the CDK-cyclin complex inhibitors. This protein blocks the phosphorylation of Rb that, in a hypo-phosphorylated state, can interact with E2F transcription factor, inhibiting expression of pro-proliferative and pro-replication genes (see "The cell cycle and checkpoints" chapter) (Takahashi et al. 2007).

Apoptosis

This process consists in a programmed cell death as a consequence of a specific sequence of events. The apoptosis mechanism depends on the activity of a cystein-aspartate protease family, the caspases, synthetized as inactive enzymes (pro-caspases) and activated by a proteolytic cleavage performed by an initiator caspase. Once cleaved, the caspases cleave others caspases amplifying the signalling and triggering the degradation of all cellular components. The initiator caspases can be activated trough two main pathways: the extrinsic and the intrinsic way. The first relies on extra-cellular factors that bind specific cellular receptors localised on the cellular membrane, like the well-known TNF (tumour necrosis factor) receptor. The second process consists in a response to stress as a DNA damage or an hypoxic condition and requires the release from the mitochondria of the cytochrome C, component of the respiratory chain. This step is essential for the apoptosome formation, a quaternary protein structure formed by Apaf1 monomers, responsible for the activation of the initiator caspases (Lawton 2016). The intrinsic way is finely regulated by p53 that, upon DNA damage, is phosphorylated in an ATM-dependent manner. This event leads to p53-dependent transcription activation of pro-apoptotic genes that neutralizes the action of anti-apoptotic factors and

promotes the formation of pores in mitochondria outer membrane. These events lead to the cytochrome C spreading in the cytoplasm, favouring the apoptosome formation (Lawton 2016).

Defects in the DNA damage response, genome instability and cancer

Nuclear DNA is a stable molecule thanks to both double helix structure and chromatin organization. The safeguard of genome stability, as already mentioned, relies on the ability to respond and repair DNA damages occurring during the cell lifespan. When the mechanisms ensuring a robust and effective DDR fail, the faithful transmission of a correct genome to the subsequent generation is threated.

Germ line mutations of some DDR factors have been found to be causative of the so called "Genome instability syndromes", sharing increased genome instability, enhanced cancer predisposition and in many cases a progeroid phenotype (Wolters & Schumacher 2013) (Table 2).

Disorder	Mutated gene(s)	Pathway impaired	Enhanced cancer susceptibility	Progenoid features
Ataxia telangiectasia	ATM	DDR	+	+
Bloom's syndrome	BLM	DSBs repair	+	+
Fanconi Anemia	FANCA, B, C, DI, E, F,G, H, I, L, M, N, O, P, Q, R, S	ICLs repair	+	+
Cockayne syndrome	CSA and CSB	NER	-	+
Li-Fraumeni syndrome	p53	DDR	+	-
Nijmegen breakage syndrome	NBS1	DSBs repair	+	+
Werner syndrome	WRN	DSBs repair, ICLs repair, MMR and BER	+	+
Xeroderma pigmentosum	XPA and XPG	NER	+	-

***Table 2**: Most studied human disorders associated with DDR genes mutations* (modified from Wolters & Schumacher 2013).

Interestingly, both hereditary and sporadic mutations of DDR players have been found with high frequency in many kind of tumours leading to genome instability, typical feature and source of high plasticity and adaptation ability of cancer cells.

Genome instability has been observed during oncogenesis since 100 years ago and today is considered the main fuel of cancer: all tumours display genetic alteration as point mutations, deletions, translocations, up to the duplication or loss of entire chromosomes (polyploidy and aneuploidy) (Jeggo et al. 2016). In hereditary and sporadic cancers the presence of genome instability is often associated with mutations in the DDR genes. As a consequence of DDR genes mutation, the un-correct DNA repair favour mutation accumulation, enhancing genome instability in a vicious circle (Negrini et al. 2010). Oncogenesis is a multistep process allowing cancer cells to grow and evolve in a micro-environment, requiring constant adaptation. When the environment changes due to inflammation or nourishment level fluctuation (hypoxia), normal cells do not posses that genetic plasticity allowing an evolution to fit the new environment, thus they stop growing or activate apoptosis. On the other hand, in pre-neoplastic cells, the increased genome instability generates different sub-populations and the most suitable to the altered environment starts to expand, due to the selective advantage (Greaves & Maley 2012). Therefore, the increased genome instability, deriving from defects in DDR and DNA repair factors, allow to pre-neoplastic cells to survive, proliferate and accumulate mutations, acquiring the typical features of cancer. Indeed, p53 is mutated in more than 50% of sporadic tumours in which a reduced expression level of many DDR factors as ATM, Brca1, Rad51, MRN and Chk2 has also been frequently detected (Soussi 2007; Broustas & Lieberman 2014). The tight interconnection between tumorigenesis and DDR defects is further demonstrated by the increased cancer predisposition typical of the hereditary syndromes caused by germ line mutations in DDR genes (Wolters & Schumacher 2013).

Despite these considerations, it has been demonstrated that cancer cells still retain the ability to repair endogenous DNA lesions, otherwise threating survival. (Samadder et al. 2016). Indeed, recently, inhibitors of DDR components have been developed, used in combination with chemotherapy to target DSB-repair deficient cancer cells (Gavande et al. 2016). Interestingly some of them have already been tested in clinical trials and the results are very promising. As an example, Olaparib (Dziadkowiec et al. 2016) is an inhibitor of the PARP-1 (poli[ADP-ribose] polymerase-1) enzyme, involved in SSB repair. Once a SSB has occurred, PARP-1 localize at the lesion and, using NAD^+ as substrate, catalyses the formation of branched ADP-ribose chains on both histones surrounding the lesion and itself. The consequent high negative charge in the damaged region induces chromatin relaxation, to favour repair, and recruitment of SSB repair factors. Initially used in combination with other chemiotherapy agents, in the last ten years is emerging a new PARP inhibitors role in cancer therapy as a single-agent (Curtin 2014). As previously mentioned, defects in HR are quite common in many cancer types. In this scenario, the PARP inhibitor Olaparib is resulting particularly interesting as a treatment for cancer displaying a low DSB repair efficiency. Several studies have analysed the mechanism of Olaparib action and proposed that, when PARP is not active, endogenous DNA SSB cannot be repaired and accumulate in cells. During S-phase SSB persistence leads to fork stalling and DSBs formation (Schultz et al. 2003). While in normal cells, these lesions are repaired through HR, in HR-deficient cancer cells these damages persist or are repaired through error-prone mechanisms, leading to chromosome aberrations and ultimately to cell death (Curtin 2014). Noteworthy, carriers of mutations in HR factors, as for example Brca1, in un-transformed cells display a wild type allele that allow the physiological accomplishment of S-phase DSB repair. It is only in tumour cells that the functional allele is lost, for loss of heterozygosity or sporadic mutation, rendering these cells HR defective and for thus sensitive to Olaparib treatment.

This confer to Olaparib a selective toxicity toward tumour cells, without harming un-transformed cells, that is one of the most important feature of cancer treatment drugs (McCabe et al. 2006; Curtin 2014). Interestingly, further studies have revealed that other HR genes, besides Brca1 and 2, sensitise cancer cells to PARP inhibitors (Gilardini Montani et al. 2013; De Felice et al. 2017; Jue et al. 2017) that for thus are very promising single-agent to treat various type of tumours.

DAXX, ATRX, H3.3 in genome instability and cancer

Recently, it has been demonstrated that H3.3 and its chaperon proteins are involved in the development of some type of cancer. Indeed, H3.3 mutations in G34 (G34R or G34V) and K27 (K27M) have been found in 31% of paediatric glioblastoma cases (Schwartzentruber et al. 2012; Gessi et al. 2013; Chan et al. 2013) (Figure 12).

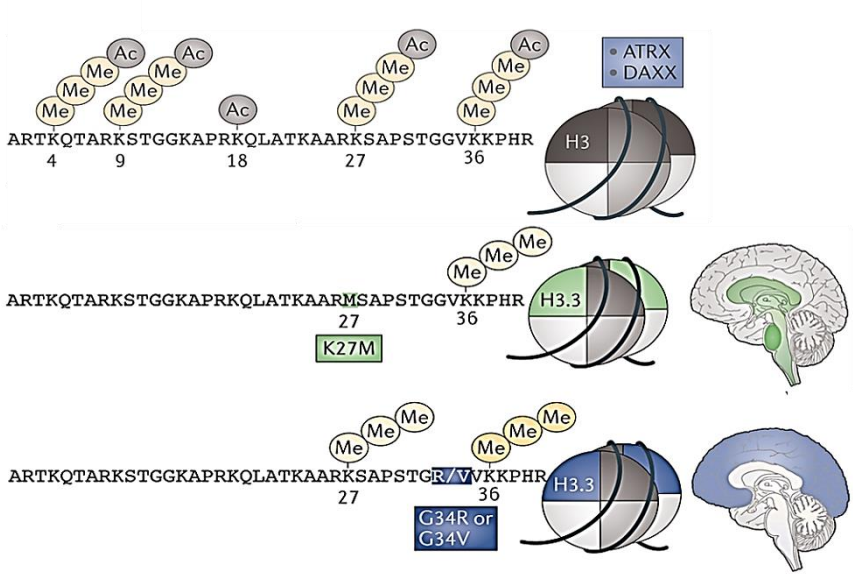

Figure 12: *H3.3 mutations in paediatric glioblastomas* (Jones & Baker 2014).

Interestingly DAXX and ATRX mutations have been reported with a 50% incidence in pediatric high-grade gliomas and strongly associated with G34V/R pediatric glioblasomas (Lulla et al. 2016). Moreover, in neuro-endocrine pancreas tumour these genes are considered a reliable and predictive marker (Appin & Brat 2015; Park et al. 2017). The connection between H3.3 mutation and central nervous system tumours is not clear yet, one possible hypothesis is that H3.3 mutations alter the expression profile of developmental and oncogenes/onco-suppressors during neuronal development (Xia & Jiao 2017). Noteworthy, DAXX, ATRX and probably H3.3 are involved in the ALT (alternative lengthening of telomeres) mechanism, an aberrant HR-based mechanism exploited by some cancer cells to elongate telomeres (Lovejoy et al. 2012). Telomerase expression and activity is normally restricted to a few cell types in human: germ cells, stem cells, active lymphocytes and epithelial cells with a high proliferative rate. All the other cells lack telomerase expression and thus are characterised by a replicative limit, determined by telomere shortening, and senescence (Chen et al. 2014). It has been reported that 85% of tumours re-activate telomerase expression to bypass the replication limit and avoid senescence while the remaining 15% adopt the ALT mechanism to maintain telomeres length, taking advantage of the HR machinery (Nabetani & Ishikawa 2011) . ALT is more frequent in sarcomas and particularly in the osteosarcomas and, interestingly, it has been discovered that mutations in ATRX or DAXX gene are essential to acquire the ALT phenotype (Heaphy et al. 2011; Lovejoy et al. 2012).

SLX4 and genome instability

Despite the absence to date of a clear correlation of SLX4 mutations and cancer predisposition SLX4 protein is considered a genome stability guardian, counteracting DNA damages and mutations accumulation, hallmark of cell transformation (Holloway et al. 2011).

As previously discussed, biallelic mutations of *SLX4 gene* have been identified in patients with a new sub-type of FA, termed FA-P (Kim et al. 2011). Since monoallelic germline mutations of all FA pathway downstream effectors (FANCD1/Brca2, FANCJ/BRIP1, FANCN/PALB2 and FANCO/Rad51C) increase breast and ovarian cancer predisposition (Somyajit et al. 2010; D'Andrea 2010; Mehrgou & Akouchekian 2016), in the last years many studies have tried to elucidate a possible SLX4 mutation-dependent breast cancer predisposition. Overall the results suggest that SLX4 mutations are associated with increased cancer risk in a small number of both Brca1/Brca2 (Landwehr et al. 2011; Fernández-Rodríguez et al. 2012; Shah et al. 2013) and non-Brca1/2 hereditary breast cancer cases (Romero et al. 2013).

Another aspect of SLX4 involvement in tumour-suppression concerns its role as a telomeres care taker. Indeed, neuroendocrine tumours and osteosarcomas display a peculiar HR-based mechanism to elongate telomeres, the ALT (as described in chapter "DAXX, ATRX, H3.3 and cancer"). Interestingly, thanks to its role in HR pathway, telomeres homeostasis maintenance and interaction with TRF2, SLX4 participates to this process. Indeed, it has been proposed that SLX4, in association with SLX1, is responsible for the telomeres trimming (Wan et al. 2013). This process is a telomere length regulation mechanism that generates DNA fragments detectable as extrachromosomal telomeric circle (TCs), found with high frequency in some ALT cancer cells (Cesare & Griffith 2004).

Relevant outstanding questions

In this context, where only a small part of player and regulator mechanisms of DNA damage response and DSBs repair has been described, many aspects have to be elucidated yet.

1. How does chromatin conformation status influences end resection and control DNA repair pathway choice? And how does chromatin conformation changes upon DNA damage induction? Are these changes permanent, signing a damaged region once the repair has occurred?

2. What are the crucial players regulating resection and DSBs pathway choice in human cells? How are these players regulated and interconnected? Are they differentially regulated upon the loss of HR?

3. Which impact on cancer could have modulation of DDR and DSB repair factors activity/interplay? A deeper understanding of HR defects could better the cancer patient outcome?

These questions in my opinion are the most common and urgent issues.

In both my PhD projects we analysed and tried to dissect different aspects of these questions.

Aims of the project

In this thesis I'm presenting the work related to two different projects both involved in improving the understanding of double strand break repair pathway choice. In particular I've focused my PhD work on two different proteins both involved in this process through the regulation of 53BP1 recruitment at the lesion: DAXX and SLX4. Indeed, here I demonstrate that DAXX, through deposition of H3.3 at the DSB, modulates 53BP1 localization at the damage regulating DNA repair pathway choice towards HR. In addition, I've started working on SLX4 that, as already discussed, in *S. Cerevisiae* display a pro-resection activity, counteracting Rad9 (53BP1) accumulation at the lesion. Here I report data that confirm this pro-resection role of SLX4 in human cells.

Aim 1: To study the role of DAXX S424 and S712 phosphorylation in the DNA damage response.

The DSBs are one of the most dangerous lesion to face for cells, since if not timely and properly repaired, they can lead to genome instability, considered to be the fuel of cancer. Eukaryotic cells rely on two main pathways to accomplish the repair: the NHEJ and the HR. The balancing of these two processes depends both on cell cycle regulation and chromatin compaction (as previously discussed in Part I, see "DNA repair pathway choice: a cell cycle and chromatin based decision" chapter), ensuring the choice of the most suitable mechanism to faithfully restore an undamaged genome. To efficiently perform a specific repair pathway, damage-induced post-translational modification and histone variants deposition are required (Thompson et al. 2013; Price & D'Andrea 2014). In the last ten years, the involvement in the DDR of a growing number of chromatin remodellers, writer and reader enzymes and histone chaperones, is emerging (Dabin et al. 2016; Stadler &

Richly 2017). DAXX protein has been reported to be phosphorylated by the apical kinases of DDR, ATM and ATR, upon DNA damage (Stokes et al. 2007; Matsuoka et al. 2007). Intriguingly, DAXX is a chaperone dedicated to H3.3, a variant of the histone H3. This histone is conserved throughout the evolution and can undergo specific PTMs, different from H3.1, shaping the pattern of modification of the nucleosome. In my first two years of PhD, I aimed to understand the role of DAXX phosphorylation in regulating H3.3 deposition upon DSBs induction, in human cells. Moreover, I aimed to verify a possible involvement of DAXX-dependent H3.3 deposition and modifications in influencing the DSB repair pathway choice. This could shed light on a new mechanism of DSBs repair pathway choice and deepen our understanding of how mutation of both DAXX and H3.3 lead to cancer onset, particularly glioblastoma.

Aim 2: To evaluate the involvement of the SLX4 protein in regulating resection, in human cells.

As previously discussed (see "SLX4 protein" chapter) an increasing number of evidences are strongly suggesting the involvement of SLX4 in modulating the resection process, essential to repair a DSB through HR. Indeed in *S. cerevisiae* it has been demonstrated that SLX4 competes with Rad9 (53BP1 homologue) for the binding with Dpb11 (TopBP1 homologue), dampening the checkpoint and favouring resection and, therefore, HR (Dibitetto et al. 2016). Interestingly, both the interaction SLX4-TopBP1 and 53BP1-TopBP1 are conserved in human cells, where the DSB repair pathway choice involves also the tumour suppressor Brca1 (Liu, Cussiol, Dibitetto, Sims, Twayana, Weiss, Freire, Marini, Pellicioli, Smolka, et al. 2017). Noteworthy, preliminary data of our lab (shown in Part III) confirm SLX4 pro-resection role in human cells. Starting from these evidences I aimed to

evaluate the conservation of SLX4 role as a pro-resection/HR factor in human cells, unravel the molecular mechanism of resection modulation by SLX4 and the possible interplay with Brca1 protein. In addition I'm evaluating resection efficiency in the Fanconi Anemia patient cell line RA3331. My hypothesis is that SLX4 could be a novel player in the network leading to DSB repair through HR, modulating the modification/loading of Brca1 onto DNA.

Part II

Submitted manuscript

DAXX MODULATES DOUBLE STRAND BREAKS REPAIR PATHWAY CHOICE THROUGH H3.3 DEPOSITION

Simona Aliprandi[1], Laura Zannini[2], Clara Ricci[2], Domenico Delia[2], Marco Muzi-Falconi[1], Giacomo Buscemi[1]

[1]Department of Biosciences, Università degli Studi di Milano, via Celoria 26, 20133 Milan, Italy. [2]Department of Experimental Oncology, Fondazione IRCCS Istituto Nazionale dei Tumori, Via Amadeo 42, 20133 Milan, Italy.

Corresponding author: G. Buscemi, giacomo.buscemi@unimi.it

Running Title: DAXX tunes DNA repair by H3.3 deposition

ABSTRACT

DNA double strand breaks (DSBs) are produced by normal cellular processes and are induced by genotoxic agents, among which several chemotherapeutics. Misprocessing of DSBs leads to pathological alterations and to the elevated genome instability observed in cancer cells. DSBs are repaired by homologous recombination (HR) and by non homologous end joining (NHEJ). The proper balance between the two pathways is modulated, through an elusive mechanism, by 53BP1 recruitment. Here we report that DAXX, a chaperone involved in loading H3.3 mainly at telomeric and centromeric regions, plays a fundamental role at DSBs. In human cells, DSBs-induced ATM/ATR-dependent phosphorylation of DAXX on serine 424 and 712 promotes DAXX binding to and deposition of H3.3 on chromatin nearby DNA breaks. Enrichment of H3.3 at damage sites regulates 53BP1 relocalization at DSBs and the choice between HR and NHEJ repair pathways. H3.3-specific post translational modifications, particularly K36 methylation, play a relevant role in these events. Altogether these findings reveal that DAXX and H3.3 are critical in determining DSB repair pathway choice, and their mutation may promote tumorigenesis enhancing genome instability.

Keywords: ATM/ DAXX/DNA repair/Double strand breaks/histone variant

INTRODUCTION

The DNA damage response (DDR) is a complex network of pathways that senses and repairs DNA, eventually activating a transient block of cell cycle progression (Ciccia & Elledge, 2010). As a consequence, DDR alterations are necessary events during tumorigenesis to increase the mutation rate, tolerate hyper-proliferation stress and avoid DDR-dependent apoptosis or senescence. DNA double-strand breaks (DSBs) are the most hazardous DNA lesions due to their ability to trigger chromosomal alterations if not repaired timely and accurately. Since DNA lesions occur in the context of the chromatin landscape, chromatin remodelling steps characterize any stage of the DDR. In the last years several histone post translation modifications and chromatin remodelling factors have been associated with DNA lesion recognition, signalling modulation, repair and original conditions restoration (Polo & Almouzni, 2015). Histone H3.3 was recently shown to be loaded by HIRA (histone regulator A) at UV-induced damage sites to mark active genes, allowing transcription restoration after DNA repair (Adam et al, 2013). H3.3 is also recruited at UVA induced breaks, through an unknown chaperone, where it promotes DNA repair (Luijsterburg et al, 2016).

H3.3 represents 10-30% of the total cellular histone H3 pool in actively dividing human cells and differs from H3.1 for five aminoacids and for the DNA replication-independent deposition (Hake et al, 2006). These variations are sufficient to confer particular properties, also as an effect of H3.3 peculiar post translational modifications (Hake et al, 2006; Loyola et al, 2006).

DAXX (or DAP6, death associated protein six) is a multifunctional protein that physically interacts with chromatin remodelling enzymes and transcription factors (Salomoni & Khelifi, 2006), suggesting a role in regulating gene expression. Generally thought to influence cell

growth, apoptosis and autophagy (Tang et al, 2015), DAXX has been more recently associated with a specific chaperone activity responsible for the deposition of the histone variant H3.3 inside chromatin (Drane et al, 2010). Differently from HIRA, which deposes H3.3 at transcriptionally active gene promoter and bodies (Hake et al, 2006), DAXX loads H3.3 at pericentromeric heterochromatin and telomeres through the interaction with the DNA helicase ATRX (Lewis et al, 2010). Significantly, ATRX and DAXX mutations (Lovejoy et al, 2012) may promote alternative lengthening of telomeres (ALT), an homologous recombination based mechanism that elongates telomeres in telomerase-negative cancer cells. DAXX activity at chromosome ends is supported by its presence in PML nuclear bodies (PML-NBs), aggregates of proteins that colocalize with telomeres in ALT positive cells (Lallemand-Breitenbach & de The, 2010).

The alteration of DAXX/ATRX/H3.3 activity at telomeres explains the effects of DAXX and ATRX mutations found in ALT positive pancreatic neuroendocrine tumors, neuroblastomas and adrenocortical carcinomas (Salomoni, 2013). At the same time, H3.3 function in oncogene expression regulation (Bjerke et al, 2013) could explain the effects of H3.3 and DAXX/ATRX mutations in gliomas, particularly paediatric glioblastoma. A role for H3.3 in the DNA damage response was previously attributed to HIRA (Yang et al, 2013) and CHD2 remodelling factor (Luijsterburg et al, 2016) activity.

Here we report for the first time that DAXX is the chaperone that regulates histone H3.3 deposition at DSBs and this has a critical effect on the actual repair of the lesions. Indeed, we show that DAXX affects the kinetics of 53BP1 recruitment at DSBs and leads alterations in the balance between HR and NHEJ. This new function of DAXX depends upon ATM/ATR-dependent phosphorylation of conserved serine residues on DAXX. We provide evidence for a crucial role of these phosphorylations in modulating DAXX/H3.3 interaction and H3.3 deposition at DSB sites, to promote DDR factors recruitment and DNA

repair pathway choice. Overall, our results demonstrate that deregulation of DAXX-dependent H3.3 deposition leads to low fidelity repair and genome instability, suggesting a new role for these proteins during carcinogenesis.

RESULTS

H3.3 histone is loaded by DAXX at DNA breaks

The configuration of chromatin strongly influences DNA damage sensing and repair. Histone variants, histone modifications and proteins that, reading such modifications, associate to chromatin regulate the assembly of DDR and repair proteins at the site of damage and modulate processing of lesion. After exposure of U2OS, HEK293T or MRC5 cells to the DSBs inducing and chemotherapeutic agent bleomycin (BLE) we evaluated the ratio of H3.3 to total H3 in chromatin at different timepoints. In all these cell lines, we observed an accumulation of the H3.3 fraction at 3hrs after damage (Fig. 1A, mock samples and Fig S1A). In U2OS we were able to detect this accumulation already at 1hr after BLE addition (Fig. 1A). Incorporation of histones in assembled nucleosomes is promoted by specific chaperones. DAXX has been reported to be involved in replication-independent H3.3 loading; therefore we investigated its possible role in the DNA damage-induced H3.3 incorporation. Silencing DAXX in U2OS and HEK293T cells (Fig. S1B and S1C) we noted that following BLE-induced DSBs, H3.3 loading on damaged chromosomes is dependent on DAXX presence (Fig. 1A and Fig. S1D). On the contrary, HIRA presence is not relevant in this context (Fig. S1E and S1F). Since U2OS cells are ATRX *null* (Newhart et al, 2012), we concluded that a form of DAXX different from the DAXX/ATRX complex active at telomeres and centromeres (Lewis et al, 2010) is involved in this process. This result was further confirmed by the finding that H3.3 accumulation in

chromatin is retained in HEK293T cells silenced for ATRX (Fig S1G). To determine if H3.3 deposition in response to DSBs is widespread or localized at damage sites, we purified γ-H2AX and H2AX containing chromatin. Indeed, while histone H2AX is diffused in the genome, its phosphorylated counterpart, γ-H2AX, is enriched at DNA breaks after damage (Iacovoni et al, 2010). Immunopurifications were conducted on oligonucleosomes preparations (Fig. S1H, (Goodarzi et al, 2008)) to evaluate the presence of H3.3 and γ-H2AX or H2AX in the same or, at least, in adjacent nucleosomes. We found that H3.3 association with H2AX is not different before and after BLE treatment (Fig. 1B, upper panels), demonstrating that after DNA damage H3.3 is not further incorporated in H2AX-containing nucleosomes. On the contrary, immunoprecipitating equal amounts of γ-H2AX at 1 and 3hrs after BLE, the fraction of H3.3 co-purifying with γ-H2AX rose at 3hrs (Fig. 1B, lower panels, mock samples). These data demonstrate an increased deposition of H3.3 in the vicinity of γ-H2AX after DSB formation. Notably, γ-H2AX/H3.3 association strongly decreased between 1 and 3hrs (Fig. 1B, lower panels, shDAXX samples) in shDAXX cells similarly treated. To confirm these data using a different approach, we performed chromatin immunoprecipitation (ChIP) experiments on U2OS cells containing a DSB derived from an I-SceI cut site (Gunn & Stark, 2012) expressing FLAG-H3.3 histone. ChIP with an anti-FLAG antibody followed by quantitative real-time PCR using primer located at 500 and 1300 nucleotides from the break revealed that H3.3 accumulates specifically at 500 nucleotides from damage site, and not at GAPDH gene (Fig. 1C), coherently with a previously published observation (Yang et al, 2013). Notably, in accordance with data obtained with oligonucleosome analysis, H3.3 enrichment at 500 nucleotides from the DSB is undetectable in siDAXX cells (Fig. 1C).Indeed, a decrease in H3.3 presence is present at both sites tested in absence of DAXX, suggesting that DAXX activity is important for

H3.3 accumulation nearby the break, but also to maintain the presence of this histone variant as far as 1300 nucleotides from the lesion.

To investigate the mechanism responsible for the DAXX-dependent loading of H3.3 at damage site we initially determined if DAXX localizes at DSBs. Immunofluorescence analysis confirmed previous observation that DAXX is located exclusively in the nucleus, with discrete bright spots (5-20 per cell), mainly colocalizing with PML-bodies (Fig S1I; Salomoni, 2013). Intriguingly, we also found that DAXX spots increase in response to BLE treatment (Fig. S1I) and that a fraction of both exogenous (Fig. 1D) or endogenous (Fig. 1E) DAXX spots are juxtaposed or overlapping with a fraction of γ-H2AX foci. To confirm this observation we performed an *in situ* Proximity Ligation Assay (PLA) using anti-HA and γ-H2AX antibodies. The presence of individual fluorescent dots increasing in number during time after BLE in cells demonstrates that DAXX and γ-H2AX proteins are in close proximity (Fig. 1F, Fig. S1L for negative controls). To exclude that positivity was due to a fortuitous proximity of DAXX, which normally binds chromatin, with γ-H2AX, we tested in the same conditions other proteins known to localize on chromatin. ORC2, which is bound throughout the cell cycle at replicative origins (Mendez and Stillman, 2003), or active p53, a well known transcriptional factor bound on gene promoters after DNA damage occurrence (Smeenk et al., 2011), do not produce PLA positive dots with γ-H2AX in cells treated with BLE (Fig. S1M). These observations underlines the specificity and sensitivity of PLA approach. Moreover, to further confirm DAXX accumulation at damage site, we performed a ChIP and quantitative PCR analysis in U2OS containing the I-SceI cut site. Consistently, we observed that DAXX accumulates specifically at least up to 1300 nucleotides from the I-SceI break (Fig. 1G) and not at GAPDH gene body, coherently with the importance of DAXX in promoting accumulation or in maintenance of H3.3 around the break (Fig.1C).

H3.3 deposition at damage sites influences 53BP1 relocalization on DNA lesions

Chromatin remodelling and histone marking are critical events during the early steps of DNA damage detection and signalling (Polo & Almouzni, 2015). To test if DAXX deposition of H3.3 at DSBs impact on the DDR signalling, we evaluated how DAXX overexpression and silencing (Fig. S2A) affect the apical events of the DDR. We also assayed the effects of H3.3 overexpression, transiently transfecting plasmids encoding H3.3-YFP or FLAG-H3.3 that produced low levels of nuclear proteins (Fig. S2B and Fig. S2C). Tagged forms of H3.3 have been extensively employed and shown to be correctly loaded in chromatin, to undergo histone modifications and to behave physiologically (Harada et al, 2015; Delbarre et al, 2010). DAXX overexpression also has no effects on H3.3 regulated genes (Harada et al, 2015).

Initially, we evaluated γ-H2AX foci formation at DSBs. Treatment with 12μM BLE produced enumerable γ-H2AX nuclear foci (2.5±2.2 in untreated cells, 33.7±23.9 at 1hr, 52±29.3 at 3hrs) and cells with less than 5 foci were considered as negative. After 1 hour of drug treatment, only 8% of U2OS mock-transfected cells were negative for γ-H2AX (Fig. 2A) and this number decreased to less than 2% after 3hrs of exposure (Fig 2A). Similar data were obtained with cells overexpressing DAXX or H3.3 (Fig. 2A). No effects were clearly detectable also on the localization of active ATM (ATM-pS1981) at damage sites (Fig. S2D). These results demonstrate that alterations of H3.3 or DAXX protein levels do not affect DNA breaks induction, γ-H2AX foci formation and local ATM activation.

53BP1 accumulates and co-localizes with γ-H2AX at DNA breaks (Chapman et al, 2012), where it is recruited and retained by a complex network of histone post-translational modifications (Panier & Boulton, 2014). Therefore, we analysed 53BP1 foci formation (Fig.

2B) in the same conditions used for γ-H2AX and found 1.5±1.4 53BP1 foci in untreated U2OS cells, while 12μM BLE induced 18.9±13.7 and 35.4±18.6 53BP1 foci, respectively 1 and 3hrs after BLE addition. In this case, 15% negative cells (with less than five 53BP1 foci) were detectable in controls 1hr after BLE addition and this number decreased to 5% at 3hrs (Fig. 2C). Interestingly, a significant delay in 53BP1 foci formation was evident following overexpression of H3.3-YFP and DAXX (Fig. 2B and 2C). Indeed, in cells overexpressing H3.3-YFP and DAXX the fraction of 53BP1 negative cells at 1hr after BLE raised to 32% and 38%, respectively; at 3hrs both showed 28% negative cells (Fig. 2C). An analysis of the distribution of 53BP1 foci number confirmed the role of DAXX in these events, since a large accumulation of cells with fewer 53BP1 foci was clearly detectable in DAXX and H3.3 overexpressing cells (Fig. S2E). This foci number reduction was not due to a reduction of total 53BP1 protein since 53BP1 protein level was unaltered in DAXX overexpressing cells, before and after bleomycin treatment (Fig. S2F). This effect cannot be ascribed to the presence of the YFP-tag at the C-ter of H3.3, since similar results were obtained with the FLAG-tag located at the N-ter of the histone (Fig. 2C), nor to histone unbalancing, since ectopic H2B does not affect the kinetics of 53BP1 foci formation (Fig. 2C). Furthermore, this activity is specific for H3.3 variant since H3.1-GFP overexpression leaves unaltered the kinetic of 53BP1 foci formation (Fig. 2C). Intriguingly, we found that the delay in 53BP1 foci formation due to H3.3-YFP expression was undetectable in DAXX depleted cells (Fig. 2C), although downregulation of DAXX does not in itself significantly affect 53BP1 foci formation, and was not affected by silencing HIRA (Fig. S2G). These observations demonstrate that the DAXX/H3.3 and not the HIRA/H3.3 pathway is involved in modulating 53BP1 foci formation after DNA breaks induction. As expected, DAXX overexpressing/53BP1 negative cells were positive for γ-H2AX foci (Fig. 2D), demonstrating that these cells are alive and responsive to BLE. These results were also

confirmed in HEK293T cells exposed to BLE (Fig. S2H) and in AsiSI–ER-U20S cells transfected with DAXX or H3.3 (Fig. S2I), where treatment with 4-hydroxytamoxifen (4OHT) induced nuclear localization of AsiSI–ER and DSBs formation (Iacovoni et al, 2010).

It was previously established that H3.3 is loaded on chromatin independently of DNA replication (Ahmad & Henikoff, 2002). At the same time 53BP1 is loaded at DSBs throughout the cell cycle with the exclusion of mitosis (Orthwein et al., 2014). Therefore alterations of the cell cycle due to DAXX or H3.3 transfection could not account for the effects on 53BP1. However, H3.3 or DAXX overexpression does not induce a substantial modification of cell cycle distribution in cellular population before and within 6hrs after bleomycin addition (Fig. S2J). To exclude that the defect in 53BP1 foci is linked to S phase, cells transiently expressing FLAG-H3.3 were exposed to the nucleotide analogue EdU to mark replicating cells. Triple staining for FLAG-H3.3, 53BP1 and EdU demonstrated that H3.3 overexpression reduces the number of 53BP1 foci in both EdU -positive and -negative cells (Fig. S2K). Particularly, cells without 53BP1 foci were enriched in the EdU negative population when H3.3 is overexpressed (Fig S2K right), thus excluding that H3.3 activity on 53BP1 was confined to replicating cells. Similar results were obtained overexpressing DAXX (Fig. S2L). No clear cell cycle specificity for 53BP1 reduction was also detectable when cells were stained for 53BP1 and cyclin B1, to mark late S/G2 cells. Indeed, also in this case cells with reduced 53BP1 foci, due to DAXX or H3.3 overexpression, were detectable both in G1/early S and late S/G2 categories (Fig. S2M).

DAXX regulates DNA repair pathway choice, efficiency and fidelity through H3.3

Accumulation of 53BP1 at DSBs counteracts resection contributing to repress HR (Chapman et al, 2013). Therefore, we speculated that the delay in 53BP1 foci formation could produce an unbalance in DNA repair pathway choice, increasing HR in the case of DAXX overexpression and, conversely, reducing HR as consequence of DAXX silencing. As a marker for HR we tested RAD51 foci formation, since localization of this protein on resected DNA is an essential step during HR. We focused our attention on late S/G2 phase cells, where HR and NHEJ are both active (Ciccia & Elledge, 2010). To this aim, we stained cells with both anti-RAD51 and anti-cyclin B1 antibodies (Fig. S3A), since cyclin B1 accumulates in the cytoplasm of G2 cells. In accordance with the hypothesis, we observed a significant reduction of RAD51 foci in the absence of DAXX and an increase upon DAXX overexpression (Fig. 3A and Fig. S3A). These results were not influenced by RAD51 protein levels. Indeed, DAXX knock-down did not alter the amount of RAD51, whereas a slight reduction in RAD51 levels is detectable in DAXX overexpressing cells (Fig. S3B), where RAD51 foci increase. Also in this case we tested a possible role for HIRA, but no significant effects on RAD51 foci formation in G2 cells were detectable in HIRA silenced cells (Fig. S3C).

Since RAD51 accumulation at DSBs is a specific, but intermediate, step during HR, to confirm the relevance of DAXX for DNA repair we tested also BRCA1 recruitment at damage sites, which is an early event of HR pathway (Munoz et al., 2012). In this case we co-stained BRCA1 with cyclin A, which marks S/G2 cells, and with EdU to detects cells in S phase. The analysis of G2 cells produced data resembling those for RAD51 but that never reached a statistical significance (data not shown). At the same time we interestingly found that DAXX overexpression induces BRCA1 foci formation in 19% of G1 cells, which are normally negative for BRCA1 accumulation at breaks (EdU negative/cyclin A negative cells, Fig. 3B and Fig. S3D). This phenotype resembles that of 53BP1 silencing (Feng et

al., 2013), further demonstrating the negative role of DAXX in 53BP1 recruitment at damage site.

To further confirm DAXX requirement for HR, we used reporter cell lines engineered to reveal by GFP production when HR (Fig. 3C) or classic NHEJ (Fig. 3D) are utilized to repair a DSB derived from an I-SceI cut site (Gunn & Stark, 2012). Consistently with the data reported above, HR was impaired by DAXX silencing (Fig. 3C), whereas no significant effect on classic NHEJ was detected (Fig. 3D). These data were not influenced by alterations of cell cycle distribution, as demonstrated by a cytofluorimetric analysis of siCON and siDAXX cellular population (Fig. S3E). We were unable to use this assay in the context of DAXX overexpression as transient DAXX transfection, differently from inducible stable clones, affects cell cycle progression (data not shown).

Unbalancing of DNA repair pathways choice affects the efficiency of DNA breaks rejoining. To test global DNA repair, we treated U2OS cells with the radiomimetic drug neocarzinostatin (NCS) that acutely induces DNA breaks. We found that in presence of 0.5nM NCS DAXX overexpression delays 53BP1 foci formation (Fig. S3F). The same treatment leads to a peak of 26.3±9.6 γ-H2AX foci (2.5±2.2 in untreated cells), generating more than 90% positive cells (>10 γ-H2AX foci/cell), regardless of DAXX or H3.3 expression (Fig. 3E and S3G). A defect in DNA repair, suggested by the persistence of γ-H2AX foci positive cells at 8 and 24hrs after NCS exposure, was observed in cells overexpressing DAXX (Fig. 3E) and H3.3 (Fig. S3G) compared to mock transfected cells.

Since HR is a high fidelity repair mechanism, defects in this pathway could induce accumulation of unligated or aberrantly repaired DNA breaks and loss of DNA fragments detectable as micronuclei formation (Medvedeva et al, 2007). Consistently, we found that more than 45% of DAXX-depleted cells, but less than 25% of control cells, accumulate

micronuclei 24hrs after NCS exposure (Fig. 3F). A less pronounced increase in micronuclei presence is detectable also in DAXX overexpressing cells (Fig. 3F), in accordance with the fact that also NHEJ inhibition promotes micronuclei formation (Oliveira et al., 2003).

Altogether, these data demonstrate a role for the DAXX/H3.3 axis in DNA repair pathway choice and, as a consequence, in breaks rejoining fidelity.

DAXX is phosphorylated at S424 and S712 by ATM/ATR in response to DNA damage

Our findings that DAXX-H3.3 interaction and H3.3 deposition are modulated in presence of DNA breaks, prompted us to evaluate the mechanism responsible for DAXX regulation in this context. The DNA damage response to DSBs primarily involves a cascade of phosphorylation events driven by the Ataxia Telangiectasia Mutated (ATM) and the Ataxia Telangiectasia and Rad3 Related (ATR) apical kinases. Two independent screenings (Matsuoka et al, 2007; Stokes et al, 2007), suggested that upon DNA damage ATM/ATR phosphorylate DAXX on Serine 424 and Serine 712 (S424 and S712), which are specifically conserved in mammalian DAXX proteins, with the exception of S712 in mice (Fig. 4A). These residues (Fig. 4B) are not located in the region of DAXX directly in contact with H3.3 (aa 178-389, Elsasser et al, 2015), but S712 is in the PML-binding region (aa 625-740, Salomoni, 2013). To confirm that these two residues are *bona fide* targets of DNA damage-induced kinases, we developed antibodies (pS424 and pS712) against these phosphoresidues. We transiently expressed HA tagged versions of WT and S424 or S712A mutant forms of DAXX in U2OS cells and after HA immunoprecipitation we verified that these sites are phosphorylated upon BLE treatment (Fig. 4C). In addition, the sensitivity of pS712 antibody allowed us to confirm the presence of this phosphorylation also in the endogenous DAXX protein immunoprecipitated from cells exposed to BLE (Fig.

S4A). Both these sites are targeted within 1hr after the addition of BLE, thus suggesting a role in the early events of the DNA damage response (Fig. S4B).

To further characterize the phosphorylation of DAXX in relation to the type of DNA damage, we exposed cells to different genotoxic agents: 4-NQO, an UV mimetic drug, etoposide, a topoisomerase II inhibitor, 30Gy ionizing radiation (IR). At the 3hrs timepoint S424 was phosphorylated in response to BLE and 4-NQO, but only slightly in response to IR, while S712 residue was phosphoryated following BLE, IR and etoposide exposure (Fig. S4C).

To test the relative contribution of ATM and ATR to S424 and S712 phosphorylation in presence of BLE we pre-treated cells with specific ATM and ATR inhibitors (respectively, KU-55933, Hickson et al, 2004, and VE-821, Prevo et al, 2012). ATM autophosphorylation at S1981 and ATR-dependent phosphorylation of Chk1 at S345 were used as specific reporters of these kinases activity. We found that ATM inhibition completely abolished BLE-induced S712 and S424 phosphorylations, while ATR participated in a limited manner to S712 phosphorylation (Fig. 4D). Furthermore, in response to BLE, S424A mutation partially affects S712 phosphorylation and *viceversa* (Fig. 4E). Altogether, these data demonstrate that S424 and S712 are phosphorylated by ATM within 1hr in presence of DSBs.

It is common during DNA damage response that a phosphorylation event could influence the localization of the protein on DNA lesion. Therefore we analyzed by immunofluorescence (Fig. 4F) and by PLA (Fig. 4G) the localization of S424A and S712A single and double mutants. No differences were detectable between WT and phosphomutants localization (compare Fig. 4F with Fig. 1E and Fig. 4G with Fig. 1G),

indicating that DAXX localization on DNA lesions is unaffected by S424A and S712A mutations.

DAXX chaperone activity at DNA breaks is regulated by S424 and S712 phosphorylation

The finding that DAXX phosphorylation on S424 and S712 occurs rapidly in response to DSBs inducing agents led us to hypothesize that these post-translational modifications might regulate DAXX chaperone activity. To explore this possibility we initially tested the effect of S424A and S712A mutations on H3.3 deposition. For this purpose, we generated cells stably silenced for DAXX (shDAXX) expressing an inducible phosphomutant form of DAXX resistant to silencing (Fig. S5A), to exclude the effect of endogenous DAXX. Cells expressing $DAXX^{S424A}$ or $DAXX^{S712A}$, compared to $DAXX^{WT}$, showed a reduction of H3.3 presence into the chromatin after damage, in both U2OS (Fig. 5A and S5B) and HEK293T cells (Fig. S5C). As an effect of functional DAXX overexpression, H3.3 accumulation in $DAXX^{WT}$ cells is more sustained than parental U2OS (compare Fig. 5A and 1A right panel). H3.3 accumulation at the sites of damage was confirmed by testing H3.3 coimmunoprecipitation with γ-H2AX at 1hr and 3hrs after BLE exposure. Remarkably, in $DAXX^{WT}$ expressing cells γ-H2AX-H3.3 association increased from 1 to 3hrs (Fig. 5B), whereas both mutants exhibit an alteration in the kinetics. In cells expressing DAXX mutants, 1hr after BLE treatment, the amount of co-immunoprecipitated γ-H2AX-H3.3 is higher than in cells expressing the WT protein, but 3hrs after damage the γ-H2AX-H3.3 association is reduced to background levels (Fig. 5B) as it was observed for shDAXX cells (Fig. 1CB), demonstrating that phosphosite mutations affect the H3.3 loading activity of DAXX after damage. To investigate whether the physical interaction between DAXX and

H3.3 histone is impaired, we performed coimmunoprecipitation assays using HA-tagged DAXX variants. In the absence of damage H3.3 interacts with $DAXX^{WT}$ and phosphomutants in U2OS (Fig. 5C) and in HEK293T cell lines (Fig. S5D), confirming that ATRX is not relevant for this association. However, the presence of DNA breaks strongly induced DAXX-H3.3 interaction in $DAXX^{WT}$, whereas the induction was moderate with $DAXX^{S712A}$ and absent with $DAXX^{S424A}$. Figure S5D also shows that, in HEK293T cells, the physical interaction of ATRX with $DAXX^{WT}$ and $DAXX^{S712A}$ is augmented by DNA damage, while no increase was detectable with S424A mutant. These data demonstrate that DAXX phosphorylation on S424 and S712 regulates the interaction between DAXX and histone H3.3 and promotes the loading of H3.3 at damage sites. Moreover, S424 phosphorylation is also relevant for DAXX-ATRX interaction in presence of exogenous damage.

Previous work described a role for DAXX in the DDR in regulating p53 protein through the interaction with HAUSP, an ubiquitin-specific protease (Tang et al, 2015), although this function has recently been disputed (Brazina et al, 2015). We tested p53 protein levels and DAXX-HAUSP physical interaction and show that phosphosite mutations in DAXX do not have any effect on either (Fig. S5E and Fig. S5F), indicating that these phosphorylation events do not have a general effect on DAXX interactions and activity.

Remarkably, S424A and S712A mutations prevented the delay in 53BP1 foci formation induced by overexpression of DAXX (Fig. 5D). Of note, alteration of 53BP1 foci formation was not due to different levels of total 53BP1 protein (Fig S5G), nor to alteration of cell cycle progression (Fig. S5H).

These data indicate that DAXX phosphorylation by ATM/ATR influences 53BP1 recruitment at DSBs through the regulation of DAXX/H3.3 interaction and H3.3 deposition into the chromatin.

To test the relevance of DAXX phosphorylation for its activity on DNA repair, shDAXX cells expressing phosphomutant DAXX were tested for RAD51 foci formation, γ-H2AX foci resolution and micronuclei presence following DNA damage induction. Remarkably, we found that the expression of both S424A and S712A, differently from WT DAXX (Fig. 3A), reduces the number of RAD51 foci (Fig. 5E) and do not slow down DNA repair (compare Fig. 3E and Fig. 5F) but enhance micronuclei formation (Fig. 5G and Fig. S5I for alternative clones to exclude a background effect).

Altoghether these data demonstrate that DAXX chaperone activity during the DNA damage response is regulated by DAXX phosphorylation on S424 and S712 by ATMA/ATR. This phosphorylative events, as a consequence influence DNA repair choice and fidelity.

H3.3 methylation at K36 is relevant for DAXX and H3.3 regulation of 53BP1 localization

Our results demonstrate that DAXX controls H3.3 deposition on DSB-containing chromosomes, influences 53BP1 foci formation and modulates DNA repair pathway choice. To obtain a better insight into the mechanisms, we focused our attention on histone post translational modifications (PTMs). Indeed, both 53BP1 recruitment and repair choice depend on pre-existing or damage-induced PTMs (Panier & Boulton, 2014). Furthermore, it was previously shown that histone H3.3 exhibits peculiar PTMs when compared to the classical H3.1 (Hake et al, 2006; Loyola et al, 2006). Therefore, we overexpressed H3.3 and H3.1 in U2OS cells and analyzed the presence of the H3 PTMs known to be involved in 53BP1 recruitment and DNA repair (van Attikum & Gasser, 2009) on histones extracted

from purified chromatin. We found that while K79me, K4me3, K9Ac and K9me3 were present at the same level in exogenous H3.3 and H3.1 (Fig. 6A), K36 di- and tri-methylation were enriched in H3.3 (Fig. 6A). In any case, PTMs tested on exogenous histones were unaffected by BLE treatment (Fig. 6A). Similar results were obtained in HEK293T cells, although the differences between H3.3 and H3.1 were less prominent (Fig. S6A).

To confirm these observations we expressed in U2OS cells a mutated form of histone H3.3. Particularly, we mutagenized K36 to R, to impede PTMs and particularly methylation, at this site. We also mutagenized K36 residue to M, since K36M mutation was found in more than 90% of human chondroblastomas (Fang et al., 2016). Remarkably, while WT H3.3 expression represses 53BP1 spots formation, both K36 mutants (within H3.3-YFP or FLAG-H3.3) retains only a limited effect on this event (Fig. 6B and Fig. S6B) suggesting that H3.3K36 PTMs could be relevant for 53BP1 recruitment at DNA lesions.

To test a possible role for K36me on DAXX-dependent activities we silenced SETD2, the histone methyltransferase mainly responsible for K36 trimethylation (Edmunds et al, 2008), in H3.3 overexpressing cells and we found that depletion of this protein severely reduced K36me3 on both endogenous and exogenous H3.3 (Fig. 6C). Intriguingly, depression of H3.3-K36 tri-methylation partially rescued the retarded recruitment of 53BP1 at damage sites due to overexpression of DAXX and H3.3 (Fig. 6D). These data indicate a role for K36me3 on DAXX/H3.3 dependent recruitment of 53BP1 at damage sites.

DISCUSSION

Here, we describe a new activity of DAXX/H3.3 in the cellular response to DSBs. Indeed, we found that following formation of DSBs, histone H3.3 is loaded by DAXX at damage

sites. Such chromatin modification and the associated tri-methylation of H3.3 at lysine 36 modulate the recruitment of 53BP1 and influence DNA repair pathway choice. This new function of DAXX is controlled by the DNA damage response (DDR) apical kinases, ATM and ATR, through phosphorylation of S424 and S712.

Upon formation of DSBs, cells trigger the DDR that marks the lesion and activates the correct repair mechanisms (Ciccia & Elledge, 2010). We discovered that human cells exposed to the chemotherapeutic and DNA damaging agent bleomycin (BLE) transiently accumulate H3.3 in chromatin and this histone variant is closely associated to γ-H2AX, an early marker of DNA breaks found in a region that spans up to Mb from the lesion (Iacovoni et al, 2010). Furthermore, the H3.3 association with γ-H2AX increases with the time of BLE exposure and does not occur with H2AX, which is widespread on chromatin, demonstrating that H3.3 accumulates at damage sites and not everywhere in the genome. A more sensitive analysis performed by ChIP revealed that H3.3 accumulation is limited to a region very close to a DNA break. Up to now, damage-induced H3.3 accumulation was only detected at UV lesions (Adam et al, 2013) or after laser microirradiation (Luijsterburg et al, 2016). In both cases DAXX was not found to be responsible of H3.3 deposition. In this work we show that H3.3 accumulation at DSBs is almost exclusively DAXX-dependent but HIRA-independent. Indeed, using three different experimental approaches (chromatin purification, γ-H2AX/H3.3 association and ChIP followed by quantitative real time PCR) we demonstrated that H3.3 accumulation at DNA breaks is strongly impaired in the absence of DAXX protein. Therefore, DNA breaks promote histone turnover and H3.3 accumulation at damage sites, and this process depends on DAXX. These conclusions were further supported by the presence of DAXX nearby a fraction of DNA break as demonstrated by classical immunofluorescence, proximity ligation assay and ChIP. DAXX presence seems to span more than H3.3 accumulation region, up to 1300 nucleotides from the break.

However, it is important to note that DAXX depletion afflicts also H3.3 presence at 1300 nucleotides, suggesting that DAXX is relevant to accumulate H3.3 closely to broken DNA ends but also to maintain H3.3 presence in a more widespread region. An unknown negative signal could regulate the amount of H3.3 loaded by DAXX as a function of distance from the break site. Importantly, we obtained these data in a cell line which is negative for ATRX protein but also in an ATRX silenced background, thus excluding a role for this helicase in DAXX loading of H3.3 at DNA lesions. This indicates that DAXX functions in two independent pathways: at telomeres and centromers in complex with ATRX and at DSBs, possibly in complex with an alternative chromatin remodeller. Accordingly to this conclusion, we primarily tested DAXX activity on DNA repair and genome stability in ATRX-negative cells to exclude a contribution from telomeres and centromeres.

To investigate the possible role of H3.3 at damage sites, we evaluated the recruitment of sensors and apical kinases to breaks, which are tightly regulated by chromatin status (Panier & Boulton, 2014). We found that overexpression of H3.3 or wild type DAXX increased the loading of H3.3 on damaged chromatin and caused a delayed formation of 53BP1 foci. DAXX silencing *per se* had no effect on 53BP1 foci formation: this is not an unexpected result since 53BP1 is rapidly localized on any DSB, so we could not attend an increase in 53BP1 foci in a DAXX-knockdown background. However, DAXX silencing strongly reduced the effect of H3.3 overexpression on 53BP1 foci and this effect was not obtained with HIRA silencing, confirming this chaperone as irrelevant for DAXX/H3.3 activity at DSBs and for 53BP1 relocalization. This indicates that the recruitment of 53BP1 at damage sites can be altered by the specific DAXX-dependent massive incorporation of H3.3 in the DSB region. These data were confirmed also in cells damaged by AsiSI restriction enzyme, which is known to produce DNA breaks specifically in euchromatin

(Aymard et al, 2014), suggesting that the DAXX/H3.3 pathway may be preferentially active at breaks occurring within transcribed regions. This is in agreement with the observation that DAXX protein localizes only on a fraction of DNA breaks induced by BLE. Altogether, we conclude that the DAXX/H3.3 pathway is a novel regulator of 53BP1 relocalization at DNA breaks. Importantly, this activity is not cell cycle phase specific, confirming that H3.3 loading by DAXX is replication-independent.

We then asked whether, altering 53BP1 recruitment, DAXX may affect the DNA damage response and repair. 53BP1 has an undefined role in the arrest of cell cycle at the G2/M checkpoint (Wang et al, 2002), but we did not find any effect of DAXX knock-down or overexpression on G2 arrest (data not shown). Importantly, 53BP1 plays a prominent role in regulating DSBs repair balance. NHEJ repair is fast, error prone and active in any phase of the cell cycle. HR is error-free, but slow and active exclusively in S and G2 phases, when a sister chromatid is available. Furthermore, it was suggested that HR is responsible for repairing less than 20% of the breaks occurring in G2 (Karanam et al, 2012) and occurs preferentially at DSB within transcribed sequences (Aymard et al, 2014). HR requires DSB ends to be resected by nucleolytic activities in order to generate ssDNA tails for strand invasion (Ciccia & Elledge, 2010). A finely regulated 53BP1 localization on DNA breaks, both in time and positioning, represses the access of HR factors, like BRCA1, and DNA resection, thus disfavouring the HR pathway (Zimmermann et al, 2013; Chapman et al, 2012). Coherently, the delayed 53BP1 foci formation due to increased H3.3 deposition by DAXX unbalances NHEJ/HR pathway choice, facilitating HR. Indeed, we observed that DAXX overexpression increases the accumulation of BRCA1 and RAD51 on damage while DAXX silencing has the opposite effect. Interestingly, in DAXX overexpressing cells, BRCA1 relocalization on DNA lesions partially occurs also in G1, a phase of the cell cycle when this protein should be excluded by damage. These data resemble those obtained by

53BP1 silencing (Feng et al., 2013), again underlining the inhibitory activity of DAXX on 53BP1 relocalization after damage. As a consequence, we expected that DAXX could influences HR/NHEJ balancing. Indeed, using a GFP based approach to study formation of the HR repair product we were able to reveal a reduction of HR activity in DAXX silenced cells, in absence of any cell cycle progression alterations.

Unbalancing DNA repair pathways can lead to slower breaks rejoining and low repair fidelity. Consistently, cells overexpressing DAXX and H3.3 exhibit a delay in DSB rejoining with a slightly increased genome instability that could derive from alternative-NHEJ pathways (Ferguson et al, 2000). Conversely, DAXX silencing or expression of DAXX mutants reduces HR leading to an increase in micronuclei formation. This event is DNA damage-dependent and occurs in ATRX negative cells, indicating that the genomic rearrangements originate from misregulated repair pathways and not from a DAXX/ATRX-dependent instability at telomeres or centromeres. On the whole we have found that DAXX has a role, through H3.3, in DNA repair in response to bleomycin, neocarzinostatin and restriction enzyme induced DSBs, therefore irrespectively to the DSBs inducing agent.

Recently, it was shown that H3.3 is loaded by CHD2 chromatin remodeller protein on clustered DSBs induced by laser microirradiation, and that H3.3 silencing reduces NHEJ repair (Luijsterburg et al, 2016). Furthermore, since DAXX/ATRX/H3.3 pathway is able to repress ALT, it was suggested that H3.3 deposition could repress the HR process that characterizes this pathway (Conomos et al, 2013). These two facts seem in contrast with our data demonstrating that H3.3 or DAXX overexpression promotes HR. However, apart from differences in damaging treatments and experimental approaches, and the fact that it is still unknown how DAXX represses ALT, many factors could influence the final outcome of H3.3 deposition. Particularly, it is important to point out three aspects. First, different chaperone or chaperone/helicase complexes could load different H3.3 histone subsets,

characterized by specific PTMs and since H3.3 is loaded in complex with H4 (Elsasser et al, 2012), H3.3 could also act through H4 PTMs. Second, H3.3 could be subjected to different PTMs depending on the different context where it is loaded (i.e. transcribed or untranscribed regions or different cell cycle phase). Third, H3.3 function could be influenced by the chromatin context. The importance of this aspect is underlined by the fact that H3.3 deposition correlates with opening chromatin activity at transcribed regions (Chen et al, 2013), but it is also enriched at highly heterochromatic centromeric and telomeric regions (Lewis et al, 2010) and at silenced retroviral elements (Elsasser et al, 2015).

Once defined the role for DAXX in H3.3 deposition at DSBs, we explored the molecular mechanism regulating DAXX histone chaperone activity in response to a DNA damage. We took advantage of previously described high-throughput screening that identified DAXX as a putative ATM/ATR substrate (Matsuoka et al, 2007; Stokes et al, 2007). ATM and ATR are the main upstream regulators of the DDR in human cells: while ATM is the most relevant apical kinase in response to DSBs, in presence of these lesions ATR can be also activated by ATM or can backup ATM activity (Ciccia & Elledge, 2010). The above mentioned works also determined S424 and S712 as possible target residues in DAXX. However up to now only S564 has been described as an ATM substrate with a specific activity in DAXX/p53 pathway regulation (Tang et al, 2013). To investigate the possible involvement of damage-induced DAXX phosphorylation in the repair of DSBs, we generated phosphospecific antibodies against S424 and S712 and demonstrated that they are indeed targeted preferentially by ATM in human cells exposed to DSBs inducing agents. We also generated human cell lines stably silenced for endogenous DAXX and expressing inducible WT or Serine-to-Alanine mutants for these residues. Interestingly, we found that the expression of $DAXX^{WT}$, but not phosphomutant versions, is able to provide

the function required for H3.3-γ-H2AX complex formation after damage. These data further corroborate the evidence that turnover and accumulation of H3.3 at DNA breaks substantially rely on the DNA damage-dependent activity of DAXX.

Successively, we asked how the H3.3 chaperone activity of DAXX was modulated in response to DNA damage. One hypothesis was that DAXX relocalization on DNA lesion is sufficient to target H3.3 loading. However, we found that S424, S712 and the double mutant did not alter DAXX localization at DNA breaks. On the contrary, the DNA damage induced DAXX/H3.3 interaction is strongly impaired in S424A and S712A mutants, similarly to the H3.3-γ-H2AX interaction. These data depict a model where DAXX is recruited at the sites of damage, but it needs site specific, DNA damage- and ATM-dependent phosphorylation events in order to enhance interaction with H3.3 and modify the chromatin around the lesion. Further analyses also showed that S424 phosphorylation regulates DAXX-ATRX interaction after DSBs, this aspect is particularly interesting and will need further investigation. Similarly, it would be intriguing to study the role of PML bodies in DAXX localization on damage, also in cosideration of the fact that S712 residue is located inside a PML-interacting region of DAXX.

We next wondered how H3.3 deposition nearby a DNA break could influence DNA repair. This histone variant shows peculiar PTMs and this aspect could suggest a possible mechanism for H3.3 activity. Indeed, we provide evidence that H3.3 inside chromatin accumulates higher levels of K36 di- and tri-methylation compared to H3.1, coherently with previous works (Hake et al, 2006; Loyola et al, 2006). Interestingly, both through the mutagenesis of K36 residue to arginine and through silencing the K36 trimethylase SETD2, we were able to restore the wild type kinetics of 53BP1 foci formation after damage, in the presence of DAXX or H3.3 overexpression, suggesting for the first time that

K36me3 may affect 53BP1 recruitment at damage site. Coherently with what we obtained with DAXX and H3.3, it was previously published that K36me2 promotes the recruitment at damage sites of Nbs1/Mre11 complex (Cao et al, 2016), which is critical to start resection during HR. Furthermore, in agreement with our data, H3K36me3 and SETD2 were described as relevant to promote HR if DSB occurs within transcribed regions (Pfister et al, 2014; Aymard et al, 2014). We propose that H3.3 deposition could contribute to locally maintain or even enrich K36 methylated histones. This will favour HR versus NHEJ for the repair of lesions occurring in a specific transcription context. However, we cannot exclude that other mechanisms could be involved in H3.3 regulation of DNA repair.

Strikingly, K36 methylation seems altered in two H3.3 mutations (G34R and G34V) that are common in cerebral hemispheric paediatric glioblastoma (Schwartzentruber et al, 2012) and in K36M mutation found in chondroblastoma. Consistently, about 15% of paediatric glioblastoma showed SETD2 inactivation (Fontebasso et al, 2013). SETD2 mutations were also described as affecting DNA repair in renal cancer (Kanu et al, 2015). ATRX (or rarely DAXX) mutations were found in 100% of G34-H3.3 mutant cases (Schwartzentruber et al, 2012); (Behjati et al, 2013), indicating that ATRX/ALT axis is not overlapping with G34 mutations. Of note, we found that K36M mutation is unable to delay 53BP1 recruitment compared to wild type H3.3. Therefore, previous evidence and our findings suggest that DAXX and H3.3 alterations could favour tumorigenesis through multiple aspects: acquisition of ALT, enhanced transcription of oncogenes and increased genomic instability due to imprecise repair. As a consequence, DAXX/H3.3 pathway could be relevant for diagnosis and therapy of some particularly aggressive forms of cancer.

MATHERIAL AND METHODS

Cells, transfections and treatments. Human osteosarcoma cell line U2OS, EJ5-GFP and DR-GFP U2OS (Gunn & Stark, 2012) and human embryonic kidney cell line HEK293T were cultured in Dulbecco's modified Eagle's medium (DMEM) with 10% fetal bovine serum (FBS). Cells were maintained at 37°C in a humidified atmosphere containing 5% CO2. Stably transduced cell lines were selected in medium containing 600µg/ml G418, 10µg/ml blasticidin and 1.8µg/ml puromycin. To induce DAXX expression, doxocyclin was added at 0.8-1.2µg/ml. Cells were transfected using Lipofectamine 3000 or RNAiMAX according to manufacturer instructions. Bleomycin treatments were performed at 12 or 120µM. Neocarzinostatin was used at a concentration of 0.2 or 0.5nM, 4-NQO and etoposide was added at 10µM. Cells were irradiated using a ^{137}Ce source. The ATM (KU-55933) or ATR (VE821) inhibitors were added, respectively, at 10 and 2µM, 1hr before bleomycin. Arsenic trioxide was added at 1µM for 18hrs.

Antibodies. Antibodies are listed in Supplemental Experimental Procedures, Table S1. DAXX phospho-S424 and phospho-712 antibodies were generated by ImmunoGlobe. They were negatively purified against specific unphosphorylated peptides and, for phospo-S424 antibody against a phosphorylated S712 peptide and viceversa. Finally, they were positively purified using their own specific phospho-peptides.

Expression vectors and siRNAs. U2OS cell lines silenced for DAXX were obtained by stable transfection of shDAXX sequence cloned in the pENTER U6 vector of the BLOCK-iT™ U6 RNAi Entry Vectors. Human DAXX cDNA was cloned in the pcDNA3-HA vector for transient transfections or in the pTRE3G vector of the Tet-ON 3G Inducible Expression System for stable transfections. The DAXX cDNA sequence for the Tet-ON system contains two silent mutations within the region targeted by the DAXX shRNA to escape the

silencing. Silencing sequences are listed in Supplemental Experimental Procedures, Table S2. H3.3-YFP plasmid was obtained from Addgene (#8693). H3.3 gene was successively cloned in the pcDNA3-FLAG vector.

Immunofluorescence. Immunofluorescence assays were performed as previously described (Carlessi et al, 2010). Antibodies concentrations are listed in Supplemental Table S1. EdU staining was performed with the Click-it EdU assay kit. *In situ* Proximity ligation assays were performed as previously described (Soderberg et al, 2006). Images were captured with a Leica Microsystems DMRA2 microscope equipped with a DFC450C camera.

Cell extracts. Cells were routinely lysed with Laemmli or ELB buffer. Chromatin purification was performed as previously reported (Mendez & Stillman, 2000). Histones were extracted from chromatin fraction by Laemmli buffer or acid extraction (Shechter et al, 2007). Western blots were performed with the antibodies listed in Supplemental Table S1. Densitometric analyses were done with the ImageQuant software.

Immunoprecipitations. Immunoprecipitations were performed as in (Magni et al, 2014). Oligonucleosome preparation and γ-H2AX immunoprecipitation was previously described (Magni et al, 2015).

Chromatin immunoprecipitation and quantitative real time PCR. Chromatin immunoprecipitations were performed essentially as described in ref. Briefly, U2OS-DR-GFP cells were transfected with mock or SceI encoding vectors and, 48hrs, later fixed with 1% formaldehyde. For DAXX depletion, cells were transfected with control or DAXX siRNAs and 24hrs later with FLAG-H3.3 and mock or SceI vectors. Cells were then lysed in RIPA buffer and sonicated with Bioruptor Plus sonication device (Diagenode). Immunoprecipitations were performed with 2µg of anti-DAXX (Santa Cruz Biotechnology)

or anti-FLAG-M2 (Sigma) antibodies. Immunoprecipitated DNA was purified with the Chromatin IP DNA Purification kit (Active Motif) and analyzed by real-time PCR with a 7900HT Fast Real-Time PCR system (Thermo-Fisher) and Fast SYBR Green Master Mix (Thermo Fisher). Results were calculated with the percent input method and expressed as the ratio of the DNA immunoprecipitated after SceI expression and the DNA immunoprecipitated from mock transfected cells. Primer used are: DR-GFP+500for 5'-AGCTCGCCGACCACTACCAG-3', DR-GFP+500rev 5'-CGTTGGGGTCTTTGCTCAGG-3', DR-GFP+1300for 5'-CCCCCGTAGCTCCAATCCTT-3', DR-GFP+1300rev 5'-CCAGGAGCGGATCGAAATTG-3', GAPDHfor 5'-AATCCCATCACCATCTTCCA-3' GAPDHrev 5'-TGGACTCCACGACGTACTCA-3'.

NHEJ and HR reporter assays. To evaluate repair pathways incidence, U2OS EJ5-GFP and DR-GFP cells were silenced for DAXX, BRCA1 and control. After 48hrs cells were transfected with the I-SceI expression plasmid (pCBASceI, Addgene, #26477) in combination with a reduced amount of DAXX, BRCA1 or control siRNA; 96hrs after the initial silencing, cells were harvested and GFP-positive cells were detected by flow cytometry using a BD FACSCantoII (more than 20,000 events acquired). Data were analyzed using FlowJo.

ACKNOWLEDGMENTS

We thank Prof. J. Stark and Prof. S. Piccolo for providing cell lines, G. Abolafio and C. Chiodoni for flow cytometry assistance, members of the M.M.F., P. Plevani and A. Pellicioli labs for comments and suggestions. This work was partially supported by MIUR (PRIN) and AIRC grants to M.M.F.

AUTHOR CONTRIBUTIONS

Conceptualization and Methodology: G.B., D.D. and M.M.F.; Investigation and Validation: S.A., L.Z., C.R., G.B.; Supervision, Data curation, Visualization: G.B.; Writing-Original draft: G.B. and M.M.Z.; Review & Editing: D.D., L.Z. and S.A.

REFERENCES

Adam S, Polo SE, & Almouzni G (2013) Transcription recovery after DNA damage requires chromatin priming by the H3.3 histone chaperone HIRA. *Cell* **155**: 94-106

Ahmad K & Henikoff S (2002) Histone H3 variants specify modes of chromatin assembly. *Proc Natl Acad Sci U S A* **99 Suppl 4**: 16477-16484

Aymard F, Bugler B, Schmidt CK, Guillou E, Caron P, Briois S, Iacovoni JS, Daburon V, Miller KM, Jackson SP, & Legube G (2014) Transcriptionally active chromatin recruits homologous recombination at DNA double-strand breaks. *Nat Struct Mol Biol* **21**: 366-374

Behjati S, Tarpey PS, Presneau N, Scheipl S, Pillay N, Van Loo P, Wedge DC, Cooke SL, Gundem G, Davies H, Nik-Zainal S, Martin S, McLaren S, Goody V, Robinson B, Butler A, Teague JW, Halai D, Khatri B, Myklebost O et al (2013) Distinct H3F3A and H3F3B driver mutations define chondroblastoma and giant cell tumor of bone. *Nat Genet* **45**: 1479-1482

Bjerke L, Mackay A, Nandhabalan M, Burford A, Jury A, Popov S, Bax DA, Carvalho D, Taylor KR, Vinci M, Bajrami I, McGonnell IM, Lord CJ, Reis RM, Hargrave D, Ashworth A, Workman P, & Jones C (2013) Histone H3.3. mutations drive pediatric glioblastoma through upregulation of MYCN. *Cancer Discov* **3**: 512-519

Brazina J, Svadlenka J, Macurek L, Andera L, Hodny Z, Bartek J, & Hanzlikova H (2015) DNA damage-induced regulatory interplay between DAXX, p53, ATM kinase and Wip1 phosphatase. *Cell Cycle* **14**: 375-387

Cao LL, Wei F, Du Y, Song B, Wang D, Shen C, Lu X, Cao Z, Yang Q, Gao Y, Wang L, Zhao Y, Wang H, Yang Y, & Zhu WG (2016) ATM-mediated KDM2A phosphorylation is required for the DNA damage repair. *Oncogene* **35**: 301-313

Carlessi L, Buscemi G, Fontanella E, & Delia D (2010) A protein phosphatase feedback mechanism regulates the basal phosphorylation of Chk2 kinase in the absence of DNA damage. *Biochim Biophys Acta* **1803**: 1213-1223

Chapman JR, Barral P, Vannier JB, Borel V, Steger M, Tomas-Loba A, Sartori AA, Adams IR, Batista FD, & Boulton SJ (2013) RIF1 is essential for 53BP1-dependent nonhomologous end joining and suppression of DNA double-strand break resection. *Mol Cell* **49**: 858-871

Chapman JR, Sossick AJ, Boulton SJ, & Jackson SP (2012) BRCA1-associated exclusion of 53BP1 from DNA damage sites underlies temporal control of DNA repair. *J Cell Sci* **125**: 3529-3534

Chen P, Zhao J, Wang Y, Wang M, Long H, Liang D, Huang L, Wen Z, Li W, Li X, Feng H, Zhao H, Zhu P, Li M, Wang QF, & Li G (2013) H3.3 actively marks enhancers and primes gene transcription via opening higher-ordered chromatin. *Genes Dev* **27**: 2109-2124

Ciccia A & Elledge SJ (2010) The DNA damage response: making it safe to play with knives. *Mol Cell* **40**: 179-204

Conomos D, Pickett HA, & Reddel RR (2013) Alternative lengthening of telomeres: remodeling the telomere architecture. *Front Oncol* **3**: 27

Delbarre E, Jacobsen BM, Reiner AH, Sorensen AL, Kuntziger T, & Collas P (2010) Chromatin environment of histone variant H3.3 revealed by quantitative imaging and genome-scale chromatin and DNA immunoprecipitation. *Mol Biol Cell* **21**: 1872-1884

Drane P, Ouararhni K, Depaux A, Shuaib M, & Hamiche A (2010) The death-associated protein DAXX is a novel histone chaperone involved in the replication-independent deposition of H3.3. *Genes Dev* **24**: 1253-1265

Edmunds JW, Mahadevan LC, & Clayton AL (2008) Dynamic histone H3 methylation during gene induction: HYPB/Setd2 mediates all H3K36 trimethylation. *EMBO J* **27**: 406-420

Elsasser SJ, Huang H, Lewis PW, Chin JW, Allis CD, & Patel DJ (2012) DAXX envelops a histone H3.3-H4 dimer for H3.3-specific recognition. *Nature* **491**: 560-565

Elsasser SJ, Noh KM, Diaz N, Allis CD, & Banaszynski LA (2015) Histone H3.3 is required for endogenous retroviral element silencing in embryonic stem cells. *Nature* **522**: 240-244

Ferguson DO, Sekiguchi JM, Frank KM, Gao Y, Sharpless NE, Gu Y, Manis J, DePinho RA, & Alt FW (2000) The interplay between nonhomologous end-joining and cell cycle checkpoint factors in development, genomic stability, and tumorigenesis. *Cold Spring Harb Symp Quant Biol* **65**: 395-403

Fontebasso AM, Schwartzentruber J, Khuong-Quang DA, Liu XY, Sturm D, Korshunov A, Jones DT, Witt H, Kool M, Albrecht S, Fleming A, Hadjadj D, Busche S, Lepage P,

Montpetit A, Staffa A, Gerges N, Zakrzewska M, Zakrzewski K, Liberski PP et al (2013) Mutations in SETD2 and genes affecting histone H3K36 methylation target hemispheric high-grade gliomas. *Acta Neuropathol* **125**: 659-669

Goodarzi AA, Noon AT, Deckbar D, Ziv Y, Shiloh Y, Lobrich M, & Jeggo PA (2008) ATM signaling facilitates repair of DNA double-strand breaks associated with heterochromatin. *Mol Cell* **31**: 167-177

Gunn A & Stark JM (2012) I-SceI-based assays to examine distinct repair outcomes of mammalian chromosomal double strand breaks. *Methods Mol Biol* **920**: 379-391

Hake SB, Garcia BA, Duncan EM, Kauer M, Dellaire G, Shabanowitz J, Bazett-Jones DP, Allis CD, & Hunt DF (2006) Expression patterns and post-translational modifications associated with mammalian histone H3 variants. *J Biol Chem* **281**: 559-568

Hands KJ, Cuchet-Lourenco D, Everett RD, & Hay RT (2014) PML isoforms in response to arsenic: high-resolution analysis of PML body structure and degradation. *J Cell Sci* **127**: 365-375

Harada A, Maehara K, Sato Y, Konno D, Tachibana T, Kimura H, & Ohkawa Y (2015) Incorporation of histone H3.1 suppresses the lineage potential of skeletal muscle. *Nucleic Acids Res* **43**: 775-786

Heaphy CM, de Wilde RF, Jiao Y, Klein AP, Edil BH, Shi C, Bettegowda C, Rodriguez FJ, Eberhart CG, Hebbar S, Offerhaus GJ, McLendon R, Rasheed BA, He Y, Yan H, Bigner DD, Oba-Shinjo SM, Marie SK, Riggins GJ, Kinzler KW et al (2011) Altered telomeres in tumors with ATRX and DAXX mutations. *Science* **333**: 425

Hickson I, Zhao Y, Richardson CJ, Green SJ, Martin NM, Orr AI, Reaper PM, Jackson SP, Curtin NJ, & Smith GC (2004) Identification and characterization of a novel and specific inhibitor of the ataxia-telangiectasia mutated kinase ATM. *Cancer Res* **64**: 9152-9159

Iacovoni JS, Caron P, Lassadi I, Nicolas E, Massip L, Trouche D, & Legube G (2010) High-resolution profiling of gammaH2AX around DNA double strand breaks in the mammalian genome. *EMBO J* **29**: 1446-1457

Kanu N, Gronroos E, Martinez P, Burrell RA, Yi Goh X, Bartkova J, Maya-Mendoza A, Mistrik M, Rowan AJ, Patel H, Rabinowitz A, East P, Wilson G, Santos CR, McGranahan N, Gulati S, Gerlinger M, Birkbak NJ, Joshi T, Alexandrov LB et al (2015) SETD2 loss-of-function promotes renal cancer branched evolution through replication stress and impaired DNA repair. *Oncogene* **34**: 5699-5708

Karanam K, Kafri R, Loewer A, & Lahav G (2012) Quantitative live cell imaging reveals a gradual shift between DNA repair mechanisms and a maximal use of HR in mid S phase. *Mol Cell* **47**: 320-329

Lallemand-Breitenbach V & de The H (2010) PML nuclear bodies. *Cold Spring Harb Perspect Biol* **2**: a000661

Lewis PW, Elsaesser SJ, Noh KM, Stadler SC, & Allis CD (2010) Daxx is an H3.3-specific histone chaperone and cooperates with ATRX in replication-independent chromatin assembly at telomeres. *Proc Natl Acad Sci U S A* **107**: 14075-14080

Lovejoy CA, Li W, Reisenweber S, Thongthip S, Bruno J, de Lange T, De S, Petrini JH, Sung PA, Jasin M, Rosenbluh J, Zwang Y, Weir BA, Hatton C, Ivanova E, Macconaill L, Hanna M, Hahn WC, Lue NF, Reddel RR et al (2012) Loss of ATRX, genome instability,

and an altered DNA damage response are hallmarks of the alternative lengthening of telomeres pathway. *PLoS Genet* **8**: e1002772

Loyola A, Bonaldi T, Roche D, Imhof A, & Almouzni G (2006) PTMs on H3 variants before chromatin assembly potentiate their final epigenetic state. *Mol Cell* **24**: 309-316

Luijsterburg MS, de Krijger I, Wiegant WW, Shah RG, Smeenk G, de Groot AJ, Pines A, Vertegaal AC, Jacobs JJ, Shah GM, & van Attikum H (2016) PARP1 Links CHD2-Mediated Chromatin Expansion and H3.3 Deposition to DNA Repair by Non-homologous End-Joining. *Mol Cell* **61**: 547-562

Magni M, Ruscica V, Buscemi G, Kim JE, Nachimuthu BT, Fontanella E, Delia D, & Zannini L (2014) Chk2 and REGgamma-dependent DBC1 regulation in DNA damage induced apoptosis. *Nucleic Acids Res* **42**: 13150-13160

Magni M, Ruscica V, Restelli M, Fontanella E, Buscemi G, & Zannini L (2015) CCAR2/DBC1 is required for Chk2-dependent KAP1 phosphorylation and repair of DNA damage. *Oncotarget* **6**: 17817-17831

Matsuoka S, Ballif BA, Smogorzewska A, McDonald ER,3rd, Hurov KE, Luo J, Bakalarski CE, Zhao Z, Solimini N, Lerenthal Y, Shiloh Y, Gygi SP, & Elledge SJ (2007) ATM and ATR substrate analysis reveals extensive protein networks responsive to DNA damage. *Science* **316**: 1160-1166

Medvedeva NG, Panyutin IV, Panyutin IG, & Neumann RD (2007) Phosphorylation of histone H2AX in radiation-induced micronuclei. *Radiat Res* **168**: 493-498

Mendez J & Stillman B (2000) Chromatin association of human origin recognition complex, cdc6, and minichromosome maintenance proteins during the cell cycle: assembly of prereplication complexes in late mitosis. *Mol Cell Biol* **20**: 8602-8612

Newhart A, Rafalska-Metcalf IU, Yang T, Negorev DG, & Janicki SM (2012) Single-cell analysis of Daxx and ATRX-dependent transcriptional repression. *J Cell Sci* **125**: 5489-5501

Panier S & Boulton SJ (2014) Double-strand break repair: 53BP1 comes into focus. *Nat Rev Mol Cell Biol* **15**: 7-18

Pfister SX, Ahrabi S, Zalmas LP, Sarkar S, Aymard F, Bachrati CZ, Helleday T, Legube G, La Thangue NB, Porter AC, & Humphrey TC (2014) SETD2-dependent histone H3K36 trimethylation is required for homologous recombination repair and genome stability. *Cell Rep* **7**: 2006-2018

Polo SE & Almouzni G (2015) Chromatin dynamics after DNA damage: The legacy of the access-repair-restore model. *DNA Repair (Amst)* **36**: 114-121

Prevo R, Fokas E, Reaper PM, Charlton PA, Pollard JR, McKenna WG, Muschel RJ, & Brunner TB (2012) The novel ATR inhibitor VE-821 increases sensitivity of pancreatic cancer cells to radiation and chemotherapy. *Cancer Biol Ther* **13**: 1072-1081

Salomoni P (2013) The PML-Interacting Protein DAXX: Histone Loading Gets into the Picture. *Front Oncol* **3**: 152

Salomoni P & Khelifi AF (2006) Daxx: death or survival protein? *Trends Cell Biol* **16**: 97-104

Schwartzentruber J, Korshunov A, Liu XY, Jones DT, Pfaff E, Jacob K, Sturm D, Fontebasso AM, Quang DA, Tonjes M, Hovestadt V, Albrecht S, Kool M, Nantel A, Konermann C, Lindroth A, Jager N, Rausch T, Ryzhova M, Korbel JO et al (2012) Driver mutations in histone H3.3 and chromatin remodelling genes in paediatric glioblastoma. *Nature* **482**: 226-231

Shechter D, Dormann HL, Allis CD, & Hake SB (2007) Extraction, purification and analysis of histones. *Nat Protoc* **2**: 1445-1457

Soderberg O, Gullberg M, Jarvius M, Ridderstrale K, Leuchowius KJ, Jarvius J, Wester K, Hydbring P, Bahram F, Larsson LG, & Landegren U (2006) Direct observation of individual endogenous protein complexes in situ by proximity ligation. *Nat Methods* **3**: 995-1000

Stokes MP, Rush J, Macneill J, Ren JM, Sprott K, Nardone J, Yang V, Beausoleil SA, Gygi SP, Livingstone M, Zhang H, Polakiewicz RD, & Comb MJ (2007) Profiling of UV-induced ATM/ATR signaling pathways. *Proc Natl Acad Sci U S A* **104**: 19855-19860

Tang J, Agrawal T, Cheng Q, Qu L, Brewer MD, Chen J, & Yang X (2013) Phosphorylation of Daxx by ATM contributes to DNA damage-induced p53 activation. *PLoS One* **8**: e55813

Tang SY, Wan YP, & Wu YM (2015) Death domain associated protein (Daxx), a multi-functional protein. *Cell Mol Biol Lett* **20**: 788-797

van Attikum H & Gasser SM (2009) Crosstalk between histone modifications during the DNA damage response. *Trends Cell Biol* **19**: 207-217

Wang B, Matsuoka S, Carpenter PB, & Elledge SJ (2002) 53BP1, a mediator of the DNA damage checkpoint. *Science* **298**: 1435-1438

Yang X, Li L, Liang J, Shi L, Yang J, Yi X, Zhang D, Han X, Yu N, & Shang Y (2013) Histone acetyltransferase 1 promotes homologous recombination in DNA repair by facilitating histone turnover. *J Biol Chem* **288**: 18271-18282

Zimmermann M, Lottersberger F, Buonomo SB, Sfeir A, & de Lange T (2013) 53BP1 regulates DSB repair using Rif1 to control 5' end resection. *Science* **339**: 700-704

FIGURE LEGENDS

Figure 1. H3.3 histone variant is enriched at DSBs in a DAXX-dependent manner. (A) Purified chromatin samples from U2OS cells collected at the indicated times after BLE addition were assayed by immunoblot. H3.3 signals were normalized against those of H3 and the relative quantification of band intensities is shown as fold change, considering as 1 the untreated sample. The graph reports the means and standard deviations of three independent experiments. ***(B)*** Immunoprecipitations were conducted with specific antibodies against H2AX (upper) or γ-H2AX (lower) on oligonucleosome preparations obtained from mock or shDAXX U2OS cells exposed to BLE and collected at the indicated timepoints. Immunoprecipitates (IP) and total cell extracts (Input) were analysed by immunoblot. ***(C)*** U2OS cells containing an exogenously introduced I-SceI site were transfected with control (siCON) and DAXX (siDAXX) silencing. After 24hrs cells were transfected with either I-SceI expression vector (+I-SceI) or an empty vector (mock) in combination with a FLAG-H3.3 construct. Chromatin for ChIP analysis was prepared 2 days after the second transfection and immunoprecipitations were conducted with an anti-FLAG antibody. Quantitative PCR were performed with primers at 500 or 1300bp from the break or localized in the GAPDH gene. Real-time PCR values, normalized to input DNAs and to the values obtained with unrelated IgG, were considered as 1 for mock. Fold induction for I-SceI samples was calculated and the mean of three independent experiment

plotted. Statistical significance were obtained with a Student's t-test. *p<0.05 **p<0.01. ***(D)*** U2OS cells or ***(E)*** U2OS cells overexpressing $DAXX^{WT}$ were treated with 12μM BLE for 3hrs, fixed and tested by immunofluorescence with DAXX (green) and γ-H2AX (red) specific antibodies. Nuclei were stained with DAPI (blue). Scale bar: 2μm. The graph shows the relative intensities for the green and red channel (a.u.=arbitrary unit) along the line scan (white arrow) to estimate colocalization. ***(F)*** DAXX interaction with DSBs marker γ-H2AX detected by *in situ* PLA. Cells expressing HA-$DAXX^{WT}$ were left untreated (untr) or exposed to 12μM BLE. The interactions were visualized as red fluorescent spots. Nuclei were stained with DAPI (blue). Scale bar: 10μm. Negative and positive controls are shown as Supplementary Figure S1L and S1M. ***(G)*** U2OS cells containing an exogenously introduced I-SceI site were transfected with a I-SceI expression vector (+I-SceI) or an empty vector (mock). Chromatin for ChIP analysis was prepared 2 days after the transfection and immunoprecipitation was conducted with an anti-DAXX antibody. Quantitative PCR, calculations and plotting were performed as in (C).

Figure 2. DAXX and H3.3 overexpression delays 53BP1 foci formation at damage site. (A) U2OS cells were transfected with an empty vector or with H3.3-YFP or HA-$DAXX^{WT}$. Immunostaining of these cells with γ-H2AX antibody (in combination with HA antibody in the case of HA-DAXX) at the indicated times after 12μM BLE treatment, allowed to count cells positive for transfection and with less than 5 foci. ***(B)*** Upper panels: examples of 53BP1 staining in cells left untreated or 1hr after 12μM BLE addition. Nuclei were stained with DAPI (blue). Lower panels: HA-DAXX (stained with an anti-HA antibody, green), or H3.3-YFP (green) overexpression leads to the accumulation of 53BP1 foci negative cells (white arrows) 1hr after 12μM BLE addition. Nuclei were stained with DAPI (blue). Scale bar: 10μm. ***(C)*** U2OS or U2OS shDAXX cells were transfected with the indicated constructs. Cells were treated as in (A), but testing 53BP1 foci. Cells with less

than 5 foci were considered as negative. ***(D)*** Double immunostaining of 53BP1 (red) and γ-H2AX (green) of U2OS cells overexpressing $DAXX^{WT}$. Nuclei were stained with DAPI (blue). Scale bar: 10μm. In (A) and (C) charts represent the means and standard deviations (s.d.) of at least three independent experiments. For a single experiment 300 cells were scored for each cell line. *p<0.01 **p<0.001 ***p<0.0001.

Figure 3. DAXX impacts on DNA repair pathway choice, efficiency and fidelity. (A) U2OS cells stably silenced for DAXX and expressing in an inducible manner HA-DAXX WT were immunostained with anti-cyclin B (high cytoplasmic signal reveal G2 cells) and anti-RAD51 antibodies 2hrs after the exposure to 12μM BLE. RAD51 foci were enumerated within cyclin B positive cells. The graph shows the mean ±s.d. foci number per G2 cells obtained from three independent experiments. At least 100 cells were scored for each experiment. **p<0.001 statistical significance obtained with a Student's t-test**. *(B)*** Same cells as in (A) were immunostained with anti-cyclin A (nuclear signal reveal S and G2 cells), EdU (nuclear signal reveal S phase cells) and anti-BRCA1 antibodies 1hr after the exposure to 12μM BLE. BRCA1 foci were counted within cells double negative for EdU and cyclin A (G1 cells). The graph shows the mean percentage ±s.d. of G1 cells with more than 5 foci obtained from three independent experiments. At least 100 G1 cells were scored for each experiment. *p<0.01 statistical significance obtained with a Student's t-test**. *(C, D)*** Schematic representation of the DR-GFP (B) and EJ5-GFP (C) reporters used to monitor, respectively, homologous recombination (HR) and non-homologous end joining (NHEJ). DR-GFP-U2OS cells and EJ5-GFP-U2OS cells with DAXX (siDAXX), BRCA1 (siBRCA1) or control (siCON) knockdown were transfected with pCBASceI or empty vector (no I-SceI). After 72hrs, samples were analysed for GFP-positive cells by flow cytometry. BRCA1, an essential component of HR (Munoz et al., 2012) was used as a positive control. The values in the graph are mean±s.d. of three independent experiments

normalized to those of control silenced GFP positive cells. *p<0.01. ***(E)*** U2OS cells (mock) stably silenced for DAXX (shDAXX) and expressing in an inducible manner HA-DXX^{WT} (shDAXX+WT) were immunostained for γ-H2AX before and at different time points after 0.5nM NCS addition. Cells with more than 10 foci were considered negative for DNA repair activity. ***p<0.0001 statistical significance obtained with a Student's t-test. ***(F)*** DAPI staining of DNA was used to reveal micronuclei (white arrows) before and 24hrs after NCS treatment, using the same cells as in (E). Scale bar: 10μm. The chart represents the means and standard deviations of at least three independent experiments. For each experiment 1000 cells for sample were scored. *p<0.01.

Figure 4. DAXX protein is phosphorylated at Serine 424 and Serine 712 by ATM/ATR kinases after DSBs induction. (A) The alignment of DAXX regions spanning S424 and S712 among the indicated organisms is shown. ATM/ATR consensuses (SQ) at S424 and S712 are highlighted in grey (other SQ/TQ consensus are present in the same region). ***(B)*** Schematic representation of human DAXX protein with structural and functional domains. S424 and S712 position are indicated. ***(C)*** U2OS cells expressing HA-tagged WT, S424A and S712A forms of DAXX, treated or untreated with BLE, were used to immunoprecipitate the ectopic protein and immunoblotted with phospho-specific antibodies against S424 (left) and S712 (right). Total lysates were tested in parallel (Input); *= non specific bands. ***(D)*** U2OS cells transfected with HA-DAXX were pre-treated with 10μM of the ATM inhibitor KU55933 (ATMi), 2μM of the ATR inhibitor VE-822 (ATRi), or DMSO (vehicle). One hour later 120μM BLE was added and after 3hrs cells lysed. Immunoblot analysis of the total lysates obtained were performed with the indicated antibodies. ***(E)*** Cells expressing WT and phosphomutant forms of DAXX were treated with 120μM BLE and 3hrs later harvested. Total lysates were tested with the indicated antibodies. Total DAXX and vinculin are used as a loading control. ***(F)*** U2OS cells overexpressing HA-DAXX$^{S424A/S712A}$ were

tested by immunofluorescence with HA (green) and γ-H2AX (red) specific antibodies. Nuclei were stained with DAPI (blue). Scale bar: 2μm. The graph shows the relative intensities for the green and red channel (a.u.=arbitrary unit) along the line scan (white arrow) to estimate colocalization. See also Figure 1D. ***(G)*** Cells expressing HA-DAXX^{WT} or phosphomutants were exposed to 12μM BLE and fixed 3hrs after BLE addition. DAXX interaction with DSBs marker γ-H2AX detected was detected by *in situ* PLA. The interactions were visualized as red fluorescent spots. Nuclei were stained with DAPI (blue). Scale bar: 10μm.

Figure 5. H3.3-DAXX interaction and H3.3 deposition at damage site are impaired by S424 and S712 mutation. (A) Purified chromatin samples from U2OS cells, transfected with the indicated forms of DAXX, were assayed by immunoblot. Samples were collected at the indicated times after BLE addition. H3.3 signals were normalized to total H3 levels. Data are shown considering as 1 the untreated sample. The chart represents the means and standard deviations of three independent experiments. ***(B)*** Oligonucleosomes (see Fig. 1B and S1C) were obtained from U2OS cells expressing a WT or mutant form of DAXX, exposed for the indicated time to 120μM BLE. Immunoprecipitation were conducted with a γ-H2AX antibody. Immunocomplexes (IP) and protein levels in total cell extracts (Input) were analysed by immunoblot. ***(C)*** U2OS cells were transfected with WT or mutant forms of DAXX. Lysates were obtained before (-) and after 3hrs BLE exposure (+). HA-DAXX was immunoprecipitated with an anti-HA antibody (IP). H3.3 presence was determined by immunoblot. Actin levels are used as loading control. ***(D)*** U2OS shDAXX+HA-DAXX^{WT}, HA- DAXX^{S424A} or HA-DAXX^{S712A} cells fixed 1 and 3hrs after 12μM BLE addition were co-immunostained with anti-HA and -53BP1 antibodies. Cells positive for HA and with less than five 53BP1 foci were considered as negative. At least three independent experiments were conducted and for each experiment 300 cells for sample

were scored. ***(E)*** The same cells as in (D) were immunostained with anti-cyclin B (high cytoplasmic signal reveal G2 cells) and anti-RAD51 antibodies 2hrs after the exposure to 12μM BLE. RAD51 foci were enumerated within cyclin B positive cells. See also Figure 3A. The graph shows the mean foci number per G2 cells obtained from independent experiments. At least 100 cells were scored for each experiment. ***(F)*** The same cells as in (D) were immunostained for γ-H2AX before and at different time points after 0.5nM NCS addition. Cells with more than 10 foci were considered negative for DNA repair activity. See also Figure 3E. At least 300 cells for sample were scored. ***(G)*** The same cells as in (D) were stained with DAPI staining of DNA was used to reveal micronuclei before and 24hrs after NCS treatment (See also Figure 3F). For (D), (E), (F) and (G) graphs the means and s.d. of at least three independent experiments are shown. Statistical significance was obtained with a Student's t-test *p<0.01 **p<0.001.

Figure 6. H3.3-K36 methylation contributes to delay 53BP1 recruitment at damage site. (A) Post translational modifications of histone H3 were assessed on chromatin extracted from U2OS cells expressing H3.3-YFP, H3.1-YFP or no exogenous histones (empty). Cells were treated for the indicated times with 120μM BLE. Chromatin was purified from total protein extract and analysed by immunoblotting. GFP signals show the expression levels of H3.3-YFP and H3.1-YFP. °non specific band. ***(B)*** Cells expressing WT or a mutated form of H3.3-YFP (lysine 36 to arginine or to methionine) were treated with 12μM BLE and fixed 1 or 3hrs after. 53BP1 foci were enumerated and cells with less than 5 spots considered as negative. At least three independent experiments were conducted and for each experiment 300 cells for sample were scored. Statistical significance was obtained with a Student's t-test *p<0.01 **p<0.001. ***(C)*** Cells with SETD2 (two different sequences) or control (siCON) silencing, overexpressing (+) or not (-) H3.3-YFP protein,

were tested for K36 di- and tri-methylation of H3.3-YFP and endogenous H3 using specific antibodies and cells. Cells were treated and chromatin purified as in (A). ***(D)*** Cells transfected with silencing (siCON or siSTED2) in combination with H3.3-YFP or HA-DAXX were tested for 53BP1 foci formation by immunofluorescence after the addition of 12μM BLE. YFP or anti-HA positive cells were scored for 53BP1 foci and those with less than 5 foci were considered as negative. For a single experiment 300 cells were scored for each cell line. Graph collects the means and s.d. of three independent experiments.

SUPPLEMENTAL MATHERIAL:

SUPPLEMENTAL FIGURE LEGENDS

Figure S1. (A) Purified chromatin samples from MRC5 and HEK293T cells collected at the indicated times after BLE addition were assayed by immunoblot. H3.3 signals were normalized against those of H3 and the relative quantification of band intensities is shown as fold change, considering as 1 the untreated sample. The graph reports the means and s.d. of three independent experiments. **(B)** Stable (shDAXX) and **(C)** transient DAXX silencing (siDAXX) were tested by immunoblotting using actin to as a loading control. **(D)** Purified chromatin samples obtained from siDAXX or siCON HEK293T tested for H3.3 and total H3 at the indicated times after BLE addition. H3.3 signals were normalized by total H3 levels and the relative quantification of band intensities is shown, considering as 1 the untreated sample. **(E)** Western blot performed on total lysates from U2OS cells transiently silenced with two different HIRA siRNA (siHIRA #1 and #2). Actin represents the loading

control. **(F)** Purified chromatin samples obtained from siHIRAs and mock U2OS tested for H3.3 and total H3 at the indicated times after BLE addition. Relative quantification of band intensities is shown and obtained as in (A). **(G)** ATRX-silenced HEK293T or siCON cells were treated with BLE for the indicated times and tested for ATRX, H3.3 and H3 protein levels. **(H)** Oligonucleosome preparations as in (Goodarzi et al., 2008) were tested by electrophoresis with 0.1 and 1Kb ladders as a marker. **(I)** DAXX (green) immunostaining of U2OS cells expressing HA-DAXX^{WT} treated for 3hrs with 12μM BLE. DAPI (blue) dyes nuclear DNA. **(J)** Single antibody controls for in situ proximity ligation assays (PLA). Cells expressing HA-DAXX WT or empty vector were exposed for 3hrs to 12μM BLE before fixation. PLA was conducted as in Fig. 1F with the indicated antibodies. Cell nuclei were stained with DAPI (blue). **(K)** Antibodies against 53BP1, ORC2 and p53 phosphorylated at S15 were used as positive and negative controls for protein colocalization with γ-H2AX at DNA breaks revealed by PLA. PLA was conducted as in Fig. 1F. Cell nuclei were stained with DAPI (blue) In (I), (J) and (K) panels, scale bar represents 10μm.

Figure S2. (A) U2OS shDAXX cell lines expressing WT form of DAXX under the control of a doxycyclin-inducible promoter were tested for DAXX expression. Cells were exposed to 1μg/ml of doxycicline 24hrs before the exposure to 120μM BLE and successively harvested at the indicated time points. Actin was used as loading control. **(B)** Western blot and **(C)** immunofluorescence analyses of H3.3-YFP and FLAG-H3.3 protein levels and localization, expressed in U2OS cells. Scale bar represents 10μm. **(D)** U2OS cells, transfected with YFP, H3.3-YFP, mock and HA-DAXX were tested by immunofluorescence for pS1981-ATM foci formation 1 and 3hrs after 12μM BLE exposure. The number of foci per cell was counted and the graph shows representative results. **(E)** Graph depicting the distribution of 53BP1 foci number from immunofluorescence analyses in mock, H3.3 and DAXX overexpressing U2OS cells exposed to 12μM BLE. 100 cells were enumerated,

median and standard errors are shown. In the 3hrs graph less than 8 cells for each cell line are outside the range of the scale. **(F)** 53BP1 protein levels were detected by western blotting. Samples were collected before and after BLE from mock, shDAXX and shDAXX+DAXX^{WT} cells. Actin is used as a loading control. **(G)** U2OS cells silenced for HIRA (see Figure S1E) were concurrently transfected with H3.3-YFP or an empty vector and tested by immunofluorescence for 53BP1 foci formation 1 and 3hrs after 12μM BLE addition. The graph shows representative results. **(H)** Same as (F) for HEK293T cells. **(I)** Same as (F) for DivA cells transfected with mock, DAXX and H3.3. 4OHT was added to promote AsiSI translocation into the nucleus 4hrs before cell fixation. **(J)** Cells expressing the indicated constructs were exposed to 1μg/ml of doxycicline 24hrs before the treatment with 12μM BLE and harvested 6hrs later. Cell cycle distribution evaluation was performed by DNA staining and cytofluorimetric analysis. Data in the graph are the mean of three independent experiments. **(K)** U2OS cells transfected with FLAG-H3.3 and exposed to 3hrs BLE were initially stained with Click-iT EdU (green) to label S phase cells and successively immunostained with anti-53BP1 (red) and FLAG (blue) antibodies. Representative images are shown. Arrows point EdU positive (upper) or EdU negative (lower) FLAG-H3.3 positive/53BP1 negative cells. The graph shows the distribution of 53BP1 negative cells between EdU positive (+) and EdU negative (-) cells. **(L)** As in (K) but with the overexpression of DAXX revealed by an anti HA antibody. In (K) and (L) panels, scale bar represents 10μm**. (M)** Cells transfected with the indicated constructs were exposed to 12μM BLE and fixed after 1 (upper panel) or 3hrs (lower panel). Samples were co-stained with anti-53BP1 and -cyclin B1 antibodies. 53BP1 foci were enumerated and cells negative for a cyclin B1 cytoplasmic staining were considered as in G1 or early S phase of the cell cycle.

Figure S3. (A) Representative images of U2OS treated for 2hrs with 12μM BLE, fixed and co-stained with anti-RAD51 and -cyclin B1 antibodies. Cells with cytoplasmic staining of cyclin B1 are in G2 phase of the cell cycle. Scale bar represents 10μm**. (B)** RAD51 protein levels evaluation for cells silenced or overexpressing DAXX in a doxycicline inducible background (+ or – doxycicline) and treated for the indicated time with 12μM BLE. **(C)** RAD51 foci number in G2 cells for siCON and siHIRA cells (see also Fig. S7C) exposed for 2hrs to 12μM BLE. **(D)** Mock and shDAXX cells expressing WT HA-DAXX were fixed 1hr after 12μM BLE. Initially samples were labelled with click-iT-EdU (green, S phase cells), successively immunostained with anti cyclin A (blue, nuclear staining in S and G2 phase cells) and BRCA1 (red). Examples of G1 (EdU negative/cyclin A negative), S (EdU positive/cyclin A positive) and G2 (EdU negative/cyclin A positive) cells are indicated. BRCA1 foci were counted in G2 and G1 cells. Scale bar represents 10μm. **(E)** The siCON and siDAXX dells used for Fig. 3C were tested for cell cycle distribution evaluation by DNA staining and cytofluorimetric analysis. **(F)** Graph showing the fraction of U2OS cells with less than five 53BP1 foci/cell, evaluated by immunofluorescence of cells treated with 0.5nM neocarzinostatin. Data from a representative experiment are shown. **(G)** Graph showing the median and s.d. of a time course analysis of U2OS cells positive for γ-H2AX foci number evaluated by immunofluorescence. Cells expressing or not H3.3-YFP were treated with 0.5nM neocarzinostatin.

Figure S4. (A) Endogenous DAXX was immunoprecipitated from U2OS cells. Immunocomplexes were probed with p712 antibody. shDAXX cells were immunoprecipitated as a control. Total lysates (Input) were also loaded. *non specific bands. **(B)** U2OS cells transfected with HA-DAXX (WT, S424A or S712A) were treated with 120μM BLE and starved 1hr later. Immunoblot analysis of total lysates were

performed with the indicated antibodies. **(C)** U2OS cells as in (B) were treated with 120μM BLE, 10μM 4-Nitroquinoline 1-oxide (NQO), 10μM etoposide (ETO) or 30Gy ionizing radiation (IR). After 3hrs, cells were lysed and immunoprecipitations, carried out with an HA antibody, were loaded on gels and western blotted. Extracts from S424A or S712A expressing cells treated with BLE were loaded as a control for antibody specificity.

Figure S5. (A) U2OS shDAXX cell lines expressing WT and phosphomutant forms of DAXX under the control of a doxycyclin-inducible promoter were tested for DAXX expression. Cells were exposed to 1μg/ml of doxycicline 24hrs before the exposure to 120μM BLE and successively harvested at the indicated time points. Actin was used as loading control. **(B)** Purified chromatin samples obtained from U2OS shDAXX+DAXX^{WT} or +DAXX^{S424A} or +DAXX^{S712A} cells induced 24hrs with doxycicline and tested for H3.3 and total H3 at the indicated time after BLE addition. **(C)** Purified chromatin samples from HEK293T cells collected at 3hrs after 120μM BLE addition were assayed by immunoblot. H3.3 signals were normalized against those of H3 and the relative quantification of band intensities is shown as fold change, considering as 1 the untreated sample. **(D)** HEK293T cells were transfected with WT or mutant forms of DAXX. Lysates were obtained before (-) and after 3hrs BLE exposure (+). HA-DAXX was immunoprecipitated with an anti-HA antibody (IP). H3.3 presence was determined by immunoblot. Actin levels are used as loading control. **(E)** p53 protein levels tested by western blotting on total lysates from U2OS shDAXX+DAXX^{WT} or +DAXX^{S424A} or +DAXX^{S712A} cells induced with doxycicline 24hrs before exposure to BLE for the indictaed times. Actin is used as a loading control. **(F)** HA-DAXX immunoprecipitations with an anti-HA antibody were performed in U2OS shDAXX+DAXX^{WT} or +DAXX^{S424A} or +DAXX^{S712A} cells induced 24hrs with doxycicline. Cells were also treated with BLE for 3hrs (+) or left untreated (-). Immunocomplexes and inputs

were tested for HAUSP presence with a specific antibody. Vinculin is used as a loading control. **(G)** 53BP1 protein levels were detected by western blotting. Samples were collected before and after BLE from shDAXX+DAXX^{WT}, shDAXX+DAXX^{S424A} and shDAXX+DAXX^{S712A} cells induced 24hrs with doxycicline. Actin is used as a loading control. **(H)** Cells expressing the indicated constructs were exposed to 1μg/ml of doxycicline 24hrs before the treatment with 12μM BLE and harvested 6hrs later. Cell cycle distribution evaluation was performed by DNA staining and cytofluorimetric analysis. Data in the graph are the mean of three independent experiments. **(I)** Graph showing the median and s.d. of micronuclei test in three clones alternative to those shown in Figure 5G.

Figure S6. (A) Post translational modifications of histone H3, H3.1-YFP and H3.3-YFP were tested on chromatin extracted from HEK293T cells. Cells were treated for the indicated time with BLE 120μM. *non specific band. **(B)** FLAG-H3.3K36 residue was mutated to R or to M. These constructs were transfected in U2OS cells, successively treated with 12μM BLE for 1 or 3hrs. Cells were fixed and stained for 53BP1 to enumerate 53BP1 foci. Cells with less than 5 spots considered as negative.

Figure 1

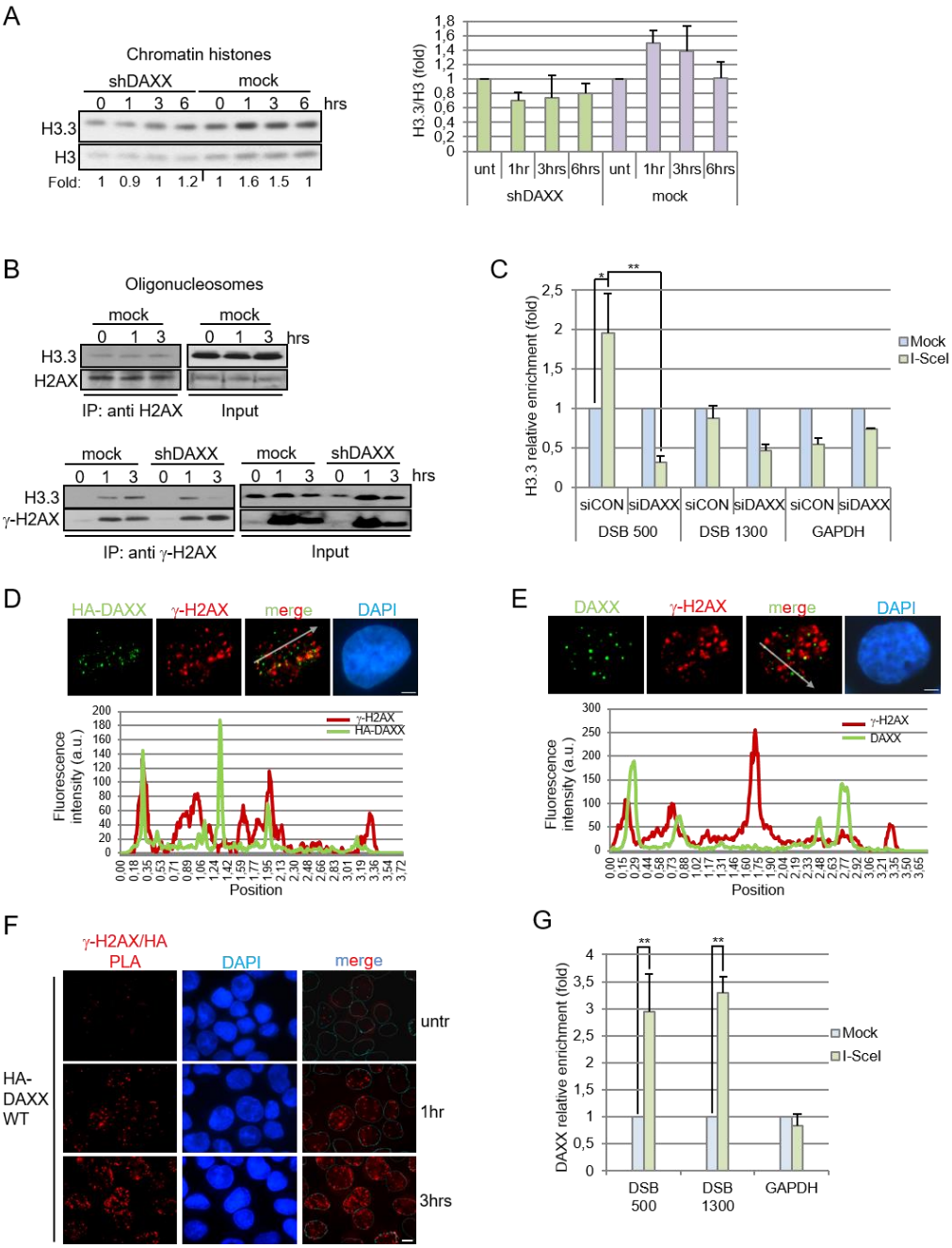
A
Chromatin histones
shDAXX
mock
0 1 3 6 0 1 3 6 hrs
H3.3
H3
Fold: 1 0.9 1 1.2 1 1.6 1.5 1
H3.3/H3 (fold)
unt 1hr 3hrs 6hrs unt 1hr 3hrs 6hrs
shDAXX
mock
B
Oligonucleosomes
mock mock
0 1 3 0 1 3 hrs
H3.3
H2AX
IP: anti H2AX
Input
mock shDAXX mock shDAXX
0 1 3 0 1 3 0 1 3 0 1 3 hrs
H3.3
γ-H2AX
IP: anti γ-H2AX
Input
C
H3.3 relative enrichment (fold)
Mock
I-SceI
siCON siDAXX siCON siDAXX siCON siDAXX
DSB 500
DSB 1300
GAPDH
D
HA-DAXX
γ-H2AX
merge
DAPI
Fluorescence intensity (a.u.)
γ-H2AX
HA-DAXX
Position
E
DAXX
γ-H2AX
merge
DAPI
Fluorescence intensity (a.u.)
γ-H2AX
DAXX
Position
F
γ-H2AX/HA PLA
DAPI
merge
HA-DAXX WT
untr
1hr
3hrs
G
DAXX relative enrichment (fold)
Mock
I-SceI
DSB 500
DSB 1300
GAPDH

Figure 2

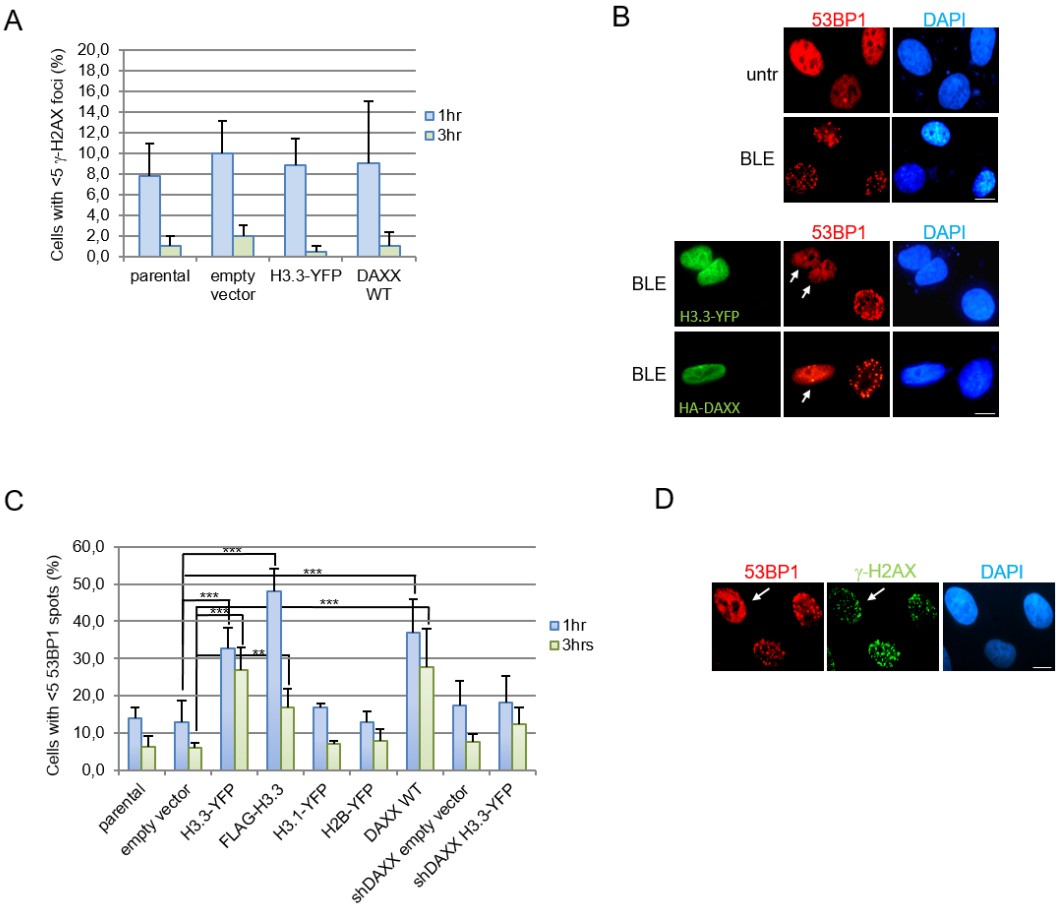
A
Cells with <5 γ-H2AX foci (%)
20,0
18,0
16,0
14,0
12,0
10,0
8,0
6,0
4,0
2,0
0,0
1hr
3hr
parental
empty vector
H3.3-YFP
DAXX WT
B
53BP1
DAPI
untr
BLE
53BP1
DAPI
BLE
H3.3-YFP
BLE
HA-DAXX
C
Cells with <5 53BP1 spots (%)
60,0
50,0
40,0
30,0
20,0
10,0
0,0
***
***
***
***
***
**
1hr
3hrs
parental
empty vector
H3.3-YFP
FLAG-H3.3
H3.1-YFP
H2B-YFP
DAXX WT
shDAXX empty vector
shDAXX H3.3-YFP
D
53BP1
γ-H2AX
DAPI

Figure 3

Aliprandi_Fig3

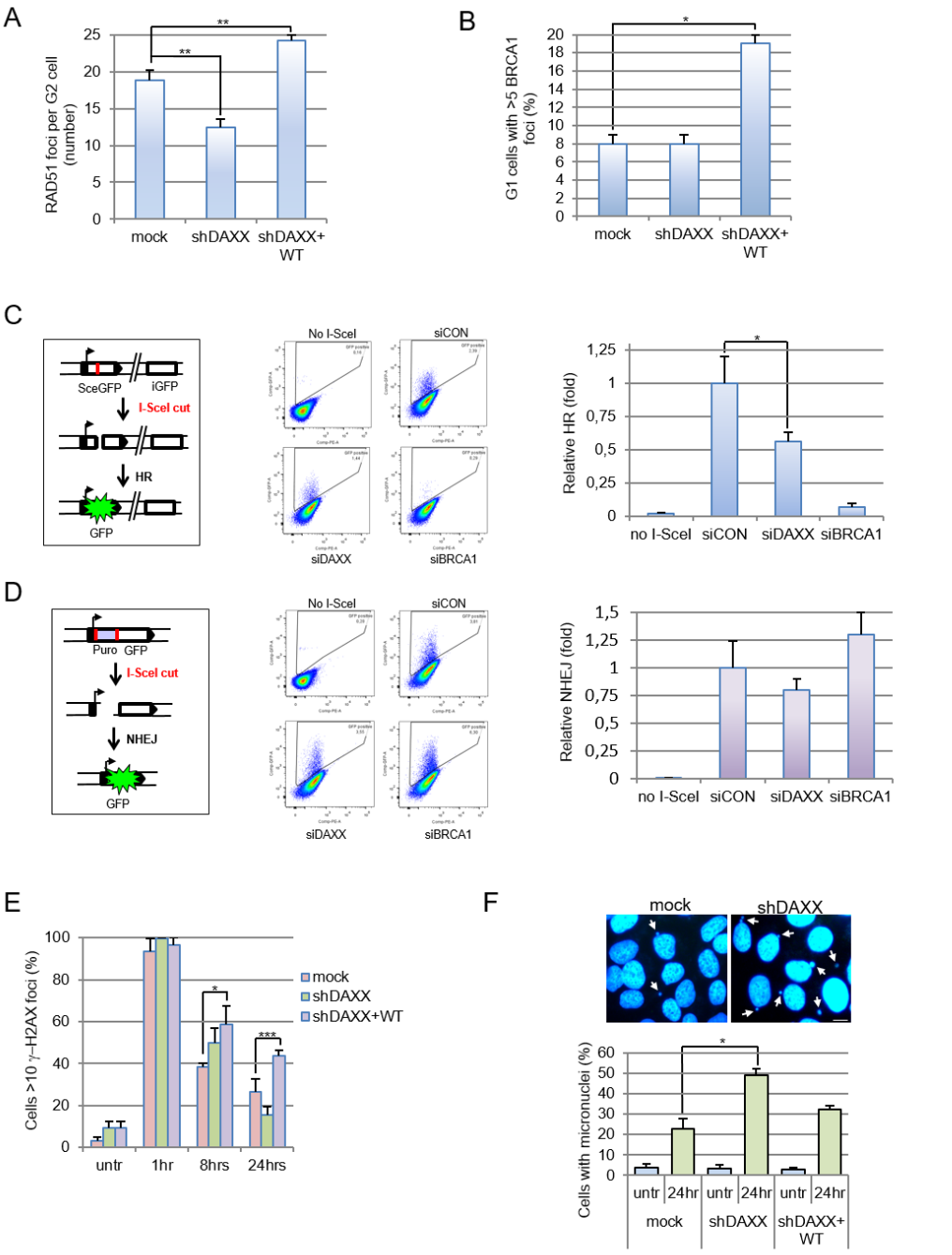

Figure 4

A

```
H. sapiens        414  DSGEGPSGMASQGCPSASRAET  435
C. aethiops       414  DSGEGPIGMASQGCPSASRAET  435
C. familiaris     414  DSGEGPSGMASQECPTTSKPET  435
M. musculus       420  ESGEGPSGMASQECPTTSKAET  441
R. norvegicus     411  DSGEGPSGVASQEDPTTPKAET  432
D. rerio          415  -----VNGQQS-----E-SKE-  424
D. melanogaster  1512  KRGPAARGNVIRKKRAANGRIF  1533

H. sapiens        702  SPARLSQTPHSQPPRPRTCKTS  723
C. aethiops       698  SPAQLSQTPQSQPPRPSTYKTS  719
C. familiaris     699  SQAQLSQTPQSQPSRPSTYKMS  720
M. musculus       701  SPSLLLQTPQAQSLRQCIYKTS  722
R. norvegicus     693  SPSLILQTPQSQSPRPCIYKTS  714
D. rerio          678  TPPRKTARNSQATPPPKKNKVN  699
D. melanogaster        ----------------------
```

B

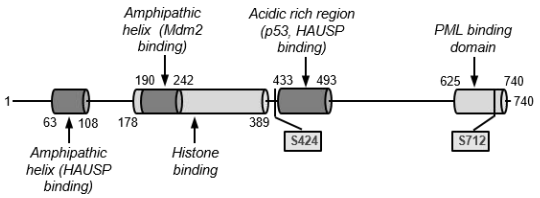

C

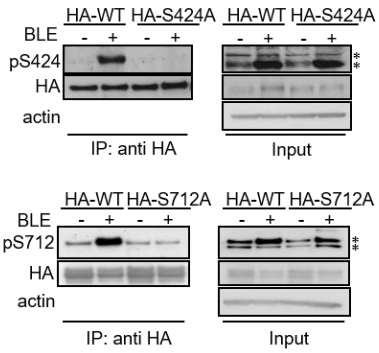

D

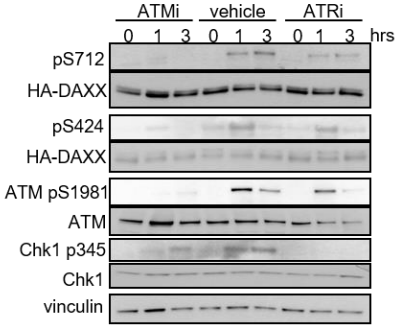

E

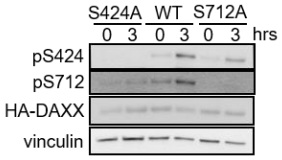

F

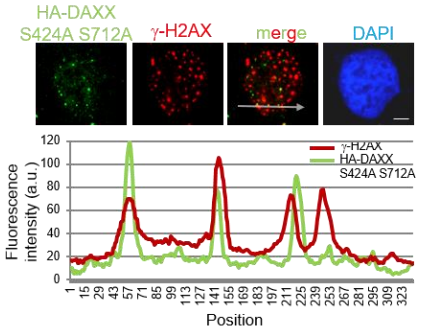

G

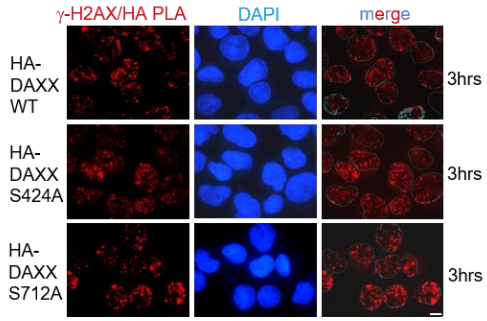

Figure 5

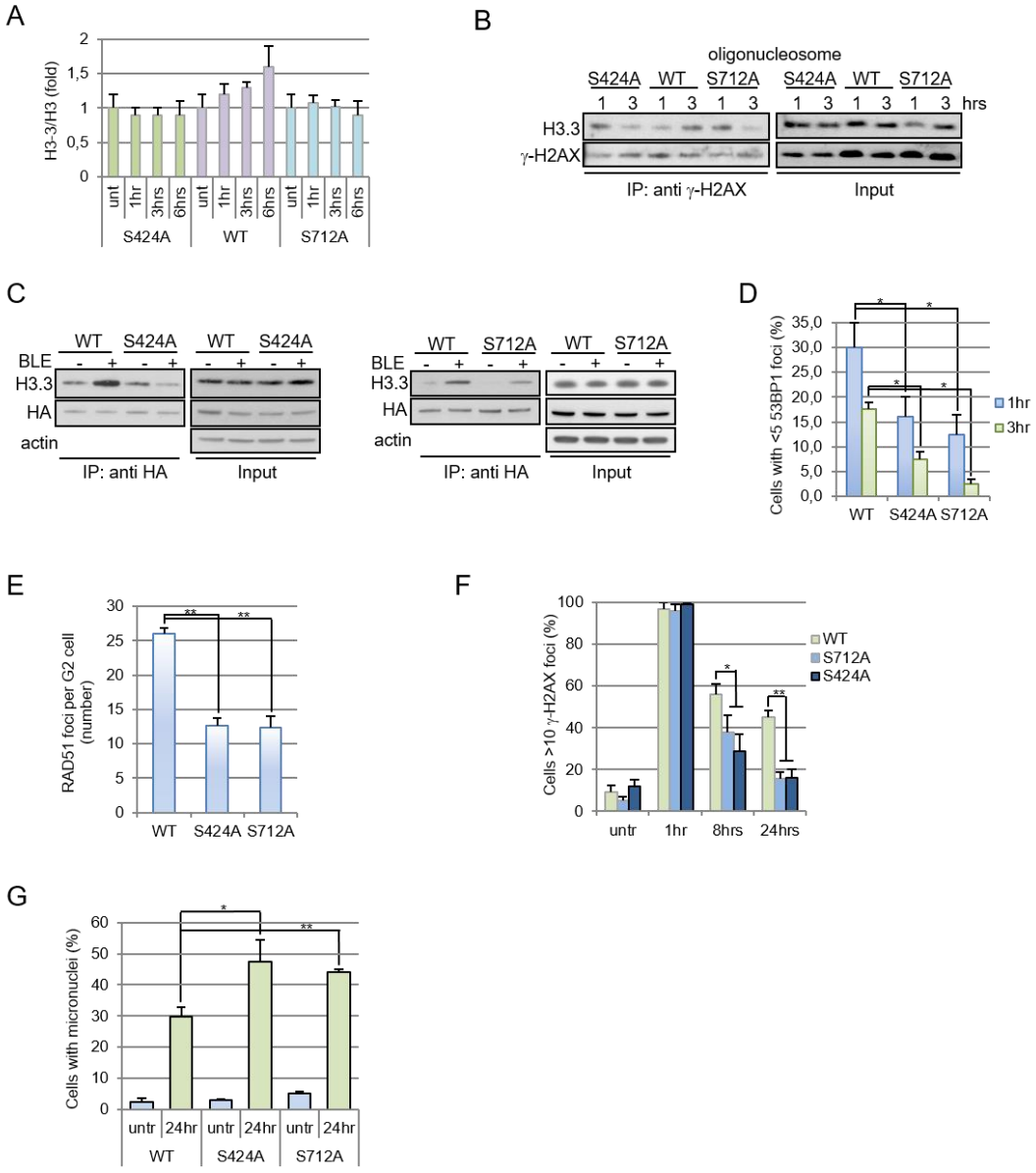
A
H3-3/H3 (fold)
unt
1hr
3hrs
6hrs
S424A
WT
S712A
B
oligonucleosome
S424A WT S712A S424A WT S712A
1 3 1 3 1 3 1 3 1 3 1 3 hrs
H3.3
γ-H2AX
IP: anti γ-H2AX
Input
C
WT S424A WT S424A
BLE
H3.3
HA
actin
IP: anti HA
Input
WT S712A WT S712A
BLE
H3.3
HA
actin
IP: anti HA
Input
D
Cells with <5 53BP1 foci (%)
1hr
3hr
WT S424A S712A
E
RAD51 foci per G2 cell (number)
WT S424A S712A
F
Cells >10 γ-H2AX foci (%)
WT
S712A
S424A
untr 1hr 8hrs 24hrs
G
Cells with micronuclei (%)
untr 24hr untr 24hr untr 24hr
WT S424A S712A

Figure 6

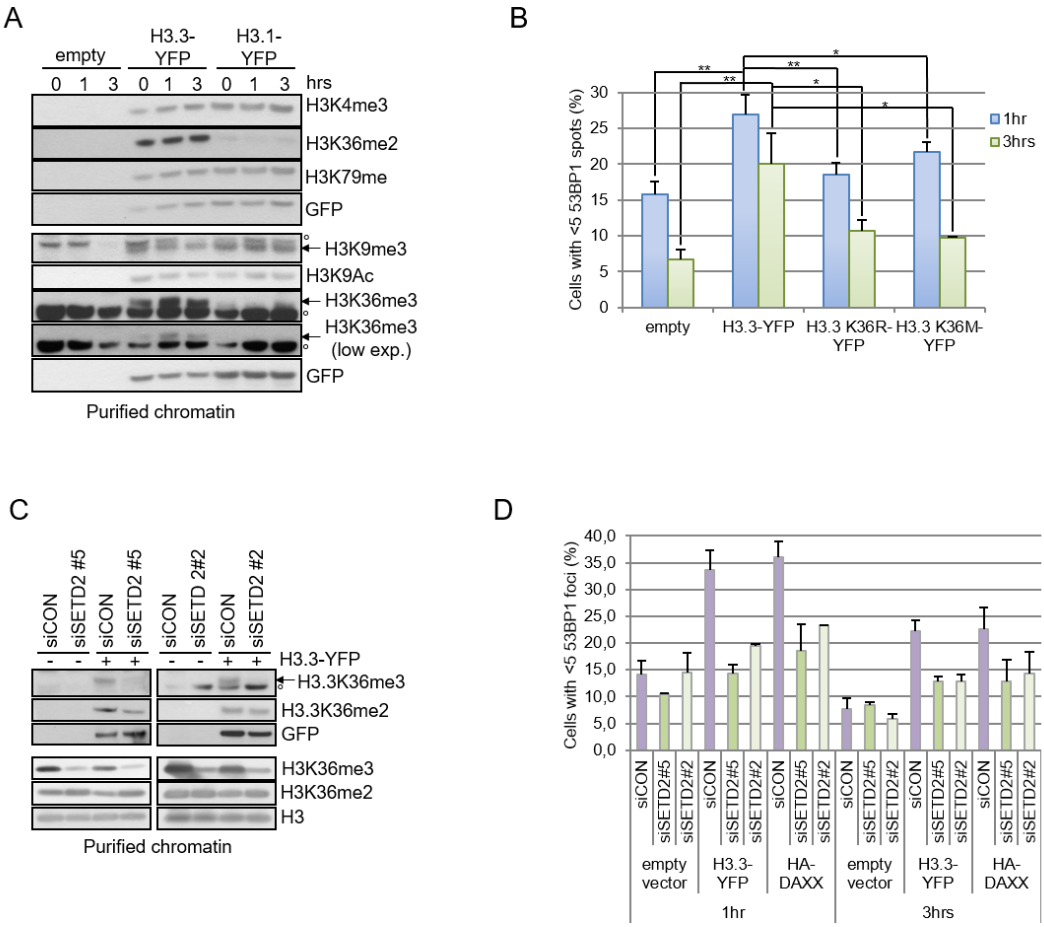
A
empty
H3.3-YFP
H3.1-YFP
0 1 3 0 1 3 0 1 3
hrs
H3K4me3
H3K36me2
H3K79me
GFP
H3K9me3
H3K9Ac
H3K36me3
H3K36me3 (low exp.)
GFP
Purified chromatin
B
Cells with <5 53BP1 spots (%)
1hr
3hrs
empty
H3.3-YFP
H3.3 K36R-YFP
H3.3 K36M-YFP
C
siCON
siSETD2 #5
siSETD 2#2
siSETD2 #2
H3.3-YFP
H3.3K36me3
H3.3K36me2
GFP
H3K36me3
H3K36me2
H3
Purified chromatin
D
Cells with <5 53BP1 foci (%)
siCON
siSETD2#5
siSETD2#2
empty vector
H3.3-YFP
HA-DAXX
1hr
3hrs

Figure S1

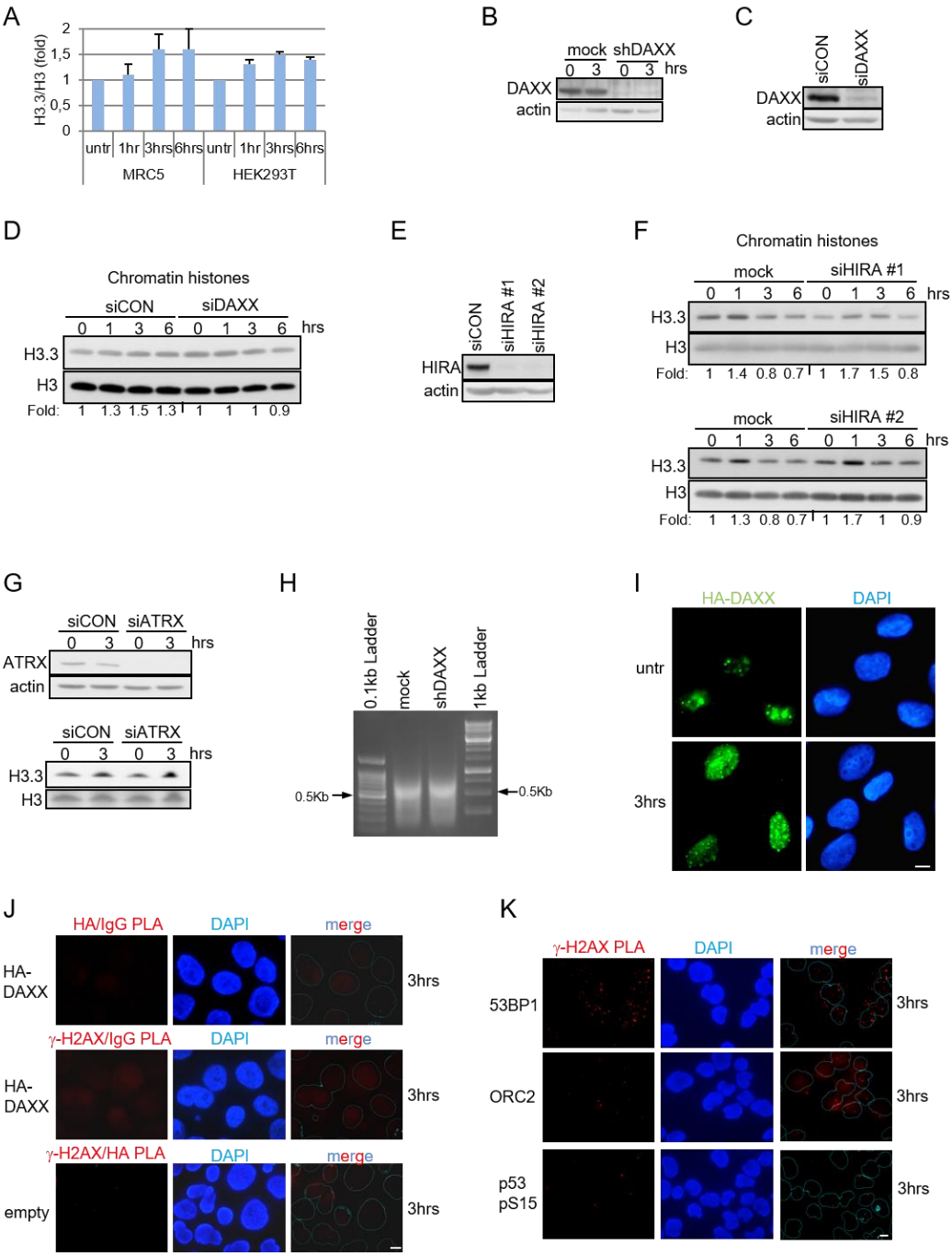
A
H3.3/H3 (fold)
2
1,5
1
0,5
0
untr 1hr 3hrs 6hrs untr 1hr 3hrs 6hrs
MRC5
HEK293T
B
mock shDAXX
0 3 0 3 hrs
DAXX
actin
C
siCON
siDAXX
DAXX
actin
D
Chromatin histones
siCON
siDAXX
0 1 3 6 0 1 3 6 hrs
H3.3
H3
Fold: 1 1.3 1.5 1.3 1 1 1 0.9
E
siCON
siHIRA #1
siHIRA #2
HIRA
actin
F
Chromatin histones
mock
siHIRA #1
0 1 3 6 0 1 3 6 hrs
H3.3
H3
Fold: 1 1.4 0.8 0.7 1 1.7 1.5 0.8
mock
siHIRA #2
0 1 3 6 0 1 3 6 hrs
H3.3
H3
Fold: 1 1.3 0.8 0.7 1 1.7 1 0.9
G
siCON siATRX
0 3 0 3 hrs
ATRX
actin
siCON siATRX
0 3 0 3 hrs
H3.3
H3
H
0.1kb Ladder
mock
shDAXX
1kb Ladder
0.5Kb
0.5Kb
I
HA-DAXX
DAPI
untr
3hrs
J
HA/IgG PLA
DAPI
merge
HA-DAXX
3hrs
γ-H2AX/IgG PLA
DAPI
merge
HA-DAXX
3hrs
γ-H2AX/HA PLA
DAPI
merge
empty
3hrs
K
γ-H2AX PLA
DAPI
merge
53BP1
3hrs
ORC2
3hrs
p53 pS15
3hrs

Figure S2

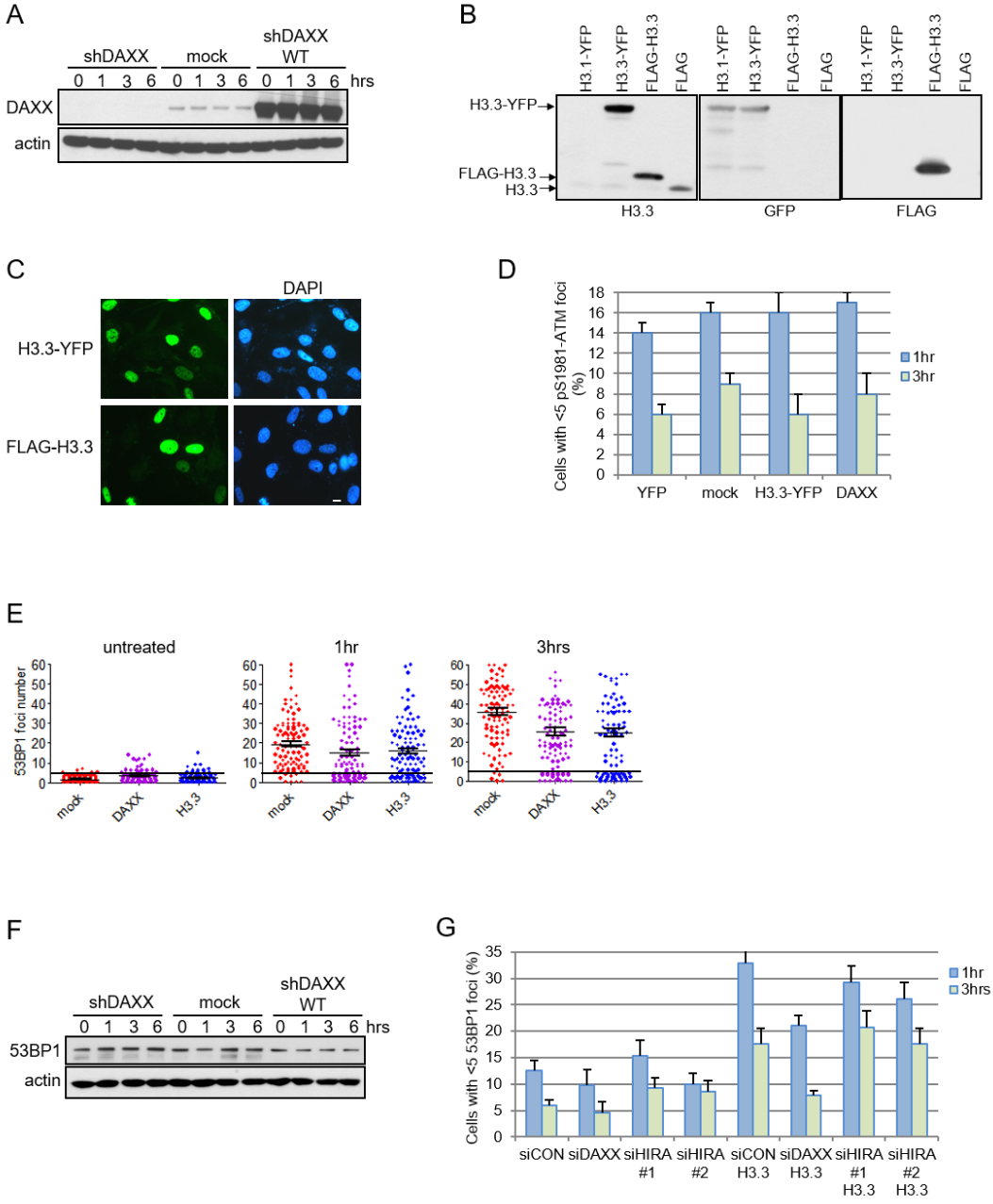
A
shDAXX
mock
shDAXX WT
0 1 3 6 0 1 3 6 0 1 3 6 hrs
DAXX
actin
B
H3.1-YFP
H3.3-YFP
FLAG-H3.3
FLAG
H3.3-YFP
FLAG-H3.3
H3.3
H3.3
GFP
FLAG
C
DAPI
H3.3-YFP
FLAG-H3.3
D
Cells with <5 pS1981-ATM foci (%)
1hr
3hr
YFP
mock
H3.3-YFP
DAXX
E
untreated
1hr
3hrs
53BP1 foci number
mock
DAXX
H3.3
F
shDAXX
mock
shDAXX WT
0 1 3 6 0 1 3 6 0 1 3 6 hrs
53BP1
actin
G
Cells with <5 53BP1 foci (%)
1hr
3hrs
siCON
siDAXX
siHIRA #1
siHIRA #2
siCON H3.3
siDAXX H3.3
siHIRA #1 H3.3
siHIRA #2 H3.3

Figure S2

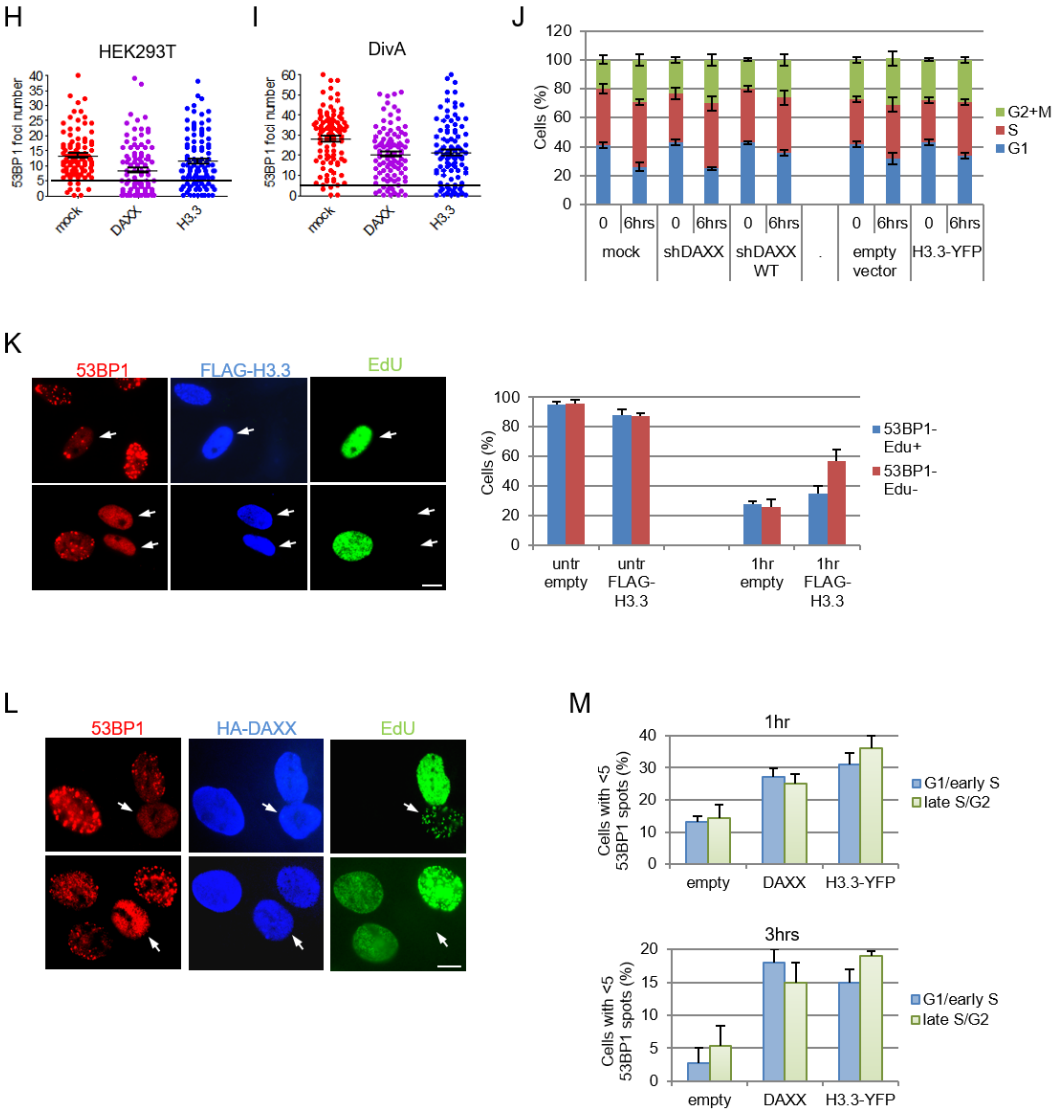
H
HEK293T
53BP1 foci number
mock
DAXX
H3.3
I
DivA
53BP1 foci number
mock
DAXX
H3.3
J
Cells (%)
G2+M
S
G1
0
6hrs
mock
shDAXX
shDAXX WT
empty vector
H3.3-YFP
K
53BP1
FLAG-H3.3
EdU
Cells (%)
53BP1-Edu+
53BP1-Edu-
untr empty
untr FLAG-H3.3
1hr empty
1hr FLAG-H3.3
L
53BP1
HA-DAXX
EdU
M
1hr
Cells with <5 53BP1 spots (%)
G1/early S
late S/G2
empty
DAXX
H3.3-YFP
3hrs
Cells with <5 53BP1 spots (%)
G1/early S
late S/G2
empty
DAXX
H3.3-YFP

Figure S3

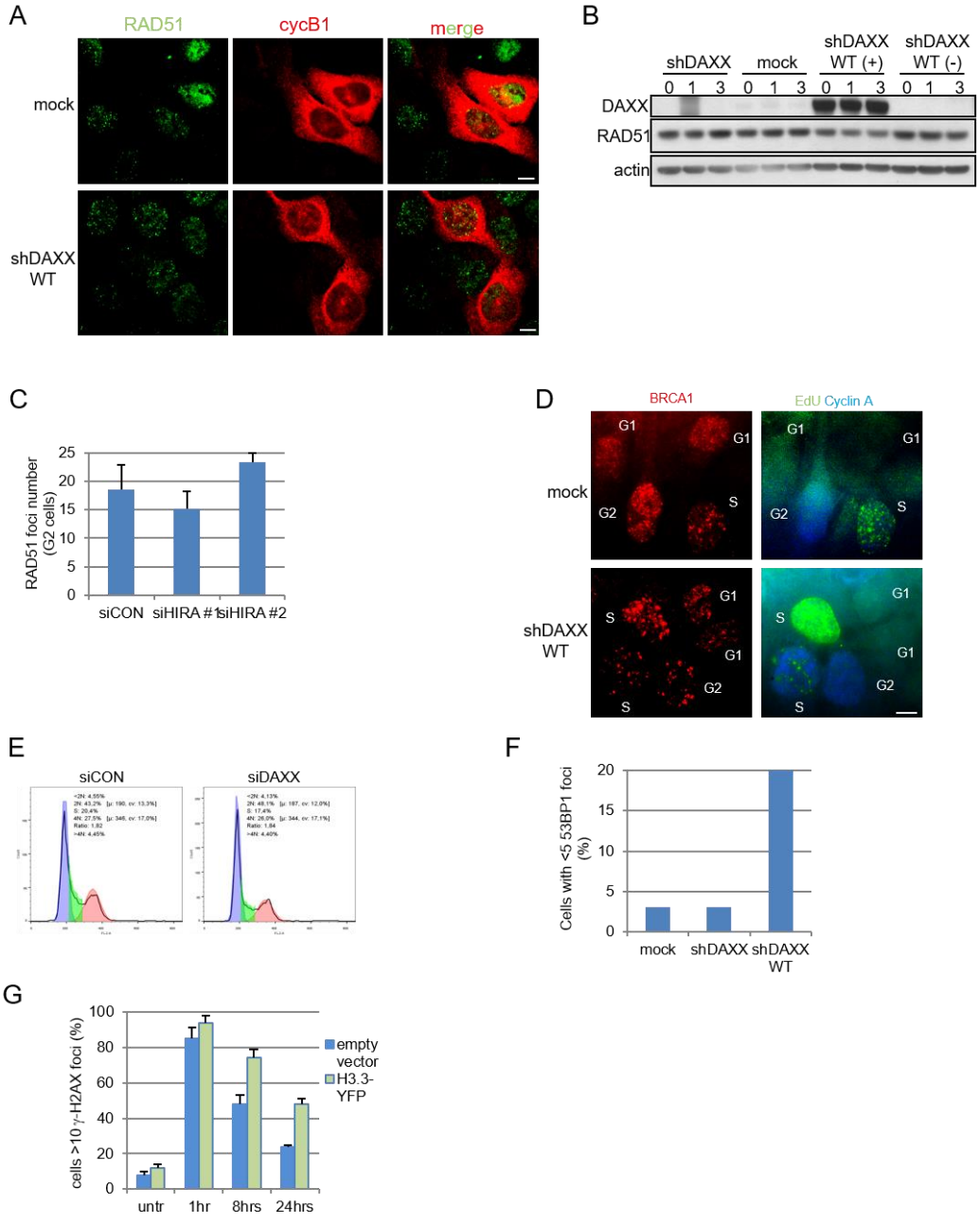
A
RAD51
cycB1
merge
mock
shDAXX WT
B
shDAXX
mock
shDAXX WT (+)
shDAXX WT (-)
0 1 3 0 1 3 0 1 3 0 1 3
DAXX
RAD51
actin
C
RAD51 foci number (G2 cells)
25
20
15
10
5
0
siCON
siHIRA #1
siHIRA #2
D
BRCA1
EdU Cyclin A
mock
shDAXX WT
G1
S
G2
E
siCON
siDAXX
F
Cells with <5 53BP1 foci (%)
20
15
10
5
0
mock
shDAXX
shDAXX WT
G
cells >10 γ-H2AX foci (%)
100
80
60
40
20
0
untr
1hr
8hrs
24hrs
empty vector
H3.3-YFP

Figure S4

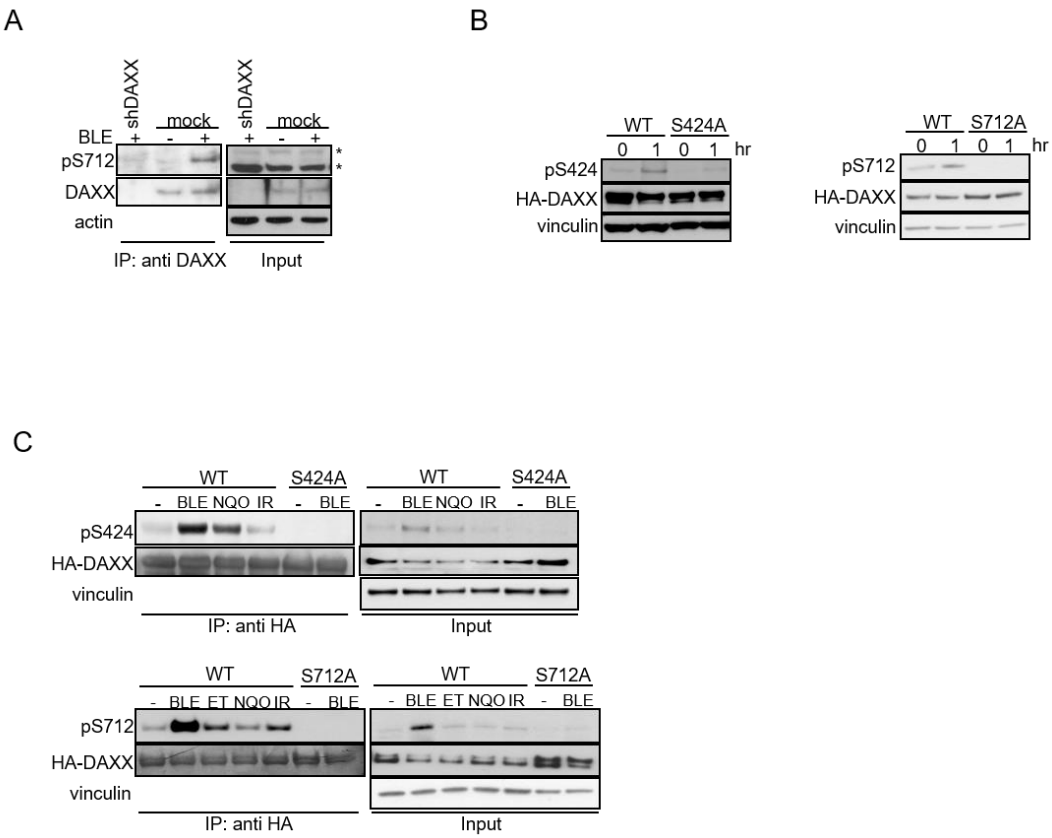
A
shDAXX
mock
shDAXX
mock
BLE
pS712
DAXX
actin
IP: anti DAXX
Input
B
WT
S424A
0 1 0 1 hr
pS424
HA-DAXX
vinculin
WT
S712A
0 1 0 1 hr
pS712
HA-DAXX
vinculin
C
WT
S424A
WT
S424A
- BLE NQO IR - BLE
- BLE NQO IR - BLE
pS424
HA-DAXX
vinculin
IP: anti HA
Input
WT
S712A
WT
S712A
- BLE ET NQO IR - BLE
- BLE ET NQO IR - BLE
pS712
HA-DAXX
vinculin
IP: anti HA
Input

Figure S5

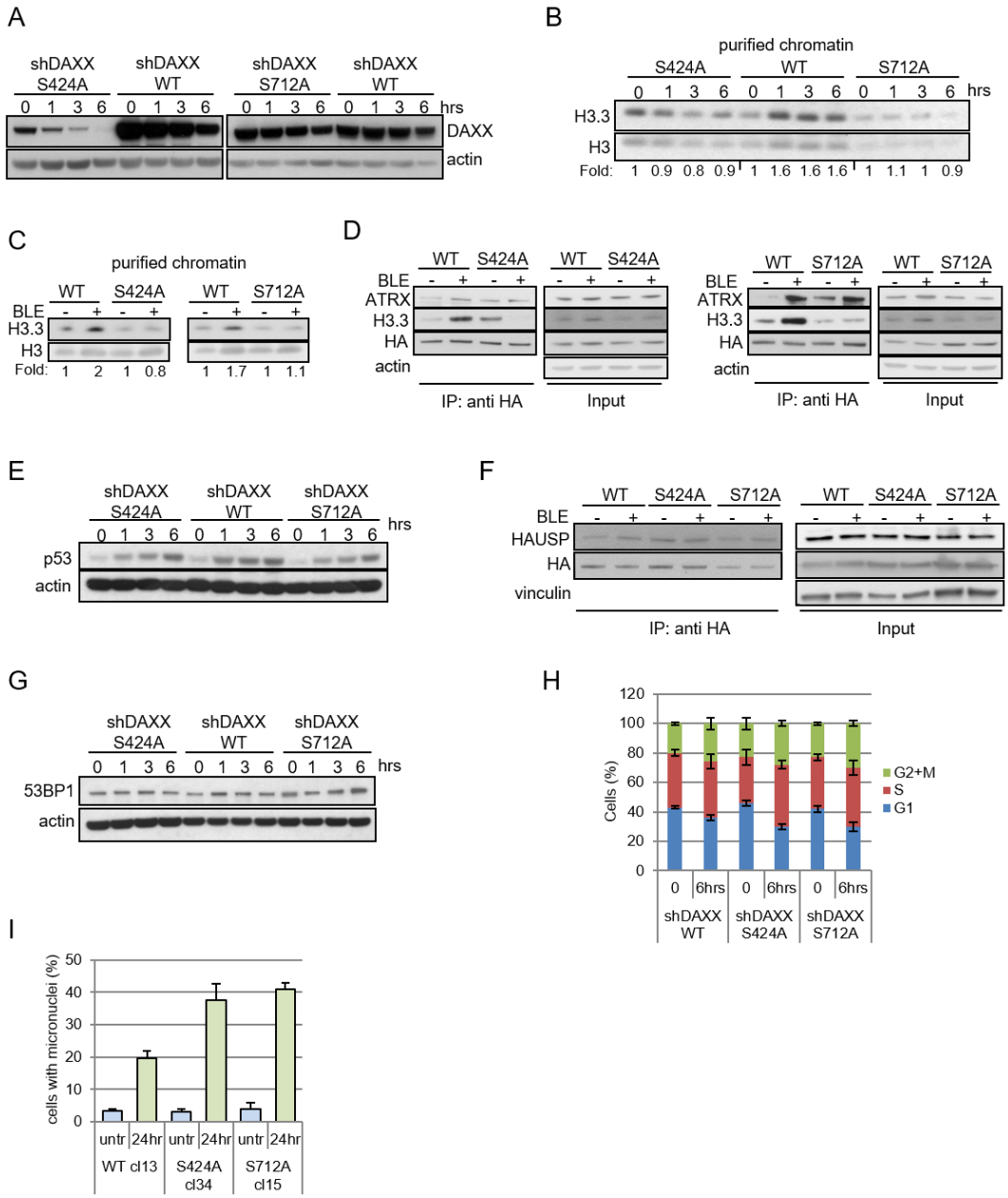
A
shDAXX S424A
shDAXX WT
shDAXX S712A
shDAXX WT
0 1 3 6 0 1 3 6 0 1 3 6 0 1 3 6 hrs
DAXX
actin
B
purified chromatin
S424A WT S712A
0 1 3 6 0 1 3 6 0 1 3 6 hrs
H3.3
H3
Fold: 1 0.9 0.8 0.9 1 1.6 1.6 1.6 1 1.1 1 0.9
C
purified chromatin
WT S424A WT S712A
BLE - + - + - + - +
H3.3
H3
Fold: 1 2 1 0.8 1 1.7 1 1.1
D
WT S424A WT S424A
BLE - + - + - + - +
ATRX
H3.3
HA
actin
IP: anti HA
Input
WT S712A WT S712A
BLE - + - + - + - +
ATRX
H3.3
HA
actin
IP: anti HA
Input
E
shDAXX S424A
shDAXX WT
shDAXX S712A
0 1 3 6 0 1 3 6 0 1 3 6 hrs
p53
actin
F
WT S424A S712A WT S424A S712A
BLE - + - + - + - + - + - +
HAUSP
HA
vinculin
IP: anti HA
Input
G
shDAXX S424A
shDAXX WT
shDAXX S712A
0 1 3 6 0 1 3 6 0 1 3 6 hrs
53BP1
actin
H
Cells (%)
120
100
80
60
40
20
0
G2+M
S
G1
0 6hrs 0 6hrs 0 6hrs
shDAXX WT
shDAXX S424A
shDAXX S712A
I
cells with micronuclei (%)
50
40
30
20
10
0
untr 24hr untr 24hr untr 24hr
WT cl13
S424A cl34
S712A cl15

Figure S6

A

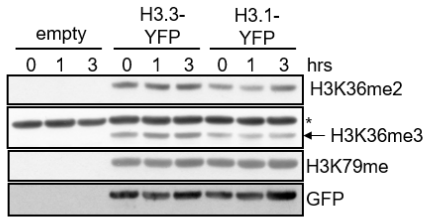
empty
H3.3-YFP
H3.1-YFP
0 1 3 0 1 3 0 1 3
hrs
H3K36me2
*
H3K36me3
H3K79me
GFP

B

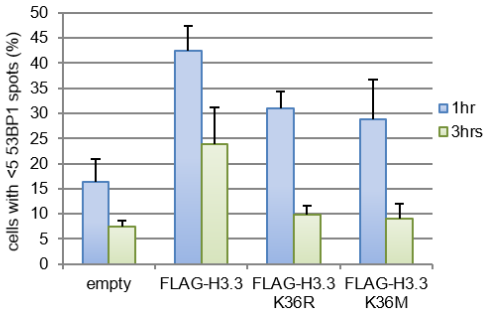
cells with <5 53BP1 spots (%)
50
45
40
35
30
25
20
15
10
5
0
empty
FLAG-H3.3
FLAG-H3.3 K36R
FLAG-H3.3 K36M
1hr
3hrs

Contribution to the paper

In this manuscript I performed the experiments for:

- Figure 1 A
- Figure 2 and 3
- Figure 4 C, D and E
- Figure 5 A, D, E, F and G
- Figure 6 A, C and D
- Figure S1 from A to E, G and I
- Figure S2 from A to D, F, G, J, L and M
- Figure S3 B, C F and G
- Figure S4 B and C
- Figure S5 A, E, G, H, I
- Figure S6 A

In addition I conceived experiments with G.B., analysed and discussed data and commented the manuscript.

Alternative discussion

In this work we provide evidence of DAXX involvement in DNA damage response and DSBs repair as a specific chaperone of the histone variant H3.3. Indeed we verified that upon DSBs occurrence DAXX is phosphorylated by ATM and ATR in S424 and S712. This event promotes H3.3 deposition by DAXX in the damage flanking region and, through H3.3k36 tri-methylation, modulates 53BP1 recruitment at the lesion committing the repair towards HR.

To face the daily challenge of DSBs human cells trigger the DDR network that promotes the repair of the lesions with the most suitable pathway, depending on cell cycle and chromatin status (Ciccia & Elledge 2010). High-throughput screening identified DAXX as a putative ATM/ATR substrates, being phosphorylated in S424 and S712 upon DNA damage (Matsuoka et al. 2007; Stokes et al. 2007). Thanks to phospho-specific antibodies that we generated against S424 and S712 and to the kind collaboration of Dr. Zannini (Fondazione IRCCS Istituto Nazionale dei Tumori, Milan and Istituto di Genetica Molecolare, CNR, Pavia, Italy), we found that upon DSBs induction by chemotherapeutic drugs, like bleomycin and neocarzinostatin, DAXX is phosphorylated on these two residues by the apical kinases of the DDR, ATM and ATR. Interestingly we observed that S424 phosphorylation is upstream and necessary to S712 phosphorylation, indicating that this two modifications act on the same pathway.

We mutagenized these two serines to alanine (S424A and S712A) and we found that the expression of these mutant forms of DAXX dramatically impair a damage-dependent DAXX/H3.3 interaction. Indeed, while in human cells, expressing DAXX wt, we detected an increase of DAXX/H3.3 co-immunoprecipitation following DSBs induction, within cells expressing S424A or S712A DAXX this increase was completely abolished. These results strongly suggested an

involvement of DAXX phosphorylation in modulating its chaperone activity. For this reasons we evaluated the amount of H3.3 specifically into the chromatin and we observed an H3.3 peak of enrichment after 1hr of bleomycin addition. This kinetic is impaired in DAXX knock-down cells and in phospho-mutants expressing cells confirming the previous hypothesis of a S424 and S712 phosphorylation involvement in DAXX chaperone activity. Further analysis, performed by Dr. Zannini demonstrated H3.3 loading at the DSB region where it interacts with γH2AX, phosphorylated form of H2AX spanning for Mb from the lesion and considered a bona fide marker of DSBs (Iacovoni et al. 2010). Moreover, we observed that H3.3 association with γH2AX increases in time and doesn't occur with H2AX, present into the chromatin independently from DNA damage. This indicates that H3.3 accumulation occur specifically at the damage region. Interestingly this H3.3 increase at the lesion depends on DAXX S424 and S712 phosphorylation since S424A and S712A expression abrogates H3.3 increased interaction with γH2AX. To further sustain these results, Dr. Zannini performed ChIP analysis of H3.3 at the DSB site and observed an enrichment of H3.3 at 500 bps from the damage. This enrichment is dramatically impaired silencing DAXX, suggesting that H3.3 accumulation occurs very close to the DNA break in a DAXX-dependent manner. Up to now accumulation of H3.3 at DNA damages sites was detected upon UV lesion (Adam et al. 2013) and laser microirradiation (Luijsterburg et al. 2016) and DAXX didn't seem to be involved in these events. whole, we verified with three different experimental approaches (ChIP, γH2AX/H3.3 co-immunoprecipitation and chromatin purification) that H3.3 enrichment at the lesion is strongly impaired in absence of DAXX. In addition, we observed that mutating S4242 and S712 into alanine reproduce the same phenotype of silencing DAXX in terms of H3.3 presence into the chromatin and γH2AX/H3.3 association. This indicates that DSBs occurrence promotes histones turnover, according to literature data (Dabin et al. 2016), and H3.3 accumulation at the lesion

in a DAXX phosphorylation-dependent manner. Interestingly, up to now, only DAXX S564 was described as an ATM target upon DNA damage, with the specific activity of p53 regulation (Tang et al. 2013) but this role has been recently disputed (Brazina et al. 2015) making of our results the first evidences of DAXX involvement in the DDR network.

Further analysis also revealed that S424 phosphorylation regulates DAXX/ATRX interaction after DSBs and that S712A afflicts DAXX localization at PML-nuclear bodies (PMLNBs). Interestingly, PMLNBs disaggregation or ATRX knock-down did not affect DAXX-dependent H3.3 deposition into the chromatin, while DAXX interaction with ATRX is essential to depose H3.3 at telomeric regions, repressing ALT mechanism (Pickett & Reddel 2015). Importantly, the data previously described demonstrating a role for DAXX in H3.3 deposition at damage site were obtained in the U2OS cells, negative for ATRX, and in some cases confirmed using 293T cell line silenced for ATRX. This allow us to exclude a possible role of the helicase ATRX in the DAXX-dependent deposition of H3.3 at the DSB. Therefore, this work underline a novel activity for DAXX and H3.3 in genome stability maintenance, which is independent from the previously described role for DAXX, ATRX and H3.3 at telomers and centromers.

DAXX role at DSBs is further supported by DAXX protein enrichment at the DSB, detected through immunofluorescence, proximity ligation assay and ChIP. First we verified, through immunofluorescence, a juxtaposition of a DAXX foci fraction with γH2AX foci, demonstrating co-localization and a possible physical interaction of these two protein upon DNA damage. This hypothesis was then verified tanks to the kind collaboration of Dr. Zannini who performed both PLA and ChIP experiments. These analyses allowed us to verify that DAXX localization and interaction with γH2AX does not rely on S424 and S712 phosphorylation. Interestingly, ChIP assay revealed that DAXX span more than H3.3, being detected

also at 1300 bps form the DSB while H3.3 enrichment has been observed only at 500 nucleotides from the damage. Noteworthy, DAXX depletion impairs H3.3 enrichment also at 1300 bps suggesting a role of DAXX not only in accumulating H3.3 close to the lesion but also in maintaining H3.3 presence in a more widespread region. A possible explanation for this observation is the presence of an unknown negative regulator or feedback loop mechanism modulating DAXX deposition of H3.3 at regions far from the damage, possibly to maintain the post-translational modification pattern (PTMs) that H3.3 enrichment could influence.

Since DDR localization at the lesion rely on chromatin modifications (Dabin et al. 2016) and H3.3 incorporation into the nucleosome could modify its stability and PTMs pattern (Szenker et al. 2011) we decided to evaluate the recruitment of sensors and apical kinases at the damage site, a series of events that are tightly regulated by chromatin conformation (Panier & Boulton 2014). We found that overexpression of H3.3 or DAXX wild type impairs 53BP1 foci formation in a cell cycle independent manner, suggesting a DAXX/H3.3 involvement in 53BP1 localization regulation and, therefore, in DSB repair pathway choice. On contrary, DAXX silencing had no effect on 53BP1 foci. This observation is not unexpected since 53BP1 co-localize with γH2AX on every DSB (Schultz et al. 2000), as a consequence an increase of 53BP1 foci is not possible but increasing the number of damages that, in any case, would not rely on DAXX activity but on bleomycin dose. Interestingly DAXX silencing strongly reduce the effect of H3.3 overexpression on 53BP1 foci while HIRA silencing did not, confirming that H3.3 role in modulating 53BP1 re-localization is HIRA independent. Moreover we demonstrate that the observed 53BP1 phenotype depends specifically on H3.3, since overexpression of another histone does not reproduce H3.3 effect. Noteworthy, in these experiments evaluated the possible phenotype of H3.3 overexpression since we wanted to mimic increased histone turnover that could putatively depends on DAXX. Moreover cells silenced for both H3.3 genes (H3.3A

and H3.3B) displayed an high rate of cell death. This is in line with the findings that knock-out mice for both H3.3 genes exhibit developmental retardation and early embryo lethality due both to cell cycle suppression and cell death (Jang et al. 2015).

Noteworthy, overexpression of DAXX phospho-mutants reduce 53PB1 localization impairment, suggesting that S424 and S712 phosphorylation are involved in 53BP1 recruitment modulation. Take together these results strongly indicate that 53BP1 recruitment at the DSBs is impaired by a massive H3.3 incorporation by DAXX. These findings were further confirmed also in cells damaged by the AsiSI restriction enzyme, known to produce DSBs specifically in euchromatin (Aymard et al. 2014), suggesting that the effect of H3.3 deposition by DAXX could preferentially occur at actively transcribe genes. This hypothesis is in agreement with the finding that DAXX localize only on a fraction of lesions induced by bleomycin treatment. Altogether these results demonstrate that DAXX-H3.3 pathway is a novel regulator of 53PB1 recruitment at DSBs.

Since 53BP1 plays a pivotal role in DSBs repair pathway choice we decided to investigate whether DAXX/H3.3-dependent impairment of 53BP1 recruitment could affect DSBs repair. As previously mentioned, human cells rely on two main pathway to repair a DSB: NHEJ and HR. The first can occur in all the phases of the cell cycle, is a fast but error prone mechanism that consist in a re-ligation of the DSBs ends. On the contrary, HR occurrence is restricted to the late S and G2 phases of the cell cycle since it requires the presence of the homology sequence, on the sister chromatid, to accomplish the repair. Furthermore, it has been suggested that HR is responsible for the repair of only a fraction of DSBs occurring in G2 phase (Karanam et al. 2012) and to preferentially occur at DSBs within transcribed regions (Aymard et al. 2014). In addition, the HR mechanism requires an extensive processing of the DSB ends, known as resection. It consists in a nucleolitic

degradation of the 5' strand to generate a 3' protruding tail of single-stranded DNA, essential for invading the homologous sequence and accomplish the repair (Symington & Gautier 2011). The positioning of 53BP1 on DSBs ends represses the access of HR factors, like Brca1, disfavouring resection and thus the HR pathway (Zimmermann & de Lange 2014). According to literature, the impaired 53BP1 foci formation due to H3.3 deposition by DAXX could unbalance the DSB repair pathway choice, promoting HR. Our hypothesis was that DAXX deposition of H3.3, affecting 53BP1 recruitment could favour HR factors recruitment. Indeed we found that DAXX overexpression increase both Brca1 and Rad51 foci accumulation upon damage induction while DAXX silencing or overexpression of DAXX phospho-mutants has the opposite effect. Rad51 is a protein known to specifically localize on resected DNA during HR (ref.). Interestingly, Brca1 localization at the lesions, in DAXX overexpressing cells, take place also in G1 when Brca1 should be excluded from the damages. This data resembles the one obtained in 53BP1 silenced cells (Feng et al. 2013) sustaining the inhibitory role of DAXX on 53BP1 localization at the DSB. These experiments sustain the previous findings of a DAXX/H3.3 pro-HR role and for these reasons we expected that DAXX could modulate the NHEJ/HR balancing.

To test this hypothesis we used a GFP based approach to study, in collaboration with G. Abolafio and Dr. Chiodoni from IRCCS Istituto Nazionale dei Tumori, the formation of HR repair product. In DAXX silenced cells we detected a reduction of HR rate, in absence of any cell cycle progression alterations, confirming the previous findings indicating a DAXX pro-HR role. Interestingly, we found that, silencing DAXX, the NHEJ rate is unharmed. A possible explanation could be that a DSBs committed to be repaired through HR cannot shift towards NHEJ, possibly due to the ends processing required by HR and to the pro-HR chromatin environment. This potentially lead to the activation of alternative-NHEJ (alt-NHEJ) or synthesis dependent strand annealing (SSA), mutagenic and error prone

pathways requiring a mild processing of the lesion ends (Ceccaldi et al. 2015). Therefore, the observed unbalancing of repair pathways could lead to a slower breaks re-joining and a decreased repair fidelity. Consistently, cells overexpressing DAXX and H3.3 display a delay in repair kinetic, evaluated through γH2AX foci expiring, and a mild increase in genome instability, detectable as micronuclei formation in response to damage induction. Conversely, DAXX silencing or expression of DAXX mutants, impairing HR, leads to an increase of micronucleated cells. These events occur in ATRX-negative cells and are DNA damage dependent, suggesting that the genomic rearrangements derive from a misregulation of DSBs repair pathway choice and not from and DAXX/ATRX-dependent telomers and centromeres instability. Taking together, our results demonstrate that DAXX plays an important role, through H3.3 deposition, in DSBs response and repair.

Recently it was demonstrated that H3.3 is loaded by the chromatin remodeller CHD2 at laser microirradiation induced DSBs and that H3.3 silencing reduces NHEJ repair (Luijsterburg et al. 2016). In addition, since the DAXX/ATRX/H3.3 axis inhibits ALT, which is an HR-based mechanism for telomers elongation, it was suggested that H3.3 deposition at the breaks could repress HR (Conomos et al. 2013). These findings seem in contrast with our results but many still unknown factors could modulate different and apparently opposite roles of H3.3 and therefore the final outcome of its deposition. Indeed, many evidence underline a dual role of H3.3 into the chromatin. It has been demonstrated that H3.3 deposition by DAXX/ATRX complex provides tri-methylation of H3.3K9, marker of constitutive heterochromatin, at telomeres and centromeres, repressing ALT (Udugama et al. 2015), and silences endogenous retroviral elements (Elsässer et al. 2015). While, HIRA-dependent deposition of H3.3 occurs in actively transcribed genes and promotes transcription restart upon UV irradiation (Adam et al. 2013). Moreover, upon neural activation H3.3 deposition by DAXX favour transcription

of genes involved in neuronal cells homeostasis (Michod et al. 2012). Taken together, these evidences suggest that H3.3 deposition outcome depends on the complex H3.3/chaperon and on the histone PTMs decorating H3.3. Indeed, the protein sequence of H3.3 differs from H3.1 just for five aminoacids but this allow H3.3 to undergo peculiar PTMs affecting the stability of the whole nucleosome (Szenker et al. 2011).

As previously described, histones PTMs are involved in DDR factors recruitment, strongly influencing the repair pathway choice. Since, as previously mentioned, H3.3 exhibit peculiar PTMs this aspect could suggest the possible mechanism of H3.3 role at the DSBs. Indeed we provide evidence that H3.3 loaded inside the chromatin before and after damage induction display increased levels of K36 di- and tri-methylation compared to H3.1, in agreement with previous works (Hake et al. 2006; Loyola et al. 2006). This result further sustain an H3.3 pro-HR since this histone mark decorates gene bodies and actively transcribed genes (Clouaire & Legube 2015) where promotes HR mechanism (Pfister et al. 2014).

Interestingly, both mutation of K36 into an alanine and silencing SETD2, the methyltransferase responsible for K36 methylation, rescue the wild type 53BP1 foci formation, in DAXX wild type or H3.3 overexpressing cell. These experiments suggest for the first time the involvement of K36 tri-methylation in regulating 53BP1 localization at the break. In addition, coherently with our result, K36Me2 was demonstrated to act as a platform for Nbs1/Mre11 complex recruitment at the DSB, resulting in an efficient resection start and, therefore, favouring HR (Cao et al. 2016). We propose that H3.3 loading into the chromatin could contribute to locally maintain and enrich K36 methylation histones, favouring HR to repair a break occurring in a specific chromatin region. However, the involvement of other factors and/or mechanisms in H3.3 regulation of DSBs repair cannot be excluded.

Strikingly, G34R and G34V mutations of H3.3, detected in 31% of paediatric glioblastoma, and K36M, found in chondroblastoma, alter K36 methylation (Schwartzentruber et al. 2012). Consistently about 15% of paediatric glioblastoma display SETD2 inactivation (Fontebasso et al. 2013) and SETD2 mutations were also described as affecting DNA repair in renal cancer (Kanu et al. 2015). ATRX (or rarely DAXX) mutations were described in 100% of G34-H3.3 mutant cases (Schwartzentruber et al. 2012), indicating that ATRX/ALT axis is not overlapping G34 mutations. Noteworthy, we have found that the expression of K36M-H3.3 mutant doesn't affect 53BP1 recruitment at DSBs differently from wild type H3.3. For this reason, previous evidences and our work suggest that DAXX and H3.3 alteration could promote tumorigenesis through different mechanisms: acquisition of ALT, oncogene transcription enhancement and increased genome instability due to unprecise repair of DSBs. As a consequence, DAXX/H3.3 axis could be relevant for diagnosis and, potentially, for development of therapies targeting particularly aggressive forms of cancer.

Part III

Unpublished data

Functional interplay between FANCP/SLX4 and Brca1 in double-strand break processing

During my last year of PhD I focused on the role of SLX4 protein in DNA damage response and double-strand breaks repair. As mentioned during the introduction (see "SLX4 protein" chapter), growing evidences both in *S. Cerevisiae* and human cells are demonstrating the important role of SLX4 as a pro-resection factor in DSBs repair and genome stability maintenance. Taking into consideration (Dibitetto et al. 2016; Liu et al. 2017) recent papers, our laboratory started investigating whether the pro-resection role of SLX4 is conserved in human cells.

The preliminary experiments have been performed in U2OS AsiSI-ER-HA cells in which DSBs can be generated in known loci of the genome thanks to the AsiSI restriction enzyme fused with the hormone binding domain of the estrogen receptor (Iacovoni et al. 2010). The resulting chimeric protein AsiSI-ER localizes in the cytoplasm in unperturbed condition while, upon 4OH-Tamoxiphen treatment, it translocates into the nucleus generating DSBs at sequence-specific sites. These loci have been already characterised and it is possible to measure percentage of single strand DNA at a particular locus using restriction digestion of genomic DNA, followed by Real-Time PCR (Paull et al. 2014; Ferrari et al., 2017 *in press*). In these cells, silenced for SLX4 we verified a 15% reduction of resected DSBs compared to the siCtrl (Fig. 13, left panel). In addition we have observed that co-silencing 53BP1 and SLX4, abrogating 53BP1-dependent resection block, rescue the phenotype (Fig. 13, right panel). Interestingly, the co-silencing of SLX4 with Brca1 doesn't produce any additive effect, suggesting that SLX4 counteract the anti-resection role of 53BP1, acting in the same pathway of Brca1 (Fig. 13, left panel).

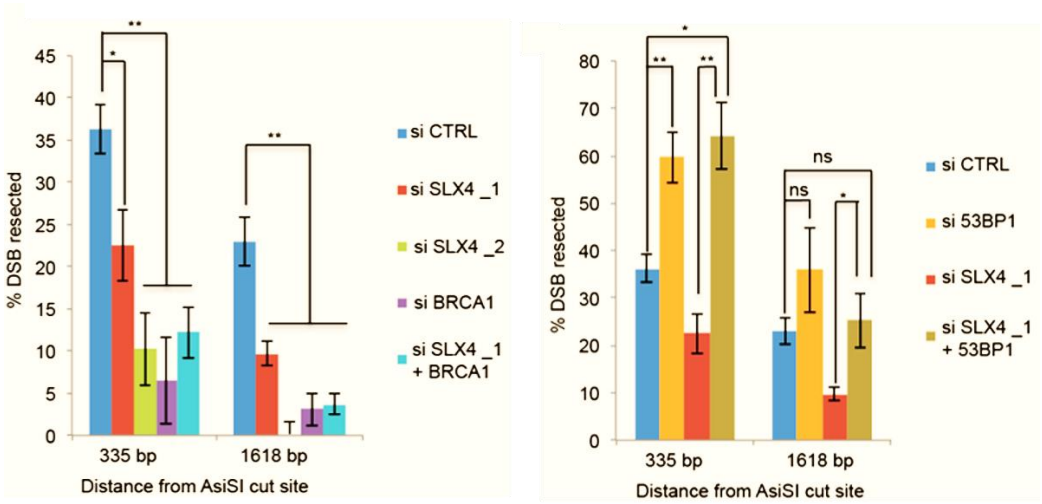

Figure 83: Resection evaluation in AsiSI cells. *AsiSI cells were treater for 4 hrs with 4OHT 300nM. Then cells were collected and DNA was extracted and digested as described in (Paull et al. 2014). Evaluation of the percentage of resected DSBs was conducted as described in (Ferrari et al., 2017 in press). P<0,0 *; P<0,0 **. (performed by S. Tawara, Prof. Achille Pellicioli laboratory, Università degli Studi di Milano).*

In 2011 it was demonstrated that SLX4 mutations are causative of a new subtype of Fanconi Anemia (Fanconi Anemia-P) and FANCP became an alias for SLX4 (Kim et al. 2011; Bakker et al. 2012). Particularly interesting for my work it is the patient-derived SLX4-null RA3331 cell line. The RA3331 cells are skin fibroblast immortalised with hTERT and transformed with the oncoproteins E6 and E7 of the HPV16 (Kim et al. 2013b), displaying two heterozygous frameshift mutations of SLX4 gene. The predicted effect of these mutations is a truncated protein of N-terminal 671 SLX4 aminoacids, but with specific antibodies raised against that region the protein is undetectable. For this reason RA3331 cells are considered SLX4-null (Kim et al. 2013b).

Taking advantage of these patient-derived cells I started analysing SLX4 role in DSB repair. First I decided to evaluate the sensitivity of RA3331 to DSBs inducing

agent bleomycin. For this purpose I infected BJ hTERT fibroblast with a retroviral plasmid containing the E6 and E7 proteins to use as a control (BJ hTERT E6E7). I treated the indicated cell lines (Fig. 14) with increasing doses of bleomycin for 3 hours and evaluated the percentage of survival 72 hours after the treatment, with Trypan Blue staining. In these experiments I verified a 50% survival reduction of RA3331 (RA), partially rescued by re-complementation of SLX4 WT (RA WT), treating cells with 10 µg/ml bleomycin (Fig. 14).

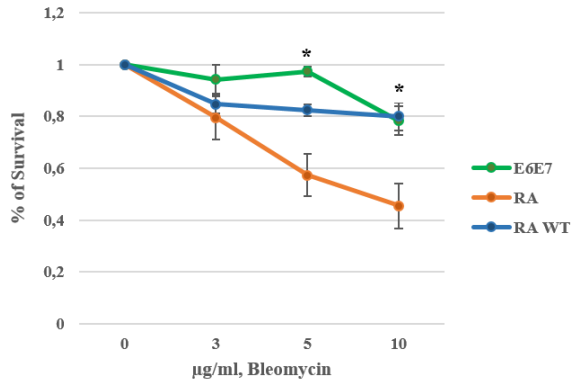

Figure 14: RA3331 cells sensitivity to bleomycin. *The indicated cell lines were treated with increasing doses of bleomycin for 3hrs. Then the bleomycin was removed, cells were washed twice with PBS let grow for 72hrs in conditioned media. Each treated sample was normalised on the untreated and the error bars represent the standard deviation of three independent experiments. P<0,05 *.*

In literature, it has already been demonstrated that mutations of factor involved in the resection process, as CtIP, EXO1 and BLM helicase (Cruz-Garcìa et al. 2014; Gravel et al. 2008), display an increased sensitivity to DSBs inducing agents. Since I observe FANCP cells sensitivity to bleomycin (Fig. 14) and a lower percentage of resected DNA in U2OS AsiSI siSLX4 (Fig. 13), I decided to evaluate resection efficiency in RA3331. To asses this point I went to Pablo Huertas laboratory (CABIMER, Sevilla, Spain) to learn and perform the SMART technique, a combing based assay that allow detection and measurement of ssDNA after exposure of cells for 24 hours to BrdU (Cruz-Garcìa et al. 2014). By this technique,

in irradiated RA3331 cells we found a 40% reduction in ssDNA length (Fig. 15) both 1,5 and 3 hours post-irradiation, compared to control cells. This result supports the hypothesis that DSB resection is defective in absence of functional SLX4. Importantly, re-complementation of SLX4 WT in RA3331 cells rescue the phenotype, confirming the pro-resection role of SLX4.

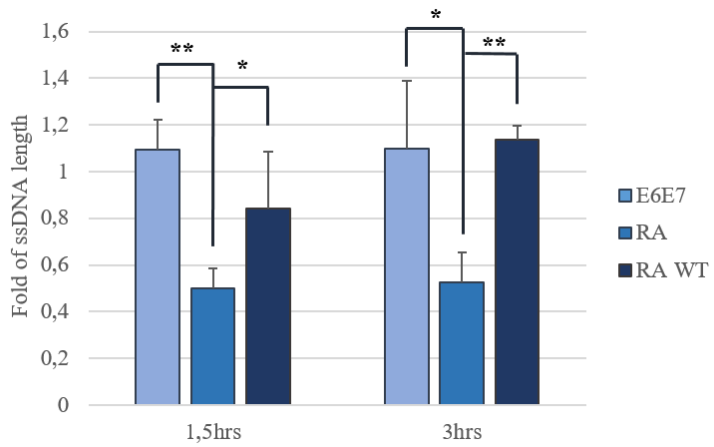

***Figure 15*: Resection evaluation in RA3331 cells.** *RA3331 and control cells were irradiated with 10Gy. After 1,5 and 3hrs cells were harvested and the SMART technique was performed as described in (Cruz-Garcìa et al. 2014) (see the "Material and methods" section). For each sample, the length of 300 fibers was measured and each irradiated sample was normalised on the untreated. The error bars represent the standard deviation of three independent experiments. Statistical significance obtained with a Student's t-test. P<0,05 *; P<0,01 **. (experiments performed by F. Mejias, Prof. Pablo Huertas laboratory, CABIMER. I performed data analysis).*

To further confirm this result I used an alternative approach to evaluate resection efficiency. It has been published that RPA32 is phosphorylated by the apical kinase DNA-PK in S4 and S8 when, upon DSB induction, it binds the ssDNA generated by the resection mechanism (Isono et al. 2017). Considering the resection defect observed RA cells with the SMART technique, I wanted to confirm the phenotype analysing RPA32 pS4/8 by western blot, expecting a decreased or delayed phosphorylation of RPA.

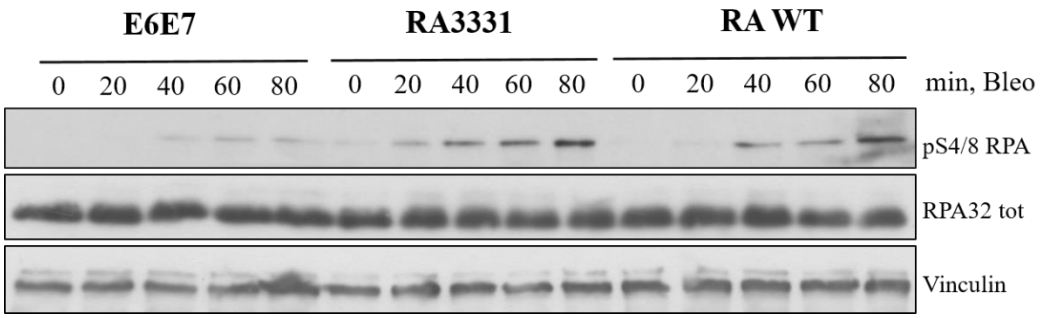

Figure 16: RPA32 phosphorylation in SLX4 depleted cells. *RA and control cells were treated for the indicated time points with 20µg/ml of bleomycin of bleomycin. Protein gel and incubation with specific antibodies was performed as indicated in "Material and methods" section. This is a representative image of 3 independent experiments.*

Strikingly, this approach revealed a faster and stronger, at least at later time points, phosphorylation of RPA32 S4 and S8 in RA3331 cells compare to control cell lines, partially rescued by the re-expression of SLX4 WT (Figure 16). This result is in contrast with our hypothesis of an impaired resection in absence of SLX4, since a faster RPA32 S4/8 phosphorylation is considered an index of efficient resection (Isono et al. 2017). A possible explanation is that resection impairment leads to an activation of the NHEJ, to repair the damages, (Brandsma & Gent 2012b) and a consequent enhanced activity of DNA-PK (Hartlerode & Scully 2009) that phosphorylates more efficiently RPA32 S4/8. This would be in agreement with our resection data but further analysis are required to verify and dissect the mechanism regulating RPA32 phosphorylation in absence of SLX4.

Since resection is an essential step, committing the DSB to be repaired through HR, I evaluated whether resection defect could affect the DSB repair process. I analysed Rad51 foci formation in U2OS siSLX4 and RA3331 cells through immunofluorescence and verified a mild decrease in Rad51 foci number in G2 cells, in absence of SLX4 (Figure 17).

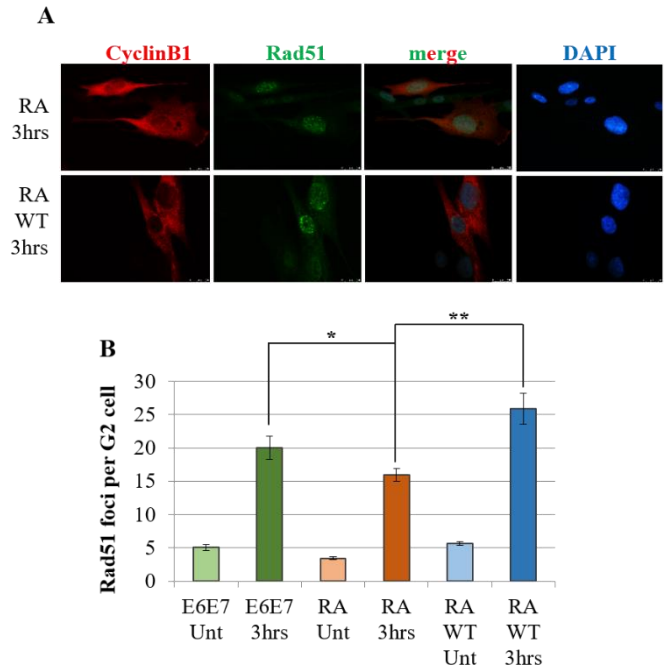

Figure 17: Absence of SLX4 affects Rad51 foci formation. A) *A representative image of the IF (see the "Material and methods" section).* ***B)*** *RAD51 foci were enumerated within cyclin B positive cells after 3hrs treatment with 20µg/ml of bleomycin. The graph shows the mean of Rad51 foci number per G2 cells obtained from three independent experiments. At least 50 cells were scored for each experiment. The error bars represent the standard deviation of at least three independent experiments. Statistical significance obtained with a Student's t-test. P<0,05 *, P<0,01 **.*

This result seem to confirm our hypothesis of an SLX4 pro-HR activity. Interestingly, the reduction of Rad51 foci number is a modest phenotype compared to the effect of SLX4 depletion on resection, both in AsiSI siSLX4 and RA3331 (Figure 13 and 15). This could suggest that an halving of resection-dependent ssDNA length is not sufficient to dramatically impair Rad51 nucleofilament formation, index of HR process, but could affect its fidelity. To address this point I evaluated the percentage of micronucleated cell after a 24hrs recovery from a bleomycin treatment. I observed a dramatic increase of the percentage of micronucleated cells in absence of SLX4, partially rescued by re-expression of SLX4 WT (Figure18).

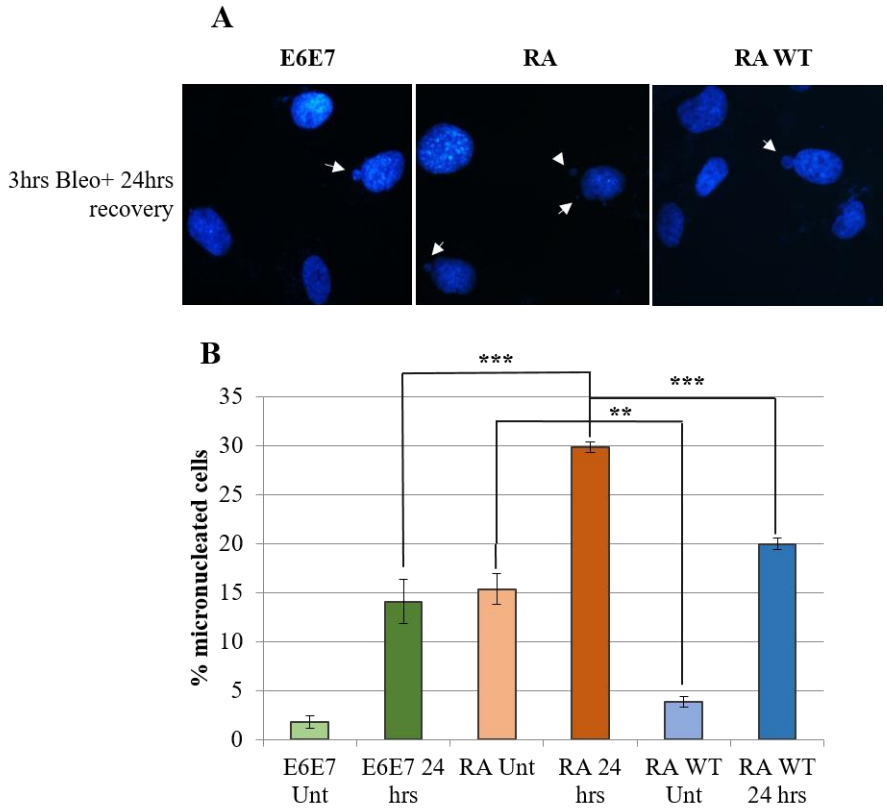

Figure 18: SLX4 depletion increases genome instability. A) A representative image of the DAPI staining. B) The indicated cell lines were treated for 3hrs with *20µg/ml of bleomycin. After three PBS washes, cells were le to recovery in conditioned media for 24hrs and then stained with ProLong Gold mounting solution (see the "Material and methods" section). At least 100 cells were scored for each experiment. The error bars represent the standard deviation of at least three independent experiments. Statistical significance obtained with a Student's t-test. P<0,01 **, P<0,001 ****

Noteworthy, the percentage of micronucleated cells in RA untreated sample is comparable to the treated sample of the control cell line, indicating an high level of endogenous damages and genome instability, in absence of SLX4. This could be due to endogenous damages improperly repaired cause of SLX4 depletion. Indeed, according to literature, SLX4 has a role in telomers homeostasis maintenance (Wan et al. 2013), in Fanconi Anemia pathway (Yamamoto et al. 2011), in double

Holliday junction resolution (Kim 2014) and, suggested by our data, in resection regulation. All these mechanisms, if misregulated, can lead to genome instability increasing micronuclei occurrence (Hengstler 2011). However, further experiments will be required to evaluate how the absence of SLX4 and the consequent resection defect affect not only HR pathway but also other repair mechanism as SSA and alt-NHEJ, both mutagenic and requiring a mild processing of DSB ends. Moreover, would be interesting to investigate how SLX4 depletion, in combination with silencing of Brca1, CtIP, and 53BP1, impact on resection efficiency.

In addition, I'm performing preliminary experiments to evaluate the involvements of SLX4 dimerization in SLX4 pro-resection activity. Indeed, as previously described (see chapter "SLX4 protein"), SXL4 localization at DNA damage region is homodimerization-dependent and relies on SLX4 BTB domains (Figure 19A). It has been published that SLX4 BTB mutants of F708 and F781 (Figure 19B) lose ICL localization and abolish associated nucleases (XPF, SLX1 and Mus81) recruitment, causing defect to ICL response (Yin et al. 2016b).

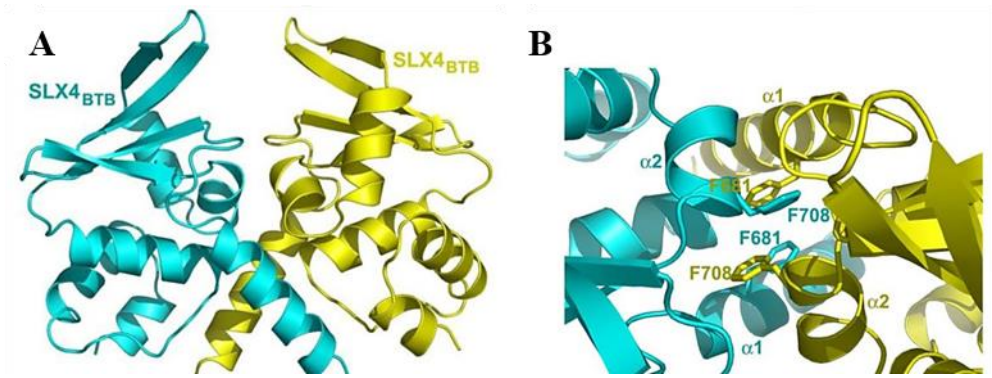

Figure 19: BTB domain mediates SLX4 dimerization. *A) Overall structure of dimeric SLX4 BTB domains. The monomers are colored in cyan and yellow. B) Enlarged view of SLX4 BTB domains dimeric interface. The aminoacids F708 and F781 are essential to preserv dimeric interface and are responsible for SLX4 dimerization and localization at ICLs.* (Yin et al. 2016b)

I'm interested in verifying whether the involvement of SLX4 in the resection process rely on its homodimerization. To asses this point I'm verifying the presence of SLX4 dimer in U2OS cell line expressing GFP-SLX4 under the control of an inducible promoter (Wilson et al. 2013), a kind gift of Jhon Rouse. In these cells I've transfected HA-SLX4, after 24 hours I induced GFP-SLX4 expression with Doxocyclin treatment. After 24 hours (48 hours from the transfection) I treated with bleomycin, for 3hrs and immunoprecipitated GFP-SLX4 to evaluat the co-immunoprecipitation of HA-SLX4.

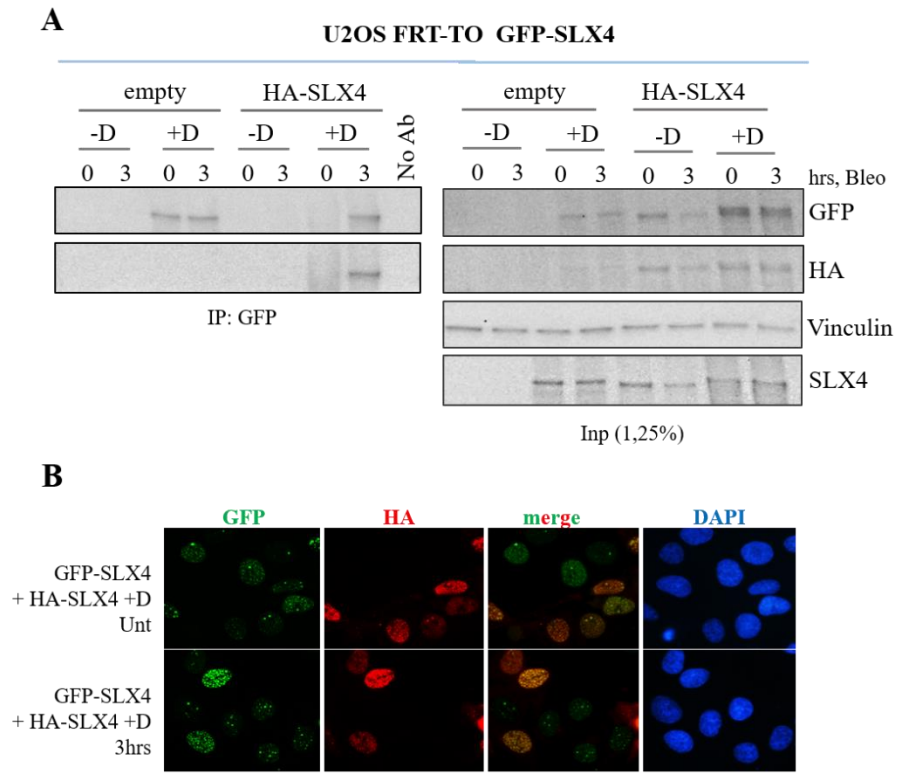

Figure 20: SLX4 dimerization. *In U2OS FRT-TO GFP-SLX4 cells was transfected HA-SLX4 and after 24hrs, GFP-SLX4 expression was induced with Doxociclin treatment (1µg/ml). After 48 hrs from the transfection cells were treated for 3 hrs with bleomycin (20µg/ml).* ***A)*** *The cells were harvested and immunoprecipitation was conducted with GFP-trap beads® Chromotech. Bands were resolved through SDS page and co-immunoprecipitation was detected with α-HA antibody.* ***B)*** *A representative image of immunofluorescence on cells treated as in A (see the "Material and methods" section).*

From these experiments I can detect HA-SLX4 co-immunoprecipitating with GFP-SLX4 conforming SLX4 dimerization at least after 3hrs of bleomycin while in the untreated sample, induced with doxocyclin, the result is not clear since seem the immunoprecipitation didn't work (Figure 20A). Starting from this preliminary evidence, taking advantage of the well-characterised crystal structure of BTB domain, in collaboration with Dr. Mastrangelo's and Milani's laboratory (CNR-Biophysics Institute, Milano, Italy) we are planning to find, by *in silico* approaches, compounds targeting F708 and F781 to stabilize or inhibit SLX4 dimer formation. With these molecules we would test resection efficiency at DSB in U2OS AsiSI-ER (see Fig. 13).

Ongoing experiments and future plans

As already mentioned previously (see “SLX4 protein” chapter), SLX4 display an E3 SUMO-ligase activity and mutations in the SLX4 SIM domains abrogates both SUMOylation of XPF and SLX4 itself, impairing SLX4 localization at laser induced DNA lesions (Guervilly et al. 2016). Moreover, it has been recently demonstrated that SLX4 directly interacts with TopBP1 at the DSB, participating to the Brca1 and 53BP1 interplay with TopBP1 (Liu et al. 2017). Taking in consideration these papers, a possible molecular mechanism of SLX4-dependent resection regulation is that SLX4 SUMOylates Brca1, stabilizing its localization at the DSB, favouring resection. To verify this hypothesis, I’m taking advantage of U2OS cell line expressing under its endogenous promoter the SUMO2 molecule, tagged with a stretch of ten His (U2OS 10xHis-SUMO2) (Hendriks et al. 2014). In these cells I’m silencing SLX4 and immunoprecipitating Brca1 to evaluate its SUMOylation status upon DSBs induction, in absence of SLX4 (Figure 21).

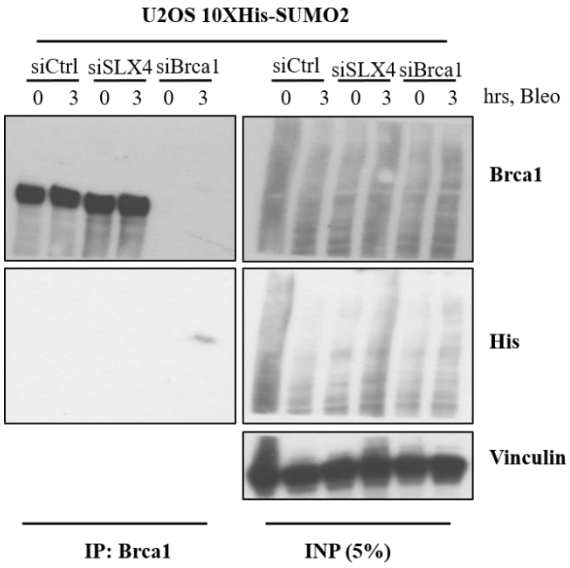

Figure 21: Brca1 SUMOylation status evalution. *Immunoprecipitation of Brca1 was performed in U2OS 10XHis-SUMO2 cells siCtrl, siSLX4 and siBrca1 treated for 3hrs with 20µg/ml of bleomycin. IP and INP bands were resolved with SDS page. Brca1 SUMOylation status was evaluated with an α-His specific antibody (see the "Material and methods" section).*

Unfortunately, up to now, after multiple trials, I couldn't detect any Brca1 SUMOylation band. This analysis will require a different approach. I'm planning to purify proteins covalently attached to 10xHis-SUMO2 molecule on Nickel-charged beads, under highly denaturing condition to abolish proteases activity (Jaffray & Hay 2006). If I manage to observe reduction of Brca1 SUMOylation status in absence of SLX4, I'm planning to mutate putative Brca1 SUMOylation sites and analyse resection efficiency. Alternatively a possible molecular mechanism for SLX4-dependent resection modulation would be that SLX4, through SIM domains, interact with SUMOylated Brca1 favouring its recruitment at the lesion. This would be in agreement with the docking platform role of SLX4 and with the findings that interacting with TopBP1, SLX4 participates to the Brca1/53BP1/TopBP1 interplay. In this case I'll verify physical interaction of both TopBP1 and SLX4 with Brca1 through Proximity Ligation Assay (PLA) and Co-

IP. Moreover, I would express the SLX4 SIM mutant to analyse a possible Brca1/TopBP1 interaction impairment, at the DSB end.

Moreover, considering also the involvement of SIM domain to SLX4 recruitment at the DSB, and taking advantage of the *in silico* approaches used for SLX4 dimerization inhibitors (see previous paragraph) I would dissect SLX4 SIM domain involvement in the resection process. Therefore, in collaboration with Dr. Mastrangelo's and Milani's laboratory (CNR-Biophysics Institute, Milano, Italy), we aim to purify and crystallize SLX4 SIM domain and develop molecules that inhibit SLX4 interaction with SUMOylated proteins. As planned for dimerization inhibitor compounds, with these new molecules, inhibiting SLX4 interaction with SUMOylated proteins, I would test resection efficiency at DSB and in U2OS AsiSI-ER (see Fig.13). It will be important to evaluate the effect of some of these novel compounds also in Brca1 defective cells, with the aim to sensitize them to Olaparib. Eventually, the more effective drugs may be successfully used in combination therapy, particularly for Olaparib resistant bracness tumors.

Material and Methods

Abbreviations

DMEM: Dulbecco's Modified Eagle Medium

DMSO: Dimetilsulfoxide

ECL: Enhanced Chemiluminescence

FBS: Fetal bovine serum

HEPES: **4-(2-Hydroxyethyl)piperazine-1-ethanesulfonic acid**

O/N: Over night

PBS: Phosphate buffer saline

Pen/Strepn: Pennicillin, Streptomycin

PPI: Protease and phosphatase inhibitors

PVDF: Polyvinylidene difluoride

Rpm: Rotations per minute

RT: room temperature

SDS: Sodium Dodecil-Sulfate

TRIS: Tris(hydroxymethyl)aminomethane

Cell culture

Solutions

- Complete media
    - DMEM High Glucose with L-Glutamine (Euroclone®)

    - FBS 10% for U2OS (and derived cell lines) and 293T, 15% for BJ hTERT E6E7, RA3331, RA3331 SLX4 WT.
    - HEPES 10 mM
    - Glutamine 2 mM
    - Pen/Strep 100U/ml di Pen e 100µg/ml Strep
    - Sodium Piruvate 1 mM
    - Non essential aminoacids: 100X
- Complete media without pen/strep
    - DMEM High Glucose with L-Glutamine (Euroclone®)
    - FBS 10% for U2OS (and derived cell lines) and 293T, 15% for BJ hTERT E6E7, RA3331, RA3331 SLX4 WT.
    - HEPES 10 mM
    - Glutamine 2 mM
    - Sodium Piruvate 1 mM
    - Non essential aminoacids: 100X
- Blasticidin 10 mg/ml in PBS 1x
- Bleomycin 10 mg/ml in PBS (Sanofi®)
- Doxocyclin 10 mg/ml in PBS
- FBS (Lonza®) Decomplemented at 56°C for 30’
- Freezing solution
    - Complete media (media and FBS concentration required for the cell line) 70%
    - FBS 20%
    - DMSO 10%
- G418 100 mg/ml in PBS
- HEPES (Lonza®)
    - HEPES 238,3 mg/L

    - NaCl 8,5 mg/L
- L-Glutamine (Euroclone®)
    - L-glutamine 200 mM
    - NaCl 145 mM
- Neocarzinostatin (Sigma®) 49,2 µM (Sigma®)
- Non essential aminoacids 100x (Lonza®)
    - L-Alanine 890 mg/ml
    - L-Asparagine 1321 mg/ml
    - L-Aspartic Acid 1330 mg/ml
    - L-Glutammic Acid 1470 mg/ml
    - L-Proline 1150 mg/ml
    - L-Serin3 1050 mg/ml
    - Glycine 750 mg/ml
- PBS 1x
    - KH_2PO 1,058 mM
    - NaCl 154, 004 mM
    - NaOH 0,010 µM
    - Na_2HPO_4 5,599 mM
- Pen/Strep (Euroclone®)
    - 10000 U Pen/ml
    - 10000 U Strep/ml
- Puromycin 1 mg/ml in PBS 1x
- Sodium piruvate (Lonza®) 11,1 mg/ml
- Tripsin-EDTA 1x in PBS (Euroclone®)
    - Tripsina 0,25% v/v 0,5g/L
    - Na_2-EDTA 0,913 mM
    - KCl 5,33 mM
    - KH_2PO_4 0,441 mM

- $NaHCO_3$ 4,17 mM
- NaCl 137,93 mM
- Na_2HPO_4-$7H_2O$ 0,336 mM

Cell lines

U-2 OS and 293 T cell lines

Both these cell lines were obtained from ATCC and were cultured in complete media 10% FBS, in an humidified incubator, at 37°C and 5% of CO_2. All cell treatment and manipulation were performed under a laminar flow hood. All the cell lines derived from U2OS (AsiSI and FRT-TO GFP-SLX4) were cultured at the same condition as above except for U2OS DR and EJ5 (a kind gift of Prof. J. Stark and Prof. S. Piccolo) that were cultured in complete media 10% w/o sodium pyruvate.

U2OS AsiSI were kept in selection adding puromycin 1µg/ml.

U2OS FRT-TO GFP-SLX4 were kept in selection adding blasticidin 1,5µg/ml and hygromycin 2µg/ml.

RA3331

This cell line deriving from a nine year male individual with Fanconi anemia, registered in the International Fanconi Anemia Registry, was a kind gift of Prof. A. Smogorzewska. RA3331 were immortalized using a catalytic subunit of telomerase (hTERT) and transformed using HPV16 E6 and E7 proteins. These cells were cultured as above except for 15% FBS. The deriving cell line R3331 SLX4 WT was a kind gift of Prof. P. Pichierri and was cultured as above adding puromycin selection 2µg/ml.

BJ h TERT E6E7

BJ hTERT were obtained by ATCC and transformed using HPV16 E6 and E7 proteins (the retroviral plasmid was a kind gift of Prof. A. Smogorzewska). These cells were cultured as above except for 15% FBS, adding G418 400µg/ml for selection.

Phoenix-AMPHO

This cell line was obtained from ATCC and used to produce retroviruses. These cells were cultured as above.

Cell lines maintenance and manipulations methods

Cells storage in liquid nitrogen and thawing

Centrifuge tripsinized cells at 1300 rpm at RT. Discard supernatant and add 1,5ml of freezing solution for each vial to freeze. Store the vials at -80°C for two days than move in liquid nitrogen. To thaw, take out from liquid nitrogen the vial of interest and incubate at 37°C. Once is completely thawed transfer cell suspension in a falcon containing 3ml of the needed cell line media and centrifuge at 1300rpm for 5'. Discard the supernatant, re-suspend in 6ml of the required media, plate the cell suspension and incubate.

Cells transfection and silencing

Cell for transfection and silencing were seeded at a confluence 70% in media w/o pen/strep. After 24hrs transfection or silencing were performed respectively with Lipofectamine®3000 and Lipofectamine® RNAiMax (Life tecnology™) according to manufacture procedures. After 24h cells were split in the needed plates. For transfected cell the DSBs inducing agent treatment was performed 48hrs

post-transfection while the silenced cells were treated with the damaging compounds after 72hrs from the silencing.

Retroviral particle production

- Day 1:
- Remove the media from a 10cm plate of Phoenix-AMPHO cells at 70% of confluence.
- Add 6ml of complete media supplemented with HEPES pH 7.3 50mM.
- Prepare two falcons: the first containing 500µl of HBS 2X, the secondo containing 500µl of water, 50µl of $CaCl_2$ and 20µg of the retroviral plasmid pMSCV HPV16 E6E7 Neo (a kind gift from Prof. A. Smogorzeska).
- While producing bubble add in the drop by drop the DNA containing mix. The add all the obtained solution drop by drop to the Phoenix-AMPHO cells and incubate O/N at 37°C, 5% CO_2.
- Day 2: Remove the cell media and add 10ml of fresh complete media.
- Day 4: Collect the cell media (that contains the virus particles) and filter it with a syringe filter (0,22µm pores). Aliquot the filtered media containing viruses and store at -80°C.

Infection

- Day 1: seed the BJ hTERT in a 6cm plate, at a confluence of 70%, in complete media.
- Day 2: thaw 1ml of retrovirus, add 1ml of complete cell media and polybrene 1:1000. Remove the media from the plate, add the mix and incubate O/N at 37°C, 5% CO_2.
- Day 3: discard the supernatant from the plate and split adding the antibiotics.

DSBs inducing agents treatment

All the damaging agents compounds were added to cell media in the required concentrations. For the survival and micronuclei experiments in RA3331 cells, after 3hrs of bleomycin treatment, cells were washed twice with PBS and then cultured in conditioned media for the needed time of recovery.

Biochemistry methods

Total lysis in SDS: tripsinized cells were centrifuged at 5000rpm for 5' at 4°C. Supernatant was discard and the pellet was re-suspended in PBS 1X. After centrifugation at 5000rpm for 5' at 4°C the pellet as re-suspended in Boiling SDS buffer (SDS 5%, Tris 0,125 M) and the sample were boiled for 10' at 95°C. After a fast spin, an equal volume of Boiling SDS buffer +PPI cocktail (Sigma ™) was added to each sample. The was performed sonication for 30'' at 40% of amplitude and lysates concentration was evaluated with µBCA (EuroClone™) according to experimental procedure at a wave length of 562nm.Than lysates were loaded in a SDS page gel (see below)

Lysis in ELB buffer for DAXX immunoprecipitations: tripsinized cells were centrifuged at 5000rpm for 5' at 4°C. Supernatant was discard and the pellet was re-suspended in PBS 1X. After centrifugation at 5000rpm for 5' at 4°C (pellet can be store at -80°C at this step) the pellet was re-suspended in 500µl of ELB buffer pH 7.4 (NaCl 150mM, HEPES 50mM, EDTA 5mM, 0,5% NP40, PPI cocktail (Sigma™)). Samples were incubated in ice for 30' and each 5' were vortexed for 30''. Then samples were centrifuged at 8000rpm for 8' at 4°C. The supernatant sonicated for 30'' at 40% of amplitude and spin. Lysates concentration was

evaluated with Bradford (BioRad™) according to experimental procedure at a wave length of 595nm. Then the IP was performed (see below).

Lysis in IP buffer for SLX4 and Brca1 immunoprecipitations: scrapered on ice cells were centrifuged at 5000rpm for 5' at 4°C. Supernatant was discard and the pellet was re-suspended in cold PBS 1X. After centrifugation at 5000rpm for 5' at 4°C (pellet can be store at -80°C at this step) the pellet was re-suspended in 500µl of cold IP buffer (NaCl 420mM, $MgCl_2$ 1mM, HEPES pH 7.5 30mM, NP40 1%, PPI cocktail (Sigma™)) and samples were incubated in ice for 50' and each 5' were vortexed for 30''. Lysates were then centrifuged at 10000rpm for 5' at 4°C and quantified with µBCA (EuroClone™) according to experimental procedure at a wave length of 562nm.

Chromatin extraction with SDS: Tripsinized cells were centrifuged at 5000rpm for 5' at 4°C. Supernatant was discard and the pellet was washed twice in in PBS 1X. After centrifugation at 5000rpm for 5' at 4°C (pellet can be store at -80°C at this step) cells were re-suspended in buffer A (HEPES pH 7.9 10mM, KCl 10mM, $MgCl_2$ 1,5mM, sucrose 0,34M, glycerol 10%, Tryton X-100 0,1%, PPI cocktail (Sigma™)) at a concentration of 2 x107cells/ml and incubated for 8' on ice. The nuclear pellet was obtained by centrifugation at 1300rcf for 5' at 4°C, washed with buffer A (same volume) and re-suspended in buffer B (EDTA 3mM, EGTA 0,2mM, PPI cocktail (Sigma™)) (2 x107cells/ml) for 30' on ice. The insoluble chromatin pellet was isolated by centrifugation at 1700rcf for 5' at 4°C, washed once with buffer B (same volume) and centrifuged at the same conditions. The final chromatin pellet was re-suspended in 15µl of Boiling SDS buffer (SDS 5%, Tris 0,125 M) and boiled at 95°C for 10'. The samples were then centrifuge at the 13000rpm for 10'' RT and Boiling SDS buffer +PPI cocktail (Sigma ™) was added in equal volume. Samples concentration was evaluated with µBCA (EuroClone™) according to experimental procedure at a wave length of 562nm.

Chromatin extraction with HCl: the final nuclear pellet was obtained as above. Once obtained it was re-suspended in HCl 0.4N at a cell density of 4 x10^7cells/ml and incubated O/N at 4°C. The day after samples were centrifuged at 3000rpm for 10' at 4°C, and was added 1/20 of the volume of NaOH 5N. Once quantitated with Bradford (BioRad™) according to experimental procedure at a wave length of 595nm, samples were stored at -80°C.

Immunoprecipitation of DAXX

During cell lysis (see above) α-HA conjugated magnetic beads (Pierce™) were washed twice in cold ELB buffer (NaCl 150mM, HEPES 50mM, EDTA 5mM, 0,5% NP40, PPI cocktail (Sigma™). Once quantified, the needed volume of cell extracts (it varies depending on samples concentration, the immunoprecipitated µg range is from 200 to 500µg) was added to the beads and incubated at 4°C on wheel for 4 hrs, while the remaining volume is stored at -80°C (when loading the protein gel will be used as input). After immunoprecipitation the supernatant (immunodepleted) was collected and stored at -80°C. The beads were washed three times with cold ELB buffer and re-suspended in 20µl of Laemly buffer (2-mercaptoethanol 0.1%, bromophenol blue 0.0005%, glycerol 10%, SDS 2%, Tris-HCl pH 6.8 63 mM) and boiled in a termomixer at 95°C for 10' at 800rpm. Samples were centrifuged at 13000rpm for 5'' at RT and then the supernatant was collected and stored at -80°C. When loading, to the needed volume of the total extract (from 1 to 5% of the IP) was added Laemly buffer and the samples were boiled.

Immunoprecipitation of SLX4

During cell lysis (see above) GFP-Trap magnetic beads (ChromoTech™) were washed twice in cold IP buffer (NaCl 420mM, $MgCl_2$ 1mM, HEPES pH 7.5 30mM, NP40 1%, PPI cocktail (Sigma™) and re-suspended in IP2 buffer (NaCl 210mM, $MgCl_2$ 1mM, HEPES pH 7.5 30mM, NP40 1%, PPI cocktail (Sigma™). Once quantified, the needed volume of cell extracts (it varies depending on samples concentration, the immunoprecipitated µg range is from 200 to 500µg) was added to the beads and incubated at 4°C on the wheel for 3 hrs, while the remaining volume is stored at -80°C (when loading the protein gel will be used as input). After immunoprecipitation the supernatant (immunodepleted) was collected and stored at -80°C. The beads were washed once with cold IP2 buffer then twice with PBS+0,1% Tryton X-100. Then 20µl of Laemly buffer was added (2-mercaptoethanol 0.1%, bromophenol blue 0.0005%, glycerol 10%, SDS 2%, Tris-HCl pH 6.8 63 mM) and boiled 95°C for 10'. The supernatant was collected and stored at -80°C. When loading, to the needed volume of the total extract (from 1 to 5% of the IP) was added the same volume of IP2 buffer and Laemly buffer, the samples were boiled and then loaded.

Immunoprecipitation of Brca1

Before starting cell lysis (see above) Dynabeads™ Protein G (Invitrogen) were conjugated with 2µg of anti-Brca1 antibody (see Table 3) for each sample, incubating at 4°C for 3hrs. Meanwhile cell extracts were prepared as described above for SLX4 IP. After the three hours of conjugation, beads+Ab were washed three times for 5' at 4°C with PBS 0,1% Tryton X-100 and the IP was conducted as described above for SLX4, except the incubation time that in this case is O/N.

SDS page and western blotting

Lysates (from 15 to 30µg) or IP were loaded on gradient protein gels Nu-page (Invitrogen™) and then transferred on PVDF membrane. The primary antibodies, listed in Table 3, were diluted in TBST BSA (NaCl 150mM, Tris-HCl pH 7.5 50 Mm, o,1% Tryton X-100, BSA 0,5%), and incubated at 4°C, O/N. The secondary antibodies, diluted in Blocking buffer [4% milk in PBST (PBS, 0,1% Tryton X-100)], were incubated at 4°C for 1hr. Chemioluminescence reaction was performed with ECL liquids 1 (Luminol 440µg/ml, P-coumaric acid 60µg/ml, Tris-HCl pH 8,5 1M) and 2 (H_2O_2 30%, Tris-HCl pH 8,5 1M) or with LiteAblot® Extended (Euroclone™). Chemioluminescent bands were detected with ChemDoc™ Touch (BioRad™).

Table 3: Antibodies used for the projects of this Thesis.

Antibody	Clone	Company	WB	IF
Actin	Clone AC-74	Sigma	1:20000	
γ-H2AX	JBW301	Upstate	1:1000	1:500
H2AX	07-627	Upstate	1:2000	
53BP1	NB100-304	Novus	1:2000	1:900
DAXX	M-112	Santa Cruz	1:1000	1:50
DAXX	DAXX-03	Acris	1:1000	1:100
HA	12CA5	Roche	1:2000	1:200
HA	H6908	Sigma		1:100
DAXX pS712	This paper *		1:100	
DAXX pS424	This paper *		1:100	
Chk2 pT68		Cell Signaling	1:1000	
Chk2	DCS-273	Enzo Life	1:800	
p53	DO1	Sigma	1:800	
Rad51	PC130	Calbiochem	1:2000	1:500
FLAG	M2	Sigma	1:1000	1:700
PML	PG-M3	Santa Cruz		1:200
ClnB1	GNS-1	BD-Pharmingen		1:200
H3.3	SP2	CosmoBio	1:10000	
H3.3B		Genetex	1:1000	

H3		Genetex	1:3000	
Chk1 pS345		Cell Signaling	1:1000	
Chk1		Cell Signaling	1:1000	
Vinculin	hVIN1	Sigma	1:50000	
H3K4Me3	Ab8580	Abcam	1:5000	
H3K36Me2	C75H12	Cell Signaling	1:1000	
H3K36Me3		ActiveMotif	1:3000	
H3K79Me1		ActiveMotif	1:1000	
H3K9Me3	Ab8898	Abcam	1:2000	
H3K9Ac	C5B11	Cell Signaling	1:1000	
H3K56Ac		Upstate	1:2000	
GFP	3E6	Invitrogen	1:1000	
HAUSP	A300-033A	Bethyl	1:4000	
HIRA	WC119.2H11	ActiveMotif	1:1000	
ATRX		Santa Cruz	1:200	
pS4/8 RPA32	A300-245-M	Bethyl	1:1000	
RPA32	NB 100-332	Novus	1:1000	
Brca1	D-9	Santa Cruz	1:200	1:100
HPV16 E6E7	C1P5	Santa Cruz	1:200	
pS2056 DNAPK		Abcam	1.500	
DNAPK		Abcam	1:1000	
CENPF		Abcam		1:400
SLX4	H00084464-B01P	Novus	1:500	
His	2366S	Cell Signaling	1:1000	

* DAXX phospho-S424 and phospho-712 antibodies were generated by ImmunoGlobe. They were negatively purified against specific unphosphorylated peptides and, for phospo-S424 antibody against a phosphorylated S712 peptide and viceversa. Finally, they were positively purified using their own specific phospho-peptides.

Immunofluorescence

Cells were seeded on a corverslip the day before the DNA damaging agent treatment. Once concluded the exposure to the drug, cells were fixed in paraformaldehyde 4% (in PBS) and washed twice for 5' at RT (fixed cells can be stored at 4°C at this step). Then samples were permeabilized for 2/5' (depending on

the protein of interest) at RT with Permeabilization buffer (HEPES 20mM, $MgCl_2$ 3mM, NaCl 5mM, sucrose 300mM, Tryton X-100 0,5%) and washed three times, 5' each, with PBS. Samples were then saturated in BSA 3% (in PBS) for 20' at RT. Primary antibody (see Table 3) were diluted in BSA 1% (in PBS) and incubated for 3hrs at RT. After three PBS washes, 5' each, samples were incubated with secondary Alexa Fluor™ antibodies in the dark for 1hr RT. Then samples were washed three times with PBS, 5' each, mounted with ProLong Gold Antifade Mountant (Thermo Fisher™) and stored at 4°C until microscope analysis (performed with Leica DMR A2 wide field).

NHEJ and HR reporter assay

U2OS EJ5-GFP and DR-GFP (a kind gift from Prof. J. Stark and Prof. S. Piccolo) cells were seeded and silenced for DAXX, BRCA1 and control. After 48hrs cells were transfected with the I-SceI expression plasmid (pCBASceI, Addgene) in combination with a reduced amount of DAXX, BRCA1 or control siRNA; 96hrs after the first silencing, cells were harvested and centrifuged at 1200 rpm for 5' at 4°C. Supernatant was discard and cold PBS was added. GFP-positive cells were detected by flow cytometry, at Department of Experimental Oncology, Fondazione IRCCS Istituto Nazionale dei Tumori, using a BD FACSCantoII (more than 20,000 events acquired). Data were analyzed using FlowJo

SMART protocol

- Day1: 5 x 10^5 cells were plated in 100 mm dishes
- Day 2: BrdU 10μM was added to the plates that were incubated for 24 hours at 37°C.
- Day 3:
    - Cells were irradiated with IR 10Gy

- After 1hr cells were washed with PBS and harvested incubating with acutase for 5'.
- Samples were resuspend in PBS and centrifuged at 400 xG for 3'. The supernatant was removed and cells were resuspend in 50µl PBS.
- Meanwhile 1% low melt point agarose in PBS was prepared and heated at 42°C.
- cell suspension was briefly heated at 42°C and 1% low melt point agarose (previously heated at 42°C) was added in a ratio 1:1.
- Plugs were generated and kept at room temperature for 25' to solidify then moved at -20°C for 5' to ensure its integrity.
- Each plug was placed in a 10ml round-bottom tube containing 500µl Lysis buffer [TE50 (10mM Tris-HCl pH 8, 50Mm EDTA) 1% L-lauril-Sarcosyl, 0,2mg/ml of K proteinase) to lyse the plugs and incubate O/N at 50°C.

- Day 4:
  - Lysis buffer was discarded and added fresh then samples were incubate at 50°C for 6 hours.
  - Plugs were washed four times at RT with 10ml of TE50 with minimum agitation for 10 minutes each wash. (plugs can be stored at this step in TE50 at 4°C)
  - the plugs were placed in new tubes for YOYO-1 staining (Thermo Fisher™).
  - 100µl of TE 1X (10mM Tris-HCl pH 8, 1mM EDTA) with 1,5µl of YOYO-1 (1mM in DMSO) were prepared for each plug. The samples were incubated in darkness for 30' at RT.
  - Meanwhile MES 1X (50mM MES hydrate, 50mM MES sodium salt) was heated at 67°C

- Plugs were washed four times with 10ml of TE 1X with minimum agitation for 10’ each wash, at RT
- Then 2,5ml MES 1X was added to each tube and samples were incubated at 65°C to melt the plugs (25’).
- Samples were then cooled at RT to 42°C and 100µl MES 1X+ β-agarase was added doing a spiral. Tubes were incubated O/N at 42°C

- Day 5:

1. Combing

- Samples were incubated at 65°C for 5’ to inactivate β-agarase, cooled to RT and DNA combing was performed.
- The coverslips were incubated at 65°C 2 hours.
- The coverslip was mounted on a slide and immunodetection was performed.

2. Immunodetection

- The coverslips were incubated for 15’ in blocking solution (PBS, 0,1% Triton, 1% BSA)
- 20µl of PBS, 0,1% Triton containing primary antibody against BrdU 1:500 were added on each coverslip, covered with another coverslip, and incubated for 45’ at RT.
- The the coverslips were washed five times, 2’ each, with PBS 0,1% Triton
- The slides were dried, mounted with ProLong Gold Antifade (Molecular Probes) and let polymerize O/N at RT. The day after slides were stored at -20°C or fiber length was evaluated at the microscope (Nikon NI-E with PLAN FLOUR40 3/0.75 PHL DLL objective). More than 200 DNA fibers length was measured with Photoshop CS4 Extended version 11.0 (Adobe Systems) (rule tool).

Bibliography

Acevedo, J., Yan, S. & Michae, W.M., 2016. Direct binding to replication protein A (RPA)-coated single-stranded DNA allows recruitment of the ATR activator topBP1 to sites of DNA damage. *Journal of Biological Chemistry*, 291(25), pp.13124–13131.

Adam, S., Polo, S.E. & Almouzni, G., 2013. Transcription recovery after DNA damage requires chromatin priming by the H3.3 histone chaperone HIRA. *Cell*, 155(1), pp.94–106. Available at: http://www.sciencedirect.com/science/article/pii/S0092867413010234.

Adamo, A. et al., 2010. Preventing Nonhomologous End Joining Suppresses DNA Repair Defects of Fanconi Anemia. *Molecular Cell*, 39(1), pp.25–35. Available at: http://dx.doi.org/10.1016/j.molcel.2010.06.026.

Ahmad, A. et al., 2008. ERCC1-XPF Endonuclease Facilitates DNA Double-Strand Break Repair. *Molecular and Cellular Biology*, 28(16), pp.5082–5092. Available at: http://mcb.asm.org/cgi/doi/10.1128/MCB.00293-08.

Alli, E. & Ford, J.M., 2015. BRCA1: Beyond double-strand break repair. *DNA Repair*, 32, pp.165–171. Available at: http://dx.doi.org/10.1016/j.dnarep.2015.04.028.

Aparicio, T. & Gautier, J., 2016. BRCA1-CtIP interaction in the repair of DNA double-strand breaks. *Molecular & Cellular Oncology*, 3(4), p.e1169343. Available at: https://www.tandfonline.com/doi/full/10.1080/23723556.2016.1169343.

Appin, C.L. & Brat, D.J., 2015. Biomarker-driven diagnosis of diffuse gliomas. *Molecular Aspects of Medicine*, 45, pp.87–96. Available at: http://dx.doi.org/10.1016/j.mam.2015.05.002.

Ashley, A.K. et al., 2014. DNA-PK phosphorylation of RPA32 Ser4 / Ser8 regulates replication stress checkpoint activation , fork restart , homologous recombination and mitotic catastrophe. *DNA Repair*, 21, pp.131–139. Available at: http://dx.doi.org/10.1016/j.dnarep.2014.04.008.

Aymard, F. et al., 2014. Transcriptionally active chromatin recruits homologous recombination at DNA double strand breaks. , 21(4), pp.366–374.

Bakhoum, S.F. & Compton, D. a, 2012. Science in medicine Chromosomal instability and cancer : a complex relationship with therapeutic potential. *The Journal of Clinical Investigation*, 122(4), pp.1138–1143.

Bakker, J.L. et al., 2012. Analysis of the Novel Fanconi Anemia Gene SLX4 / FANCP in. , pp.2011–2014.

Bernardi, R. & Pandolfi, P.P., 2007. Structure, dynamics and functions of promyelocytic leukaemia nuclear bodies. *Nature Reviews Molecular Cell Biology*, 8(12), pp.1006–1016. Available at: http://www.nature.com/doifinder/10.1038/nrm2277.

Biterge, B. & Schneider, R., 2014. Histone variants: Key players of chromatin. *Cell and Tissue Research*, 356(3), pp.457–466.

Bouwman, P. & Jonkers, J., 2012. The effects of deregulated DNA damage signalling on cancer chemotherapy response and resistance. *Nature Reviews Cancer*, 12(9), pp.587–598. Available at: http://www.nature.com/doifinder/10.1038/nrc3342.

Brandsma, I. & Gent, D.C., 2012a. Pathway choice in DNA double strand break repair: observations of a balancing act. *Genome Integr*, 3(9), pp.1–10.

Brandsma, I. & Gent, D.C., 2012b. Pathway choice in DNA double strand break repair: observations of a balancing act. *Genome integrity*, 3(9), p.9. Available at: http://www.genomeintegrity.com/content/3/1/9.

Brazina, J. et al., 2015. DNA damage-induced regulatory interplay between DAXX, p53, ATM kinase and Wip1 phosphatase. *Cell Cycle*, 14(3), pp.375–387.

Brégnard, C. et al., 2016. Upregulated LINE-1 Activity in the Fanconi Anemia Cancer Susceptibility Syndrome Leads to Spontaneous Pro-inflammatory Cytokine Production. *EBioMedicine*, 8, pp.184–194. Available at: http://dx.doi.org/10.1016/j.ebiom.2016.05.005.

Broustas, C.G. & Lieberman, H.B., 2014. DNA Damage Response Genes and the Development of Cancer Metastasis. *Radiation Research*, 181(2), pp.111–130. Available at: http://www.bioone.org/doi/10.1667/RR13515.1.

Bunting, S.F. et al., 2010. 53BP1 inhibits homologous recombination in brca1-deficient cells by blocking resection of DNA breaks. *Cell*, 141(2), pp.243–254.

Burrows, A.E. & Elledge, S.J., 2008. How ATR turns on: TopBP1 goes on ATRIP with ATR. *Genes and Development*, 22(11), pp.1416–1421.

Caldecott, K.W., 2008. Single-strand break repair and genetic disease. *Nature Reviews Genetics*, 9(6), pp.493–493. Available at: http://www.nature.com/doifinder/10.1038/nrg2380.

Cannan, W.J. & Pederson, D.S., 2016. Mechanisms and Consequences of Double-Strand DNA Break Formation in Chromatin. *Journal of Cellular Physiology*, 231(1), pp.3–14.

Cantor, S.B. et al., 2001. BACH1, a novel helicase-like protein, interacts directly with BRCA1 and contributes to its DNA repair function. *Cell*, 105(1), pp.149–160.

Cao, L.L. et al., 2016. ATM-mediated KDM2A phosphorylation is required for the DNA damage repair. *Oncogene*, 35(3), pp.301–313.

Carbone, R. et al., 2002. PML NBs associate with the hMre11 complex and p53 at sites of irradiation induced DNA damage. *Oncogene*, 21(11), pp.1633–1640.

Ceccaldi, R., Rondinelli, B. & D'Andrea, A.D., 2015. Repair Pathway Choices and Consequences at the Double-Strand Break. *Trends in Cell Biology*, 26(1), pp.52–64. Available at: http://dx.doi.org/10.1016/j.tcb.2015.07.009.

Cesare, A.J. & Griffith, J.D., 2004. Telomeric DNA in ALT cells is characterized by free telomeric circles and heterogeneous t-loops. *Mol Cell Biol*, 24(22), pp.9948–9957. Available at: http://www.ncbi.nlm.nih.gov/pmc/articles/PMC525488/pdf/1361-04.pdf.

Chan, K.M. et al., 2013. A lesson learned from the H3.3K27M mutation found in pediatric glioma A new approach to the study of the function of histone modifications in vivo? *Cell Cycle*, 12(16), pp.2546–2552.

Chang, H.H.Y. et al., 2017. Non-homologous DNA end joining and alternative pathways to double-strand break repair. *Nature Reviews Molecular Cell Biology*, 18(8), pp.495–506. Available at: http://www.nature.com/doifinder/10.1038/nrm.2017.48.

Chapman, J.R., Taylor, M.R.G. & Boulton, S.J., 2012. Playing the End Game: DNA Double-Strand Break Repair Pathway Choice. *Molecular Cell*, 47(4), pp.497–510. Available at: http://dx.doi.org/10.1016/j.molcel.2012.07.029.

Chen, P. et al., 2013. H3.3 actively marks enhancers and primes gene transcription via opening higher-ordered chromatin. *Genes and Development*, 27(19), pp.2109–2124.

Chen, X., Kamranvar, S.A. & Masucci, M.G., 2014. Tumor viruses and replicative immortality - Avoiding the telomere hurdle. *Seminars in Cancer Biology*, 26, pp.43–51. Available at: http://dx.doi.org/10.1016/j.semcancer.2014.01.006.

Cheung, T. & Rando, T., 2013. Molecular regulation of stem cell quiescence. *Nature Reviews Molecular Cell Biology*, 14(6), pp.1–26. Available at: http://www.nature.com/nrm/journal/v14/n6/abs/nrm3591.html.

Ciccia, A. & Elledge, S.J., 2011. ScienceDirect - Molecular Cell : The DNA Damage Response: Making It Safe to Play with Knives. *Molecular Cell*, 40(2), pp.179–204. Available at: https://sslvpn.rockefeller.edu/f5-w-687474703a2f2f7777772e736369656e63656469726563742e636f6d$$/science/article/pii/S1097276510007471.

Ciccia, A. & Elledge, S.J., 2010. The DNA Damage Response: Making It Safe to Play with Knives. *Molecular Cell*, 40(2), pp.179–204. Available at:

http://dx.doi.org/10.1016/j.molcel.2010.09.019.

Clouaire, T. & Legube, G., 2015. DNA double strand break repair pathway choice: a chromatin based decision? *Nucleus (Austin, Tex.)*, 6(2), pp.107–13. Available at: http://www.ncbi.nlm.nih.gov/pubmed/25675367.

Coleman, K.A. & Greenberg, R.A., 2011. The BRCA1-RAP80 complex regulates DNA repair mechanism utilization by restricting end resection. *Journal of Biological Chemistry*, 286(15), pp.13669–13680.

Conomos, D., Pickett, H.A. & Reddel, R.R., 2013. Alternative lengthening of telomeres: remodeling the telomere architecture. *Frontiers in Oncology*, 3(February), pp.1–7. Available at: http://journal.frontiersin.org/article/10.3389/fonc.2013.00027/abstract.

Courtois-Cox, S., Jones, S.L. & Cichowski, K., 2008. Many roads lead to oncogene-induced senescence. *Oncogene*, 27(20), pp.2801–2809. Available at: http://www.nature.com/doifinder/10.1038/sj.onc.1210950.

Cruz-Garcìa, A., Lopez, A. & Huertas, P., 2014. BRCA1 Accelerates CtIP-Mediated DNA-End Resection. , pp.451–459.

Curtin, N., 2014. PARP inhibitors for anticancer therapy. *Biochemical Society Transactions*, 42(1), pp.82–88. Available at: http://biochemsoctrans.org/lookup/doi/10.1042/BST20130187.

D'Andrea, A.D., 2010. Susceptibility pathways in Fanconi's anemia and breast cancer. *New England journal of medicine*, 362(20), pp.1909–1919.

D'Andrea, A.D. & Grompe, M., 2003. The Fanconi anaemia/BRCA pathway. *Nature Reviews Cancer*, 3(1), pp.23–34. Available at: http://www.nature.com/doifinder/10.1038/nrc970.

Dabin, J., Fortuny, A. & Polo, S.E., 2016. Epigenome Maintenance in Response to DNA Damage. *Molecular Cell*, 62(5), pp.712–727. Available at: http://dx.doi.org/10.1016/j.molcel.2016.04.006.

Dabin, J., Fortuny, A. & Polo, S.E., 2017. Europe PMC Funders Group Epigenome maintenance in response to DNA damage. , 62(5), pp.712–727.

Daley, J.M. & Sung, P., 2014. 53BP1, BRCA1, and the choice between recombination and end joining at DNA double-strand breaks. *Molecular and cellular biology*, 34(8), pp.1380–8. Available at: http://www.pubmedcentral.nih.gov/articlerender.fcgi?artid=3993578&tool=pmcentrez&rendertype=abstract.

Daury, L. et al., 2006. Histone H3.3 deposition at E2F-regulated genes is linked to transcription. *EMBO Reports*, 7(1), pp.66–71.

Deaton, A.M. et al., 2016. Enhancer regions show high histone H3.3 turnover that changes during differentiation. *eLife*, 5(JUN2016), pp.1–24.

Deng, C.X., 2006. BRCA1: Cell cycle checkpoint, genetic instability, DNA damage response and cancer evolution. *Nucleic Acids Research*, 34(5), pp.1416–1426.

Dibitetto, D. et al., 2016. Slx4 and Rtt107 control checkpoint signalling and DNA resection at double-strand breaks. , 44(2), pp.669–682.

Dick, F.A. & Rubin, S.M., 2013. Molecular mechanisms underlying RB protein function. *Nature Reviews Molecular Cell Biology*, 14(5), pp.297–306. Available at: http://www.nature.com/doifinder/10.1038/nrm3567.

Dunleavy, E.M., Almouzni, G. & Karpen, G.H., 2011. H3.3 is deposited at centromeres in S phase as a placeholder for newly assembled CENP-A in G_1 phase. *Nucleus*, 2(2), pp.146–157. Available at: http://www.tandfonline.com/doi/abs/10.4161/nucl.2.2.15211.

Dziadkowiec, K.N. et al., 2016. PARP inhibitors: review of mechanisms of action and BRCA1/2 mutation targeting. *Menopause review*, 15(4), pp.215–219. Available at: http://www.ncbi.nlm.nih.gov/pubmed/28250726.

Elsässer, S.J. et al., 2012. DAXX envelops a histone H3.3–H4 dimer for H3.3-specific recognition. *Nature*, 491(7425), pp.560–565. Available at: http://www.nature.com/doifinder/10.1038/nature11608.

Elsässer, S.J. et al., 2015. Histone H3.3 is required for endogenous retroviral element silencing in embryonic stem cells. *Nature*, 522(7555), pp.240–244.

Escobar-Cabrera, E. et al., 2010. Structural characterization of the DAXX N-terminal helical bundle domain and its complex with Rassf1C. *Structure*, 18(12), pp.1642–1653. Available at: http://dx.doi.org/10.1016/j.str.2010.09.016.

Escribano-Díaz, C. et al., 2013. A Cell Cycle-Dependent Regulatory Circuit Composed of 53BP1-RIF1 and BRCA1-CtIP Controls DNA Repair Pathway Choice. *Molecular Cell*, 49(5), pp.872–883.

Fekairi, S. et al., 2009. Human SLX4 Is a Holliday Junction Resolvase Subunit that Binds Multiple DNA Repair / Recombination Endonucleases. , pp.78–89.

De Felice, F. et al., 2017. Defective DNA repair mechanisms in prostate cancer: Impact of olaparib. *Drug Design, Development and Therapy*, 11, pp.547–552. Available at: https://www.dovepress.com/getfile.php?fileID=35229 http://ovidsp.ovid.com/ovidweb.cgi?T=JS&CSC=Y&NEWS=N&PAGE=fulltext&D=emex&AN=614707172 http://nt2yt7px7u.search.serialssolutions.com/?sid=OVID:Embase+%3C2017%3E&genre=article&id=pmid:28280302&id=doi:10.21.

Feng, L. et al., 2013. RIF1 counteracts BRCA1-mediated end resection during DNA repair. *Journal of Biological Chemistry*, 288(16), pp.11135–11143.

Fernández-Rodríguez, J. et al., 2012. Analysis of SLX4/FANCP in non-BRCA1/2-mutated breast cancer families. *BMC cancer*, 12(1), p.84. Available at: http://bmccancer.biomedcentral.com/articles/10.1186/1471-2407-12-84.

Ferretti, L.P., Lafranchi, L. & Sartori, A.A., 2013. Controlling DNA-end resection: A new task for CDKs. *Frontiers in Genetics*, 4(JUN), pp.1–7.

Fontebasso, A.M. et al., 2013. Mutations in SETD2 and genes affecting histone H3K36 methylation target hemispheric high-grade gliomas. *Acta Neuropathologica*, 125(5), pp.659–669.

Fregoso, O.I. & Emerman, M., 2016. Activation of the DNA damage response is a

conserved function of HIV-1 and HIV-2 Vpr that is independent of SLX4 recruitment. *mBio*.

Garner, E. et al., 2013. Article Human GEN1 and the SLX4-Associated Nucleases MUS81 and SLX1 Are Essential for the Resolution of Replication-Induced Holliday Junctions. *CellReports*, 5(1), pp.207–215. Available at: http://dx.doi.org/10.1016/j.celrep.2013.08.041.

Gaur, V. et al., 2015. structural and mechanistic analysis of the Slx1-Slx4 Endonuclease. *Cell Reports*, 10(9), pp.1467–1476. Available at: http://dx.doi.org/10.1016/j.celrep.2015.02.019.

Gavande, N.S. et al., 2016. DNA repair targeted therapy: The past or future of cancer treatment? *Pharmacology and Therapeutics*, 160, pp.65–83. Available at: http://dx.doi.org/10.1016/j.pharmthera.2016.02.003.

Gessi, M. et al., 2013. H3.3 G34R mutations in pediatric primitive neuroectodermal tumors of central nervous system (CNS-PNET) and pediatric glioblastomas: Possible diagnostic and therapeutic implications? *Journal of Neuro-Oncology*, 112(1), pp.67–72.

Gilardini Montani, M. et al., 2013. ATM-depletion in breast cancer cells confers sensitivity to PARP inhibition. *Journal of Experimental & Clinical Cancer Research*, 32(1), p.95. Available at: http://jeccr.biomedcentral.com/articles/10.1186/1756-9966-32-95.

Goldberg, A.D. et al., 2010. Distinct Factors Control Histone Variant H3.3 Localization at Specific Genomic Regions. *Cell*, 140(5), pp.678–691. Available at: http://dx.doi.org/10.1016/j.cell.2010.01.003.

Goto, H., Kasahara, K. & Inagaki, M., 2015. Novel insights into chk1 regulation by phosphorylation. *Cell structure and function*, 40(1), pp.43–50. Available at: http://www.ncbi.nlm.nih.gov/pubmed/25748360.

Gravel, S. et al., 2008. DNA helicases Sgs1 and BLM promote DNA double-strand break resection. *Genes and Development*, 22(20), pp.2767–2772.

Greaves, M. & Maley, C.C., 2012. Clonal evolution in cancer. *Nature*, 481(7381),

pp.306–313. Available at: http://www.nature.com/doifinder/10.1038/nature10762.

Greer, D.A. et al., 2003. hRad9 Rapidly Binds DNA Containing Double-Strand Breaks and Is Required for Damage-dependent Topoisomerase II β Binding Protein 1 Focus Formation hRad9 Rapidly Binds DNA Containing Double-Strand Breaks and Is Required for Damage-dependent Topoisomerase II. *Cell Cycle*, pp.4829–4835.

Grillari, J., Katinger, H. & Voglauer, R., 2007. Contributions of DNA interstrand cross-links to aging of cells and organisms. *Nucleic Acids Research*, 35(22), pp.7566–7576.

Le Guen, T. et al., 2015. Role of the double-strand break repair pathway in the maintenance of genomic stability. *Molecular & Cellular Oncology*, 2(1), p.e968020. Available at: http://www.tandfonline.com/doi/full/10.4161/23723548.2014.968020%5Cnhttp://www.ncbi.nlm.nih.gov/pubmed/27308383%5Cnhttp://www.pubmedcentral.nih.gov/articlerender.fcgi?artid=PMC4905226%5Cnhttp://www.tandfonline.com/doi/full/10.4161/23723548.2014.968020.

Guervilly, J. et al., 2015. Article The SLX4 Complex Is a SUMO E3 Ligase that Impacts on Replication Stress Outcome and Genome Stability. *Molecular Cell*, 57(1), pp.123–137. Available at: http://dx.doi.org/10.1016/j.molcel.2014.11.014.

Guervilly, J. et al., 2016. SLX4 gains weight with SUMO in genome maintenance SLX4 gains weight with SUMO in genome maintenance. , 3556(July), pp.7–9.

Guo, A. et al., 2000. The function of PML in p53-dependent apoptosis. *Nature cell biology*, 2(10), pp.730–6. Available at: http://dx.doi.org/10.1038/35036365.

Hake, S.B. et al., 2006. Expression patterns and post-translational modifications associated with mammalian histone H3 variants. *Journal of Biological Chemistry*, 281(1), pp.559–568.

Harding, S.M., Coackley, C. & Bristow, R.G., 2011. ATM-dependent phosphorylation of 53BP1 in response to genomic stress in oxic and hypoxic

cells. *Radiotherapy and Oncology*, 99(3), pp.307–312. Available at: http://dx.doi.org/10.1016/j.radonc.2011.05.039.

Hartlerode, A.J. et al., 2012. Impact of Histone H4 Lysine 20 Methylation on 53BP1 Responses to Chromosomal Double Strand Breaks. *PLoS ONE*, 7(11).

Hartlerode, A.J. & Scully, R., 2009. Mechanisms of double-strand break repair in somatic mammalian cells. *Biochemical Journal*, 423(2), pp.157–168. Available at: http://biochemj.org/lookup/doi/10.1042/BJ20090942.

Heaphy, C.M. et al., 2011. Altered Telomeres in Tumors with ATRX and DAXX Mutations. *Science*, 333(6041), pp.425–425. Available at: http://www.sciencemag.org/cgi/doi/10.1126/science.1207313.

Hendriks, I.A. et al., 2014. Uncovering global SUMOylation signaling networks in a site-specific manner. *Nature Publishing Group*, 21(10), pp.927–936. Available at: http://dx.doi.org/10.1038/nsmb.2890.

Hengstler, H.M.B.J.D.S.J.G., 2011. A comprehensive review about micronuclei : mechanisms of formation and practical aspects in genotoxicity testing. , pp.861–862.

Hoeijmakers, J.H., 2001. Genome maintenance mechanisms for preventing cancer. *Nature*, 411(6835), pp.366–74. Available at: http://www.ncbi.nlm.nih.gov/pubmed/11357144.

Hollenbach, A.D. et al., 2002. Daxx and histone deacetylase II associate with chromatin through an interaction with core histones and the chromatin-associated protein Dek. *Journal of cell science*, 115(Pt 16), pp.3319–3330.

Hollenbach, A.D. et al., 1999. The Pax3-FKHR oncoprotein is unresponsive to the Pax3-associated repressor hDaxx. *EMBO Journal*, 18(13), pp.3702–3711.

Holloway, J.K. et al., 2011. Mammalian BTBD12 (SLX4) protects against genomic instability during mammalian spermatogenesis. *PLoS Genetics*, 7(6).

Houtgraaf, J.H., Versmissen, J. & van der Giessen, W.J., 2006. A concise review of

DNA damage checkpoints and repair in mammalian cells. *Cardiovascular Revascularization Medicine*, 7(3), pp.165–172.

Hsiao, K. & Mizzen, C. a, 2013. Histone H 4 deacetylation facilitates 53 BP 1 DNA damage signaling and double-strand break repair. *Journal of molecular cell biology*, 4(3), pp.157–165. Available at: http://www.ncbi.nlm.nih.gov/pubmed/23329852.

Huertas, P. & Jackson, S.P., 2009. Human CtIP Mediates Cell Cycle Control of DNA End Resection and Double Strand Break Repair. *Journal of Biological Chemistry*, 284(14), pp.9558–9565. Available at: http://www.jbc.org/lookup/doi/10.1074/jbc.M808906200.

Iacovoni, J.S. et al., 2010. High-resolution profiling of γH2AX around DNA double strand breaks in the mammalian genome. *The EMBO Journal*, 29(8), pp.1446–1457. Available at: http://emboj.embopress.org/cgi/doi/10.1038/emboj.2010.38.

Isono, M. et al., 2017. BRCA1 Directs the Repair Pathway to Homologous Recombination by Promoting 53BP1 Dephosphorylation. *Cell Reports*, 18(2), pp.520–532. Available at: http://dx.doi.org/10.1016/j.celrep.2016.12.042.

Iyer, D.R. & Rhind, N., 2017. The intra-S checkpoint responses to DNA damage. *Genes*, 8(2).

Jacquet, K. et al., 2016. The TIP60 Complex Regulates Bivalent Chromatin Recognition by 53BP1 through Direct H4K20me Article The TIP60 Complex Regulates Bivalent Chromatin Recognition by 53BP1 through Direct H4K20me Binding and H2AK15 Acetylation. , pp.409–421.

Jaffray, E.G. & Hay, R.T., 2006. Detection of modification by ubiquitin-like proteins. *Methods*, 38(1), pp.35–38.

Jang, C. et al., 2015. Histone H3 . 3 maintains genome integrity during mammalian development. *Genes & Development*, 1, pp.1377–1392.

Jeggo, P.A., Pearl, L.H. & Carr, A.M., 2016. DNA repair, genome stability and cancer: a historical perspective. *Nature reviews. Cancer*, 16(1), pp.35–42.

Available at: http://dx.doi.org/10.1038/nrc.2015.4.

Jingjie Yi & Jianyuan Luo, 2010. SIRT1 and p53, effect on cancer, senescence and beyond. , 86(12), pp.3279–3288.

Jones, C. & Baker, S.J., 2014. Unique genetic and epigenetic mechanisms driving paediatric diffuse high-grade glioma. *Nature Publishing Group*, 14, pp.1–11. Available at: http://dx.doi.org/10.1038/nrc3811%5Cnpapers3://publication/doi/10.1038/nrc3811.

Jones, R.M. & Petermann, E., 2012. Replication fork dynamics and the DNA damage response. *Biochemical Journal*, 443(1), pp.13–26. Available at: http://biochemj.org/lookup/doi/10.1042/BJ20112100.

Jue, T.R. et al., 2017. Veliparib in combination with radiotherapy for the treatment of MGMT unmethylated glioblastoma. *Journal of Translational Medicine*, 15(1), p.61. Available at: http://translational-medicine.biomedcentral.com/articles/10.1186/s12967-017-1164-1.

Kakarougkas, A. & Jeggo, P.A., 2014. DNA DSB repair pathway choice: An orchestrated handover mechanism. *British Journal of Radiology*, 87(1035).

Kanu, N. et al., 2015. SETD2 loss-of-function promotes renal cancer branched evolution through replication stress and impaired DNA repair. *Oncogene*, 34(46), pp.5699–5708.

Karanam, K. et al., 2012. Quantitative Live Cell Imaging Reveals a Gradual Shift between DNA Repair Mechanisms and a Maximal Use of HR in Mid S Phase. *Molecular Cell*, 47(2), pp.320–329. Available at: http://dx.doi.org/10.1016/j.molcel.2012.05.052.

Khaiboullina, S.F. et al., 2013. Death-domain associated protein-6 (DAXX) mediated apoptosis in hantavirus infection is counter-balanced by activation of interferon-stimulated nuclear transcription factors. *Virology*, 443(2), pp.338–348. Available at: http://dx.doi.org/10.1016/j.virol.2013.05.024.

Kim, J. et al., 2005. Human TopBP1 Ensures Genome Integrity during Normal S

Phase Human TopBP1 Ensures Genome Integrity during Normal S Phase. *Molecular and cellular biology*, 25(24), pp.10907–10915.

Kim, Y. et al., 2011. Mutations of the SLX4 gene in Fanconi anemia. , 43(2), pp.142–147.

Kim, Y., 2014. Nuclease Delivery: Versatile Functions of SLX4/FANCP in Genome Maintenance. *Molecules and Cells*, 37(8), pp.569–574. Available at: http://www.pubmedcentral.nih.gov/articlerender.fcgi?artid=4145367&tool=pmcentrez&rendertype=abstract%5Cnhttp://www.molcells.org/journal/view.html?doi=10.14348/molcells.2014.0118.

Kim, Y. et al., 2013a. Regulation of multiple DNA repair pathways by the Fanconi anemia protein. , 121(1), pp.54–64.

Kim, Y. et al., 2013b. Regulation of multiple DNA repair pathways by the Fanconi anemia protein. *Blood journal*, 121(1), pp.54–63.

King, T. a et al., 2007. Heterogenic loss of the wild-type BRCA allele in human breast tumorigenesis. *Annals of surgical oncology*, 14(9), pp.2510–2518.

Klein Douwel, D. et al., 2014. XPF-ERCC1 Acts in Unhooking DNA Interstrand Crosslinks in Cooperation with FANCD2 and FANCP/SLX4. *Molecular Cell*, 54(3), pp.460–471.

Knudson, A.G., 1971. Mutation and Cancer: Statistical Study of Retinoblastoma. *Proceedings of the National Academy of Sciences*, 68(4), pp.820–823. Available at: http://www.pnas.org/cgi/doi/10.1073/pnas.68.4.820.

Krejci, L. et al., 2012. Homologous recombination and its regulation. *Nucleic Acids Research*, 40(13), pp.5795–5818.

Krokan, H.E. & Bjoras, M., 2013. Base excision repair. *Cold Spring Harb Perspect Biol*, 5(4), p.a012583. Available at: http://www.ncbi.nlm.nih.gov/pubmed/23545420.

Lachaud, C. et al., 2014. Distinct functional roles for the two SLX4 ubiquitin-

binding UBZ domains mutated in Fanconi anemia. , pp.2811–2817.

Laguette, N. et al., 2014. Premature activation of the slx4 complex by vpr promotes g2/m arrest and escape from innate immune sensing. *Cell*, 156(1–2), pp.134–145.

Landwehr, R., Bogdanova, N. V & Antonenkova, N., 2011. Mutation analysis of the SLX4 / FANCP gene in hereditary breast cancer. , pp.1021–1028.

Lawton, J.S., 2016. A fate worse than death. *Journal of Thoracic and Cardiovascular Surgery*, 152(1), pp.97–98. Available at: http://dx.doi.org/10.1038/nrc.2016.58.

Lewis, P.W. et al., 2010. Daxx is an H3.3-specific histone chaperone and cooperates with ATRX in replication-independent chromatin assembly at telomeres. *Proceedings Of The National Academy Of Sciences (Of The United States Of America)*, 107(32), pp.14075–14080. Available at: http://eutils.ncbi.nlm.nih.gov/entrez/eutils/elink.fcgi?dbfrom=pubmed&id=20651253&retmode=ref&cmd=prlinks%5Cnpapers2://publication/doi/10.1073/pnas.1008850107.

Li, G.-M., 2008. Mechanisms and functions of DNA mismatch repair. *Cell Research*, 18(1), pp.85–98. Available at: http://www.nature.com/doifinder/10.1038/cr.2007.115.

Lim, S. & Kaldis, P., 2013. Cdks, cyclins and CKIs: roles beyond cell cycle regulation. *Development*, 140(15), pp.3079–3093. Available at: http://dev.biologists.org/cgi/doi/10.1242/dev.091744.

Lin, D.Y. et al., 2006. Role of SUMO-Interacting Motif in Daxx SUMO Modification, Subnuclear Localization, and Repression of Sumoylated Transcription Factors. *Molecular Cell*, 24(3), pp.341–354.

Liu, K. et al., 2003. Regulation of E2F1 by BRCT Domain-Containing Protein TopBP1. *Molecular and Cellular Biology*, 23(9), pp.3287–3304. Available at: http://mcb.asm.org/cgi/doi/10.1128/MCB.23.9.3287-3304.2003.

Liu, S. et al., 2006. Claspin Operates Downstream of TopBP1 To Direct ATR

Signaling towards Chk1 Activation. *Molecular and Cellular Biology*, 26(16), pp.6056–6064. Available at: http://mcb.asm.org/cgi/doi/10.1128/MCB.00492-06.

Liu, Y., Cussiol, J.R., Dibitetto, D., Sims, J.R., Twayana, S., Weiss, R.S., Freire, R., Marini, F., Pellicioli, A., Smolka, M.B., et al., 2017. TOPBP1 Dpb11 plays a conserved role in homologous recombination DNA repair through the coordinated recruitment of 53BP1 Rad9. *DNA Repair*, 22(3), pp.165–174. Available at: http://dx.doi.org/10.1016/j.dnarep.2014.06.004.

Liu, Y., Cussiol, J.R., Dibitetto, D., Sims, J.R., Twayana, S., Weiss, R.S. & Freire, Raimundo Marini, Federica Pellicioli, Achille Smolka, M.B., 2017. TOPBP1 Dpb11 plays a conserved role in homologous recombination DNA repair through the coordinated recruitment of 53BP1 Rad9. *The Journal of Cell Biology*, 216(3), pp.623–639. Available at: http://www.ncbi.nlm.nih.gov/pubmed/28228534%0Ahttp://www.pubmedcentral.nih.gov/articlerender.fcgi?artid=PMC5350513%0Ahttp://www.jcb.org/lookup/doi/10.1083/jcb.201607031.

Liu, Y., Cussiol, J.R., Dibitetto, D., Sims, J.R., Twayana, S., Weiss, R.S., Freire, R., Marini, F., Pellicioli, A. & Smolka, M.B., 2017. TOPBP1 Dpb11 plays a conserved role in homologous recombination DNA repair through the coordinated recruitment of 53BP1 Rad9. *The Journal of Cell Biology*, 216(3), pp.623–639. Available at: http://www.ncbi.nlm.nih.gov/pubmed/28228534%0Ahttp://www.pubmedcentral.nih.gov/articlerender.fcgi?artid=PMC5350513%0Ahttp://www.jcb.org/lookup/doi/10.1083/jcb.201607031.

Löbrich, M. & Jeggo, P.A., 2007. The impact of a negligent G2/M checkpoint on genomic instability and cancer induction. *Nature Reviews Cancer*, 7(11), pp.861–869. Available at: http://www.nature.com/doifinder/10.1038/nrc2248.

Lovejoy, C.A. et al., 2012. Loss of ATRX, Genome Instability, and an Altered DNA Damage Response Are Hallmarks of the Alternative Lengthening of Telomeres Pathway. *PLoS Genetics*, 8(7), p.e1002772. Available at: http://dx.plos.org/10.1371/journal.pgen.1002772.

Loyola, A. et al., 2006. PTMs on H3 Variants before Chromatin Assembly Potentiate Their Final Epigenetic State. *Molecular Cell*, 24(2), pp.309–316.

Luijsterburg, M.S. et al., 2016. PARP1 Links CHD2-Mediated Chromatin Expansion and H3.3 Deposition to DNA Repair by Non-homologous End-Joining. *Molecular Cell*, 61(4), pp.547–562. Available at: http://linkinghub.elsevier.com/retrieve/pii/S1097276516000460.

Lulla, R.R., Saratsis, A.M. & Hashizume, R., 2016. Mutations in chromatin machinery and pediatric high-grade glioma. *Science advances*, 2(3), p.e1501354.

Ma, C.J. et al., 2017. Protein dynamics of human RPA and RAD51 on ssDNA during assembly and disassembly of the RAD51 filament. *Nucleic Acids Research*, 45(2), pp.749–761.

Malumbres, M. & Barbacid, M., 2009. Cell cycle, CDKs and cancer: a changing paradigm. *Nature Reviews Cancer*, 9(3), pp.153–166. Available at: http://www.nature.com/doifinder/10.1038/nrc2602.

Mamrak, N.E., Shimamura, A. & Howlett, N.G., 2017. Recent discoveries in the molecular pathogenesis of the inherited bone marrow failure syndrome Fanconi anemia. *Blood Reviews*, 31(3), pp.93–99. Available at: http://dx.doi.org/10.1016/j.blre.2016.10.002.

Manchado, E., Eguren, M. & Malumbres, M., 2010. The anaphase-promoting complex/cyclosome (APC/C): cell-cycle-dependent and -independent functions. *Biochemical Society Transactions*, 38(1), pp.65–71. Available at: http://biochemsoctrans.org/lookup/doi/10.1042/BST0380065.

Mao, Y.S., Zhang, B. & Spector, D.L., 2011. Biogenesis and function of nuclear bodies. *Trends in Genetics*, 27(8), pp.295–306. Available at: http://dx.doi.org/10.1016/j.tig.2011.05.006.

Matos, J. & West, S.C., 2014. Holliday junction resolution: Regulation in space and time. *DNA Repair*, 19, pp.176–181. Available at: http://dx.doi.org/10.1016/j.dnarep.2014.03.013.

Matsuoka, S. et al., 2007. ATM and ATR substrate analysis reveals extensive protein networks responsive to DNA damage. *Science*, 316(May), pp.1160–1166.

McCabe, N. et al., 2006. Deficiency in the repair of DNA damage by homologous recombination and sensitivity to poly(ADP-ribose) polymerase inhibition. *Cancer Research*, 66(16), pp.8109–8115.

Mehrgou, A. & Akouchekian, M., 2016. The importance of BRCA1 and BRCA2 genes mutations in breast cancer development. *Medical Journal of the Islamic Republic of Iran (MJIRI)*, pp.1–12. Available at: http://mjiri.iums.ac.ir.

Mertz, T.M., Harcy, V. & Roberts, S.A., 2017. Risks at the DNA Replication Fork: Effects upon Carcinogenesis and Tumor Heterogeneity. *Genes*, 8(1), p.46. Available at: http://www.mdpi.com/2073-4425/8/1/46.

Meza, J. et al., 1999. Mapping the Functional Domains of BRCA1. *Journal of Biological Chemistry*, 274(9), pp.5659–5665. Available at: citeulike-article-id:13528859%5Cnhttp://dx.doi.org/10.1074/jbc.274.9.5659.

Michod, D. et al., 2012. Calcium-Dependent Dephosphorylation of the Histone Chaperone DAXX Regulates H3.3 Loading and Transcription upon Neuronal Activation. *Neuron*, 74(1), pp.122–135. Available at: http://dx.doi.org/10.1016/j.neuron.2012.02.021.

Miller, K.M. & Jackson, S.P., 2012. Histone marks: repairing DNA breaks within the context of chromatin. *Biochemical Society transactions*, 40(2), pp.370–376. Available at: http://eutils.ncbi.nlm.nih.gov/entrez/eutils/elink.fcgi?dbfrom=pubmed&id=22435814&retmode=ref&cmd=prlinks%5Cnpapers3://publication/doi/10.1042/BST20110747.

Mimitou, E.P. & Symington, L.S., 2011. DNA end resection - unraveling the tail. *DNA Repair*, 10(3), pp.344–348.

Mordes, D.A. et al., 2008. TopBP1 activates ATR through ATRIP and a PIKK regulatory domain. *Genes and Development*, 22(11), pp.1478–1489.

Nabetani, A. & Ishikawa, F., 2011. Alternative lengthening of telomeres pathway: Recombination-mediated telomere maintenance mechanism in human cells. *Journal of Biochemistry*, 149(1), pp.5–14.

Negrini, S., Gorgoulis, V.G. & Halazonetis, T.D., 2010. Genomic instability — an evolving hallmark of cancer. *Nature Reviews Molecular Cell Biology*, 11(3), pp.220–228. Available at: http://www.nature.com/doifinder/10.1038/nrm2858.

Newell, A.E.H. et al., 2004. Interstrand crosslink-induced radials form between non-homologous chromosomes, but are absent in sex chromosomes. *DNA Repair*, 3(5), pp.535–542.

Noon, A.T. & Goodarzi, A.A., 2011. 53BP1-mediated DNA double strand break repair: Insert bad pun here. *DNA Repair*, 10(10), pp.1071–1076. Available at: http://dx.doi.org/10.1016/j.dnarep.2011.07.012.

Nussenzweig, A.T. and A., 2017. Endogenous DNA Damage as a Source of Genomic Instability in Cancer. , pp.644–656.

Panier, S. & Boulton, S.J., 2014. Double-strand break repair: 53BP1 comes into focus. *Nature Reviews Molecular Cell Biology*, 15(1), pp.7–18. Available at: http://www.nature.com/doifinder/10.1038/nrm3719.

Park, J.K. et al., 2017. DAXX / ATRX and MEN1 genes are strong prognostic markers in pancreatic neuroendocrine tumors. , 8(30), pp.49796–49806.

Paull, T.T., 2015. Mechanisms of ATM Activation. *Annual Review of Biochemistry*, 84(1), pp.711–738. Available at: http://www.annualreviews.org/doi/10.1146/annurev-biochem-060614-034335.

Paull, T.T. et al., 2014. Quantitation of DNA double-strand break resection intermediates in human cells. *Nucleic Acids Research*, 42(3), pp.1–11.

Pfister, S.X. et al., 2014. SETD2-Dependent Histone H3K36 Trimethylation Is Required for Homologous Recombination Repair and Genome Stability. *Cell Reports*, 7(6), pp.2006–2018.

Pickett, H.A. & Reddel, R.R., 2015. Molecular mechanisms of activity and derepression of alternative lengthening of telomeres. *Nat Struct Mol Biol*, 22(11), pp.875–880. Available at: http://dx.doi.org/10.1038/nsmb.3106%5Cn10.1038/nsmb.3106.

Pikor, L. et al., 2013. The detection and implication of genome instability in cancer. *Cancer and Metastasis Reviews*, 32(3–4), pp.341–352.

Pilch, D.R. et al., 2003. Characteristics of γ-H2AX foci at DNA double-strand breaks sites. *Biochemistry and Cell Biology*, 81(3), pp.123–129. Available at: http://www.nrcresearchpress.com/doi/abs/10.1139/o03-042.

Polato, F. et al., 2014. CtIP-mediated resection is essential for viability and can operate independently of BRCA1. *The Journal of Experimental Medicine*, 211(6), pp.1027–1036. Available at: http://www.jem.org/lookup/doi/10.1084/jem.20131939.

Potenski, C.J. & Klein, H.L., 2014. How the misincorporation of ribonucleotides into genomic DNA can be both harmful and helpful to cells. *Nucleic Acids Research*, 42(16), pp.10226–10234.

Price, B.D. & Andrea, A.D.D., 2014. Chromatin Remodeling at DNA Double Strand Breaks. *Cell*, 152(6), pp.1344–1354.

Puto, L. a. & Reed, J.C., 2008. Daxx represses RelB target promoters via DNA methyltransferase recruitment and DNA hypermethylation. *Genes and Development*, 22(8), pp.998–1010.

Qian & Chen, 2013. Senescence regulation by the p53 protein family. , 965, pp.37–61. Available at: http://link.springer.com/10.1007/978-1-62703-239-1.

Reinhardt, H.C. & Yaffe, M.B., 2013. Phospho-Ser/Thr-binding domains: navigating the cell cycle and DNA damage response. *Nature Reviews Molecular Cell Biology*, 14(9), pp.563–580. Available at: http://www.nature.com/doifinder/10.1038/nrm3640.

Renaud, E., Barascu, A. & Rosselli, F., 2015. Impaired TIP60-mediated H4K16 acetylation accounts for the aberrant chromatin accumulation of 53BP1 and RAP80 in Fanconi anemia pathway-deficient cells. *Nucleic Acids Research*, 44(2), pp.648–656.

Rogakou, E.P. et al., 1998. Double-stranded Brekas Induce Histone H2AX phosphorylation on Serine 139. *The Journal of Biological Chemistry*, 273(10),

pp.5858–5868. Available at: http://www.jbc.org/content/273/10/5858.full.pdf.

Rogakou, E.P. et al., 1999. Megabase Chromatin Domains Involved in DNA Double-Strand Breaks In Vivo. , 146(5), pp.905–915.

Romero, A. et al., 2013. Low prevalence of SLX4 loss-of-function mutations in non-BRCA1 / 2 breast and / or ovarian cancer families. , (October 2012), pp.883–886.

Rosen, E.M., 2013. BRCA1 in the DNA damage response and at telomeres. *Frontiers in Genetics*, 4(JUN), pp.1–14.

Sakaue, T. et al., 2017. The CUL3-SPOP-DAXX axis is a novel regulator of VEGFR2 expression in vascular endothelial cells. *Scientific Reports*, 7(February), p.42845. Available at: http://www.nature.com/articles/srep42845.

Salsman, J. et al., 2017. Myogenic differentiation triggers PML nuclear body loss and DAXX relocalization to chromocentres. *Cell Death and Disease*, 8(3), p.e2724. Available at: http://www.nature.com/doifinder/10.1038/cddis.2017.151.

Samadder, P. et al., 2016. Cancer TARGETases: DSB repair as a pharmacological target. *Pharmacology and Therapeutics*, 161, pp.111–131.

Sarma, K. & Reinberg, D., 2005. Histone variants meet their match. *Nature Reviews Molecular Cell Biology*, 6(2), pp.139–149. Available at: http://www.nature.com/doifinder/10.1038/nrm1567.

Satyanarayana, A. & Kaldis, P., 2009. Mammalian cell-cycle regulation: several Cdks, numerous cyclins and diverse compensatory mechanisms. *Oncogene*, 28(33), pp.2925–2939. Available at: http://www.nature.com/doifinder/10.1038/onc.2009.170.

Schärer, O.D., 2013. Nucleotide excision repair in Eukaryotes. *Cold Spring Harbor Perspectives in Biology*, 5(10), pp.1–19.

Schultz, L.B. et al., 2000. p53 Binding Protein 1 (53BP1) Is an Early Participant in the Cellular Response to DNA Double-Strand Breaks. *The Journal of Cell Biology*, 151(7), pp.1381–1390. Available at: http://www.jcb.org/cgi/content/full/151/7/1381.

Schultz, N. et al., 2003. Poly(ADP-ribose) polymerase (PARP-1) has a controlling role in homologous recombination. *Nucleic Acids Research*, 31(17), pp.4959–4964.

Schuster, B. et al., 2012. Whole Exome Sequencing Reveals Uncommon Mutations in the Recently Identified Fanconi Anemia Gene SLX4 / FANCP. , pp.2011–2014.

Schwartzentruber, J. et al., 2012. Corrigendum: Driver mutations in histone H3.3 and chromatin remodelling genes in paediatric glioblastoma. *Nature*, 484(7392), pp.130–130.

Shah, S. et al., 2013. Assessment of SLX4 Mutations in Hereditary Breast Cancers. , 8(6), pp.4–8.

Shibata, A. et al., 2011. Factors determining DNA double-strand break repair pathway choice in G2 phase. *The EMBO Journal*, 30(6), pp.1079–1092. Available at: http://emboj.embopress.org/cgi/doi/10.1038/emboj.2011.27.

Shibata, A., 2017. Regulation of repair pathway choice at two-ended DNA double-strand breaks. *Mutation Research/Fundamental and Molecular Mechanisms of Mutagenesis*, (March), pp.0–1. Available at: http://linkinghub.elsevier.com/retrieve/pii/S0027510717300611.

Smith, J. et al., 2010. The ATM-Chk2 and ATR-Chk1 pathways in DNA damage signaling and cancer. *Advances in cancer research*, 108, pp.73–112. Available at: http://www.ncbi.nlm.nih.gov/pubmed/21034966.

Somyajit, K., Subramanya, S. & Nagaraju, G., 2010. RAD51C: A novel cancer susceptibility gene is linked to Fanconi anemia and breast cancer. *Carcinogenesis*, 31(12), pp.2031–2038.

Song, M.S. et al., 2008. The tumour suppressor RASSF1A promotes MDM2 self-

ubiquitination by disrupting the MDM2–DAXX–HAUSP complex. *The EMBO Journal*, 27(13), pp.1863–1874. Available at: http://emboj.embopress.org/cgi/doi/10.1038/emboj.2008.115.

Soussi, T., 2007. P53 Alterations in Human Cancer: More Questions Than Answers. *Oncogene*, 26(15), pp.2145–2156.

Stadler, J. & Richly, H., 2017. Regulation of DNA repair mechanisms: How the chromatin environment regulates the DNA damage response. *International Journal of Molecular Sciences*, 18(8).

Stoepker, C. et al., 2011. is mutated in a new Fanconi anemia subtype. , 43(2).

Stokes, M.P. et al., 2007. Profiling of UV-induced ATM/ATR signaling pathways. *Proceedings of the National Academy of Sciences of the United States of America*, 104(50), pp.19855–60. Available at: http://www.pubmedcentral.nih.gov/articlerender.fcgi?artid=2148387&tool=pmcentrez&rendertype=abstract.

Stracker, T.H. & Petrini, J.H.J., 2011. The Mre11 complex: stariting from the tail. , 37(1), pp.62–70.

Sulli, G., Di Micco, R. & di Fagagna, F. d'Adda, 2012. Crosstalk between chromatin state and DNA damage response in cellular senescence and cancer. *Nature Reviews Cancer*, 12(10), pp.709–720. Available at: http://www.nature.com/doifinder/10.1038/nrc3344.

Sullivan, M. & Morgan, D.O., 2007. Finishing mitosis, one step at a time. *Nature Reviews Molecular Cell Biology*, 8(11), pp.894–903. Available at: http://www.nature.com/doifinder/10.1038/nrm2276.

Symington, L.S. & Gautier, J., 2011. Double-Strand Break End Resection and Repair Pathway Choice. *Annual Review of Genetics*, 45(1), pp.247–271. Available at: http://www.annualreviews.org/doi/10.1146/annurev-genet-110410-132435.

Szenker, E., Ray-Gallet, D. & Almouzni, G., 2011. The double face of the histone variant H3.3. *Cell Research*, 21(3), pp.421–434. Available at:

http://www.nature.com/doifinder/10.1038/cr.2011.14.

Takahashi, A., Ohtani, N. & Hara, E., 2007. Irreversibility of cellular senescence: dual roles of p16INK4a/Rb-pathway in cell cycle control. *Cell Division*, 2(1), p.10. Available at: http://celldiv.biomedcentral.com/articles/10.1186/1747-1028-2-10.

Tang, J. et al., 2004. A Novel Transcription Regulatory Complex Containing Death Domain-associated Protein and the ATR-X Syndrome Protein. *Journal of Biological Chemistry*, 279(19), pp.20369–20377.

Tang, J. et al., 2013. Phosphorylation of Daxx by ATM contributes to DNA damage-induced p53 activation. *PloS one*, 8(2), p.e55813. Available at: http://www.pubmedcentral.nih.gov/articlerender.fcgi?artid=3566025&tool=pmcentrez&rendertype=abstract.

Thomas Kuilman, Michaloglou, C. & ., 2010. The essence of senescence. *Health & Social Care in the Community*, 11(5), pp.423–430.

Thompson, L.L. et al., 2013. Regulation of chromatin structure via histone post-translational modification and the link to carcinogenesis. , pp.363–376.

Udugama, M. et al., 2015. Histone variant H3.3 provides the heterochromatic H3 lysine 9 tri-methylation mark at telomeres. *Nucleic acids research*, 43(21), pp.10227–37. Available at: http://nar.oxfordjournals.org/lookup/doi/10.1093/nar/gkv847%5Cnhttp://www.ncbi.nlm.nih.gov/pubmed/26304540.

Ueda, S. et al., 2012. Two serine phosphorylation sites in the C-terminus of Rad9 are critical for 9-1-1 binding to TopBP1 and activation of the DNA damage checkpoint response in HeLa cells. *Genes to Cells*, 17(10), pp.807–816.

Walker, M. et al., 2009. Chk1 C-terminal regulatory phosphorylation mediates checkpoint activation by de-repression of Chk1 catalytic activity. *Oncogene*, 28(24), pp.2314–23. Available at: http://www.pubmedcentral.nih.gov/articlerender.fcgi?artid=2857325&tool=pmcentrez&rendertype=abstract.

Wan, B. et al., 2013. Report SLX4 Assembles a Telomere Maintenance Toolkit by Bridging Multiple Endonucleases with Telomeres. *CellReports*, 4(5), pp.861–869. Available at: http://dx.doi.org/10.1016/j.celrep.2013.08.017.

Wang, A.T. & Smogorzewska, A., 2015. SnapShot: Fanconi anemia and associated proteins. *Cell*, 160(1–2), p.354–354.e1. Available at: http://dx.doi.org/10.1016/j.cell.2014.12.031.

Wang, A.T. & Smogorzewska, A., 2015. SnapShot: Fanconi anemia and associated proteins. *Cell*, 160(1–2), p.354–354.e1. Available at: http://dx.doi.org/10.1016/j.cell.2014.12.031.

Wang, B. et al., 2013. Abraxas and Rap80 form a novel BRCA1 protein complex required for the DNA damage response. *Science*, 316(5828), pp.1194–1198. Available at: http://www.ncbi.nlm.nih.gov/entrez/query.fcgi?cmd=Retrieve&db=PubMed&dopt=Citation&list_uids=17525340.

Wardlaw, C.P., Carr, A.M. & Oliver, A.W., 2014. TopBP1: A BRCT-scaffold protein functioning in multiple cellular pathways. *DNA Repair*, 22, pp.165–174. Available at: http://dx.doi.org/10.1016/j.dnarep.2014.06.004.

Welcsh, P.L. & King, M.C., 2001. BRCA1 and BRCA2 and the genetics of breast and ovarian cancer. *Human molecular genetics*, 10(7), pp.705–713.

Wen, H. et al., 2014. ZMYND11 links histone H3.3K36me3 to transcription elongation and tumour suppression. *Nature*, 508(7495), pp.263–8. Available at: http://www.pubmedcentral.nih.gov/articlerender.fcgi?artid=4142212&tool=pmcentrez&rendertype=abstract.

Williams, H.L., Gottesman, M.E. & Gautier, J., 2013. The differences between ICL repair during and outside of S phase. *Trends in Biochemical Sciences*, 38(8), pp.386–393. Available at: http://dx.doi.org/10.1016/j.tibs.2013.05.004.

Wilson, J.S.J. et al., 2013. Report Localization-Dependent and -Independent Roles of SLX4 in Regulating Telomeres. *CellReports*, 4(5), pp.853–860. Available at: http://dx.doi.org/10.1016/j.celrep.2013.07.033.

Wolters, S. & Schumacher, B., 2013. Genome maintenance and transcription integrity in aging and disease. *Frontiers in Genetics*, 4(FEB), pp.1–10.

Wu, J. et al., 2009. PTIP regulates 53BP1 and SMC1 at the DNA damage sites. *Journal of Biological Chemistry*, 284(27), pp.18078–18084.

Wu, L.H., Liu, Y. & Kong, D.C., 2014. Mechanism of chromosomal DNA replication initiation and replication fork stabilization in eukaryotes. *Science China Life Sciences*, 57(5), pp.482–487.

Wu, Q., Jubb, H. & Blundell, T.L., 2015. Phosphopeptide interactions with BRCA1 BRCT domains: More than just a motif. *Progress in Biophysics and Molecular Biology*, 117(2–3), pp.143–148. Available at: http://dx.doi.org/10.1016/j.pbiomolbio.2015.02.003.

Wu, Z., 2013. The concept and practice of Fanconi Anemia : from the clinical bedside to the laboratory bench. *Translational Pediatrics*, 2(3), pp.112–119.

Xia, W. & Jiao, J., 2017. Histone variant H3.3 orchestrates neural stem cell differentiation in the developing brain. *Cell Death and Differentiation*, 24(9), pp.1548–1563. Available at: http://www.nature.com/doifinder/10.1038/cdd.2017.77.

Xu, Y. et al., 2012. H2AZ controls DSB repair. , 48(5), pp.723–733.

Yamamoto, K.N. et al., 2011. Involvement of SLX4 in interstrand cross-link repair is regulated by the Fanconi anemia pathway.

Yang, K., Guo, R. & Xu, D., 2016. Non-homologous end joining: Advances and frontiers. *Acta Biochimica et Biophysica Sinica*, 48(7), pp.632–640.

Yang, X. et al., 1997. Daxx, a Novel Fas-Binding Protein That Activates JNK and Apoptosis. *Cell*, 89(7), pp.1067–1076. Available at: http://linkinghub.elsevier.com/retrieve/pii/S0092867400802949.

Yang, X. et al., 2013. Histone acetyltransferase 1 promotes homologous recombination in DNA repair by facilitating histone turnover. *Journal of*

Biological Chemistry, 288(25), pp.18271–18282.

Yao, C.J. et al., 2013. Fanconi anemia pathway-the way of DNA interstrand cross-link repair. *Pharmazie*, 68(1), pp.5–11.

Yao, Z. et al., 2014. Death domain-associated protein 6 (Daxx) selectively represses IL-6 transcription through histone deacetylase 1 (HDAC1)-mediated histone deacetylation in macrophages. *Journal of Biological Chemistry*, 289(13), pp.9372–9379.

Yin, J. et al., 2016a. Dimerization of SLX4 contributes to functioning of the SLX4-nuclease complex. *Nucleic Acids Research*, 44(10), pp.4871–4880.

Yin, J. et al., 2016b. Dimerization of SLX4 contributes to functioning of the SLX4-nuclease complex. , 44(10), pp.4871–4880.

Yu, X. & Chen, J., 2004. DNA Damage-Induced Cell Cycle Checkpoint Control Requires CtIP , a Phosphorylation-Dependent Binding Partner of BRCA1 C-Terminal Domains DNA Damage-Induced Cell Cycle Checkpoint Control Requires CtIP , a Phosphorylation-Dependent Binding Partner of BRCA1. *Molecular and Cellular Biology*, 24(21), pp.9478–9486.

Zannini, L., Delia, D. & Buscemi, G., 2014. CHK2 kinase in the DNA damage response and beyond. *Journal of Molecular Cell Biology*, 6(6), pp.442–457.

Zhao, L.Y. et al., 2004. Negative regulation of p53 functions by Daxx and the involvement of MDM2. *The Journal of biological chemistry*, 279(48), pp.50566–79. Available at: http://www.ncbi.nlm.nih.gov/pubmed/15364927.

Zimmermann, M. & de Lange, T., 2014. 53BP1: Pro choice in DNA repair. *Trends in Cell Biology*, 24(2), pp.108–117. Available at: http://linkinghub.elsevier.com/retrieve/pii/S0962892413001554.

Zimmermann, M., Lottersberger, F. & Buonomo, S.B., 2013. 53BP1 Regulates DSB Repair Using. *Science (New York, NY)*, 2(February), pp.700–705.

Ziv, Y. et al., 2006. Chromatin relaxation in response to DNA double-strand breaks

is modulated by a novel ATM- and KAP-1 dependent pathway. *Nature Cell Biology*, 8(8), pp.870–876. Available at: http://www.nature.com/doifinder/10.1038/ncb1446.

Acknowledgements

Ci sono parti più facili di quanto non sia stato il mio dottorato.

Però è stata l'esperienza più formativa, soddisfacente e sorprendente che abbia mai fatto.

Grazie alle persone meravigliose che mi hanno accompagnato lungo il cammino.

A chi ha riso con me,
a chi ha pianto con me
a chi si è commosso e arrabbiato con me
a coloro contro i quali ho dovuto combattere
a chi non era con me ma ugualmente mi è stato accanto
alla mia famiglia che insieme a me non ha mai mollato
ai colleghi diventati amici
agli amici diventati indispensabili
a me che se ci ripenso ancora non ci credo
e a te
che sei stato un fratello
e il mio padre scientifico
dedico questa tesi
che è la prima grande conquista della mia vita.
Grazie